



universität  
wien

# DISSERTATION

Titel der Dissertation

Reconstructing diet by stable isotope analysis ( $\delta^{13}\text{C}$  and  $\delta^{15}\text{N}$ ):  
Two case studies from Bronze Age and  
Early Medieval Lower Austria

Verfasserin

Mag. rer. nat. Kerstin Rumpelmayr

angestrebter akademischer Grad

Doktorin der Naturwissenschaften (Dr. rer. nat.)

Wien, 2012

Studienkennzahl:  
Dissertationsgebiet:  
Betreuerin:

A 091 419  
Chemie  
Ao. Univ.-Prof. Mag. Dr. Eva Maria Wild



## Abstract

Carbon and nitrogen stable isotope analysis is nowadays a method frequently applied for the reconstruction of past human diets. The principles of this technique were developed in the late 1970s and 1980s, when it was shown that the isotopic composition of an animal's body is correlated to that of its diet. Given that the investigated material (often bone collagen) is well enough preserved, several aspects of diet can be investigated by carbon and nitrogen isotopic signatures generally expressed as  $\delta^{13}\text{C}$  and  $\delta^{15}\text{N}$  values.  $\delta$ -values are defined as the deviation (in per mil) of the respective isotope ratio e.g.,  $^{13}\text{C}/^{12}\text{C}$  or  $^{15}\text{N}/^{14}\text{N}$ , from that of an internationally agreed reference material.  $\delta^{13}\text{C}$  and  $\delta^{15}\text{N}$  values allow the determination of a nutrition based on  $\text{C}_3$  or  $\text{C}_4$  plants (most plants in the temperate areas are of the  $\text{C}_3$  type;  $\text{C}_4$  plants like maize or millet occur in the warmer regions). Furthermore, these signatures can be used for the detection of a marine component in the diet and they contain information about the trophic level of an individual.

The goal of this work was to perform carbon and nitrogen stable isotope analysis by using human and animal skeletal remains from Austrian archaeological sites and to investigate certain aspects of diet. Two sites (both in Lower Austria) were selected for this study, the Bronze Age Cemetery of Gemeinlebarn F and the Early Medieval settlement of Thunau/Gars am Kamp. The previous archaeological and anthropological examinations suggested that both sites were inhabited by socially differentiated populations. Hence, during the stable isotope analysis special emphasis was put on the detection of variation in nutritional habits due to sociogenic or gender-related differences.

$\delta^{13}\text{C}$  and  $\delta^{15}\text{N}$  values were measured in collagen, extracted from the bone samples, by means of EA-IRMS (elemental analyzer-isotope ratio mass spectrometry) using a *CE instruments NC2500* elemental analyzer coupled to a *Micromass Optima* isotope ratio mass spectrometer. The obtained stable isotope data were examined for significant differences between social groups and the sexes using statistical hypothesis testing (MANOVA and ANOVA). However, no considerable differences between mean  $\delta$ -values of population subgroups representing distinct social categories could be found. There was only one statistically significant ANOVA result, which points to a difference in  $\delta^{15}\text{N}$  between the males and the females in Gemeinlebarn. A possible interpretation of this result is an unequal extent of animal protein consumption of the males and the females.

Nevertheless, the results of this study provide insights into the dietary habits of two ancient human populations from central Europe. The comparison of the two data sets (from Gemeinlebarn and Thunau) revealed several differences between the two populations. First, the  $\delta$ -values of the human samples from Thunau show a considerably greater variability than those from Gemeinlebarn especially with respect to the  $\delta^{13}\text{C}$  values. This implies a more heterogeneous diet for the population from Thunau compared to the investigated humans from Gemeinlebarn. In Bronze Age Gemeinlebarn the population probably relied on locally produced agricultural foodstuffs based on  $\text{C}_3$  resources, whereas the inhabitants of Early Medieval Thunau had access to more diverse diet sources. It is also noticeable that the human samples of Thunau show on average higher  $\delta^{13}\text{C}$  values than the Gemeinlebarn sample set. It is therefore likely that at least a part of Thunau's humans included  $\text{C}_4$  plants in their diet.





## Zusammenfassung

Kohlenstoff- und Stickstoffstabilisotopenanalyse wird heute häufig zur Paläodiät-Rekonstruktion angewandt. Die Grundlagen dieser Methode wurden in den späten 1970er und 1980er Jahren entwickelt. Damals wurde gezeigt, dass die Isotopensignatur des Körpergewebes eines Tieres mit jener seiner Nahrung zusammenhängt. Vorausgesetzt, dass das untersuchte Material (oft Knochenkollagen) ausreichend gut erhalten ist, können mehrere Aspekte der Diät anhand von C- und N-Isotopensignaturen untersucht werden, welche meist als  $\delta^{13}\text{C}$ - und  $\delta^{15}\text{N}$ -Werte ausgedrückt werden.  $\delta$ -Werte sind definiert als die Abweichung (in Promille) des Isotopenverhältnisses einer Probe, z.B.:  $^{13}\text{C}/^{12}\text{C}$  oder  $^{15}\text{N}/^{14}\text{N}$ , von dem eines international festgelegten Referenzmaterials.  $\delta^{13}\text{C}$ - und  $\delta^{15}\text{N}$ -Werte ermöglichen die Bestimmung einer auf  $\text{C}_3$ - oder  $\text{C}_4$ -Pflanzen basierenden Ernährung (die meisten Pflanzen in den gemäßigten Klimazonen gehören zum  $\text{C}_3$ -Typ;  $\text{C}_4$ -Pflanzen wie z.B.: Mais oder Hirse kommen in den wärmeren Regionen vor). Außerdem können  $\delta^{13}\text{C}$ - und  $\delta^{15}\text{N}$ -Werte eine marine Nahrungskomponente anzeigen und es können Informationen bezüglich des trophischen Levels eines Individuums daraus abgeleitet werden.

Das Ziel dieser Arbeit war die Durchführung von C- und N-Stabilisotopenanalysen mit menschlichen und tierischen Skelettüberresten von österreichischen Ausgrabungsstätten, um verschiedene Aspekte der Ernährungsweise zu untersuchen. Zwei Fundstätten in Niederösterreich, das bronzezeitliche Gräberfeld von Gemeinlebarn F und die frühmittelalterliche Siedlung von Thunau/Gars am Kamp, wurden für diese Paläodiätstudie ausgewählt. Die vorangegangenen archäologischen und anthropologischen Untersuchungen deuten darauf hin, dass beide Fundstätten von sozial differenzierten Populationen bewohnt wurden. Deshalb wurde während der Stabilisotopenuntersuchungen besonderes Augenmerk auf Variationen in den Ernährungsgewohnheiten aufgrund soziogener oder geschlechtsspezifischer Unterschiede gelegt.

Die  $\delta^{13}\text{C}$ - und  $\delta^{15}\text{N}$ -Werte wurden mittels EA-IRMS (**E**lemental **A**nalyzer-**I**sotope **R**atio **M**ass **S**pecrometry) in Knochenkollagen bestimmt. Für die Messungen wurde ein *CE instruments NC2500* Elementaranalysator gekoppelt an ein *Micromass Optima* Massenspektrometer eingesetzt. Die erhaltenen Stabilisotopen-Daten wurden mithilfe statistischer Hypothesentests (MANOVA und ANOVA) auf signifikante Unterschiede zwischen sozialen Gruppen und den beiden Geschlechtern untersucht. Es konnten jedoch keine bedeutsamen Unterschiede zwischen den Gruppenmittelwerten der verschiedenen sozialen Gruppen gefunden werden. Die ANOVA-Analysen ergaben ein einziges statistisch signifikantes Resultat, welches auf einen Unterschied im  $\delta^{15}\text{N}$ -Wert zwischen Frauen und Männern aus Gemeinlebarn F hindeutet. Eine mögliche Interpretation dieses Ergebnisses ist ein unterschiedlicher Diätanteil an tierischem Protein bei den beiden Geschlechtern.

Die Ergebnisse dieser Paläodiätstudie lieferten Einblicke in die Ernährungsgewohnheiten von zwei (prä)historischen menschlichen Populationen aus Zentraleuropa. Der Vergleich dieser Datensätze zeigte ernährungsbezogene Unterschiede zwischen den beiden Populationen auf. Die  $\delta$ -Werte der menschlichen Proben aus Thunau weisen eine deutlich größere Streuung auf als jene aus Gemeinlebarn. Daraus kann man auf eine heterogenere Ernährungsweise der Thunauer im Vergleich zu der untersuchten Gemeinlebarner Bevölkerung schließen. Im bronzezeitlichen Gemeinlebarn beruhte die Ernährung vermutlich auf  $\text{C}_3$ -Ressourcen aus einer lokalen landwirtschaftlichen Produktion, während die Einwohner Thunaus wahrscheinlich Zugang zu vielfältigeren Nahrungsmittelquellen hatten. Erwähnenswert ist des Weiteren, dass die menschlichen Proben von Thunau im Mittel höhere  $\delta^{13}\text{C}$ -Werte im Vergleich zu Gemeinlebarn aufweisen. Demnach ist es wahrscheinlich, dass zumindest bei einem Teil der Menschen aus Thunau  $\text{C}_4$ -Pflanzen eine Rolle in der Ernährung spielten.



# Contents

<b>1</b>	<b>Introduction</b>	<b>1</b>
1.1	Motivation . . . . .	1
1.2	Stable Isotope Ratios . . . . .	3
1.3	Isotope Effects . . . . .	4
1.3.1	Kinetic Isotope Effects in Incomplete, Unidirectional Processes	4
1.3.2	Equilibrium Isotope Effects . . . . .	6
1.4	Stable Isotopes in Palaeodietary Reconstruction . . . . .	7
1.4.1	Carbon Stable Isotope Signatures in Food Webs . . . . .	7
1.4.2	Nitrogen Stable Isotope Signatures in Food Webs . . . . .	11
1.4.3	The Sample Material: Bone Collagen . . . . .	13
<b>2</b>	<b>Materials</b>	<b>17</b>
2.1	Gemeinlebarn . . . . .	17
2.1.1	The Archaeological Site of Gemeinlebarn . . . . .	17
2.1.2	The Investigated Bone Samples from Gemeinlebarn F . . . . .	17
2.2	Thunau/Gars am Kamp . . . . .	20
2.2.1	The Archaeological Site of Thunau . . . . .	20
2.2.2	The Investigated Bone Samples from Thunau . . . . .	21
<b>3</b>	<b>Methods</b>	<b>23</b>
3.1	Bone Collagen Preparation . . . . .	23
3.1.1	Comparison of Collagen Extraction Methods . . . . .	24
3.1.2	Sample Preparation for Archaeological Bone . . . . .	28
3.2	Instrumentation: EA-IRMS . . . . .	29
3.2.1	System Configuration . . . . .	29
3.2.2	Processes during a Measurement . . . . .	31
3.2.3	Tuning of the Mass Spectrometer . . . . .	35
3.3	IRMS-measurement of Bone Collagen . . . . .	37
3.3.1	Developing a Standard Measurement Procedure for Collagen Samples . . . . .	37
3.3.2	Calibrating Laboratory Standards . . . . .	42
3.3.3	Collagen Batch-Measurements . . . . .	44
3.4	Uncertainty Estimation for EA-IRMS Measurement Results ( $\delta^{13}\text{C}$ and $\delta^{15}\text{N}$ ) . . . . .	44
3.4.1	General Overview of the Applied Mathematical Procedures . . . . .	45
3.4.2	Uncertainty Estimation for $\delta$ -values of Laboratory Standards . . . . .	49
3.4.3	Uncertainty Estimation for $\delta$ -values of Palaeodiet Samples . . . . .	53

3.5	Uncertainty Estimation for Elemental Contents . . . . .	53
3.6	Inter-Laboratory Comparison . . . . .	55
<b>4</b>	<b>Results and Discussion</b>	<b>57</b>
4.1	Collagen Preparation Methods . . . . .	57
4.2	Uncertainty analysis . . . . .	63
4.2.1	Laboratory Standards . . . . .	63
4.2.2	Palaeodiet Samples . . . . .	64
4.2.3	Conclusions . . . . .	67
4.3	Palaeodiet Reconstruction for the Skeletal Samples from Thunau/Gars am Kamp . . . . .	68
4.3.1	Stable Isotope Data of the Animal Remains . . . . .	68
4.3.2	Stable Isotope Data of the Human Remains . . . . .	70
4.3.3	Statistical Examination . . . . .	76
4.3.4	Conclusions . . . . .	80
4.4	Palaeodiet Reconstruction for the Sample-Set from Gemeinlebarn F .	81
4.4.1	Results of the Stable Isotope Analysis for the Animal Samples	81
4.4.2	Results of the Stable Isotope Analysis for the Human Samples	83
4.4.3	Statistical Examination . . . . .	86
4.4.4	Conclusions . . . . .	88
<b>5</b>	<b>Final Remarks</b>	<b>91</b>
	<b>Bibliography</b>	<b>95</b>
	<b>List of Abbreviations</b>	<b>109</b>
	<b>Acknowledgments</b>	<b>111</b>
	<b>Curriculum Vitae</b>	<b>113</b>

# 1 Introduction

## 1.1 Motivation

*"Biological evolution among hominids leading to the appearance of the genus Homo was intimately associated with changes in diet. The subsequent developments of human social and economic organization were, to a large extent, responses to changes in methods for the procurement and distribution of food."*

Michael J. DeNiro (1987), *American Scientist* **75**, 182-192.

To assess human nutritional behavior in the past, various techniques have been employed in archaeological science (see e.g., Schoeninger & Moore, 1992; Schutkowski, 2006). Important insights have for instance been gained by archaeological artifacts like tools, the examination of food remains in midden deposits or by anthropological approaches like palaeopathology or dental microwear analysis. The examination of human and animal remains by means of stable isotope analysis complements the range of these techniques, because it provides information about the nutrients that were actually consumed and subsequently incorporated into the body tissues. The analysis of carbon and nitrogen stable isotope ratios in bone collagen is therefore a frequently applied method in order to reconstruct past human diets.

The principles of this technique have been developed in the 1970s and 1980s, when its application showed the consumption of maize by prehistoric woodland Americans (van der Merwe & Vogel, 1978; Vogel & van der Merwe, 1977). First controlled diet experiments were conducted in order to understand the transfer of dietary carbon and nitrogen to body tissue (DeNiro & Epstein, 1978, 1981). These pioneering experiments demonstrated that the isotopic composition of an animal's body is correlated to the isotopic composition of its diet and therefore founded the basis for dietary reconstruction. Since then, extensive methodological work has been performed in order to address essential questions like the assessment of post mortem alteration and diagenesis of the analyzed tissues or the clarification of isotope fractionation during metabolism and possible routing of dietary nutrients (see Section 1.4). Yet, some details of the complex mechanisms behind these processes are not completely understood.

To date, numerous examples for the application of C- and N-stable isotope analysis to archaeological material have been published and reviewed by several authors (e.g., Ambrose & Krigbaum, 2003; DeNiro, 1987; Lee-Thorp, 2008; Schoeninger & Moore,

1992; van der Merwe, 1982). To give a few examples, Vogel's and van der Merwe's approach to trace the introduction of the  $C_4$  plant (see Section 1.4.1) maize into a  $C_3$  environment in the area of New York State has been extended to other regions in North America and lead to similar observations (e.g., Buikstra & Milner, 1991). It could be shown, that in Iron Age Slovenia another important  $C_4$  crop, millet, was included into the diet (Murray & Schoeninger, 1988; Schoeninger & Moore, 1992). Many authors have investigated the importance of marine versus terrestrial resources in human nutrition (e.g., Eriksson *et al.*, 2008; Richards & Hedges, 1999; Sealy & van der Merwe, 1988). In some cases, carbon and/or nitrogen stable isotope analysis has revealed or strengthened evidence for social differentiation within past human populations. For example, Richards *et al.* (1998) related differences in carbon and nitrogen isotope ratios to burial type in the case of a Late-Roman cemetery (Poundbury Camp, England). They concluded that individuals from higher status burials (mausolea and lead-lined coffins) consumed marine foods, whereas the individuals buried in wooden coffins did not. Ambrose & Krigbaum (2003) ascribed higher nitrogen isotope ratios of high status individuals (identified by grave goods) in Cahokia Mound 72, Illinois around 1050-1150 AD to consumption of larger amounts of animal protein than the low status individuals. The same interpretation is given by Le Huray & Schutkowski (2005) for elevated nitrogen isotopic ratios of a group of male individuals, possibly warriors, compared to the remaining investigated males from a Bohemian site during the La Tène period. An example from northern Europe comes from the medieval site in Sigtuna, Sweden, where the observed pattern of isotope ratios seems to reflect variation in vegetable vs. animal protein intake between the social groups (Kjellström *et al.*, 2009). The isotope data from Sigtuna also show a significant shift between males and females within a population. In several studies differences in bone isotopic composition between the sexes, which are thought to be associated with diet rather than with physiological differences (see Nitsch *et al.*, 2010), have been noticed and discussed (e.g., Dürrewächter *et al.*, 2006; Müldner & Richards, 2007a; Prowse *et al.*, 2005; Richards *et al.*, 2006).

In the presented work, the intention was to apply carbon and nitrogen stable isotope analysis to human and animal skeletal remains from archaeological sites in Austria, in order to reconstruct certain aspects of human diet (e.g., in terms of  $C_3$  versus  $C_4$  plant consumption and trophic level) with special emphasis on possible gender-related or sociogenic differences in nutritional habits. The Early Bronze Age necropolis Gemeinlebarn F and the Early Medieval burials of Thunau/Gars am Kamp were selected for this project, since the investigation of these sites by stable isotope analysis may verify earlier archaeological and anthropological studies (see below).

For the buried individuals of Gemeinlebarn F, classification into social groups was achieved using several parameters generally believed to be related to social status like grave goods or grave dimensions. An observed difference in body height of high status and low status male individuals (Teschler-Nicola, 1989) raised the question, if nutritional factors could be responsible for this effect (see Section 2.1). The presented study includes an attempt to clarify this question by means of stable isotope analysis.

The site in Thunau provides a special topographical situation, as it comprises a hill-top settlement with a manor house and a riverine settlement with graves. The

latter is thought to be an area that was used for agriculture and artisanal work (see Section 2.2). The inhabitants of both areas could therefore represent different social strata, which in turn could have influenced diet patterns.

## 1.2 Stable Isotope Ratios

Isotopes are atoms of a chemical element, with the same number of protons but different numbers of neutrons in their nuclei. This means isotopes of an element have the same atomic number, which defines a chemical element in the periodic table, but different mass numbers. Most elements are composed of more than one isotope. Carbon and nitrogen have two stable isotopes each, which are listed in table 1.1 together with their respective natural abundances.

Isotope	Abundance (%)
$^{12}\text{C}$	98.89
$^{13}\text{C}$	1.11
$^{14}\text{N}$	99.64
$^{15}\text{N}$	0.36

**Table 1.1:** Natural abundances of stable carbon and nitrogen isotopes.

The natural isotope abundances in table 1.1 are average values, but there are variations in abundances between different materials, like distinct chemical compounds (for example carbohydrates and lipids in a plant) or different reservoirs in nature (for instance the atmosphere and the biosphere). These variations in isotopic composition are due to so called "isotope effects" (see section 1.3).

It is common practice to denote natural isotope abundances in  $\delta$ -notation, which expresses the relative deviation of the isotope ratio of a sample from that of an internationally agreed reference material in per mil. The  $\delta$ -notation has become generally accepted, because most isotopic measurements are relative measurements (i.e., the isotopic compositions of the sample to be measured and a known standard material are compared) and it is more convenient for the denotation of very small differences in isotopic composition between materials as they occur in nature (e.g., Hayes, 2002). Carbon stable isotope ratios are given as  $\delta^{13}\text{C}$  values, which are defined by equation 1.1 (for a review see e.g., Coplen *et al.*, 2002; Werner & Brand, 2001),

$$\delta^{13}\text{C} = \left( \frac{^{13}\text{C}/^{12}\text{C}_{\text{spl}} - ^{13}\text{C}/^{12}\text{C}_{\text{ref}}}{^{13}\text{C}/^{12}\text{C}_{\text{ref}}} \right) \cdot 1000 \text{‰} \quad (1.1)$$

where  $^{13}\text{C}/^{12}\text{C}_{\text{spl}}$  is the ratio of the number of  $^{13}\text{C}$ -atoms to  $^{12}\text{C}$ -atoms in a sample and  $^{13}\text{C}/^{12}\text{C}_{\text{ref}}$  is the respective carbon stable isotope ratio of the international reference material. In the case of  $\delta^{13}\text{C}$  values this reference material initially was the Pee Dee Belemnite (PDB), which is composed of calcium carbonate from fossilized shells of *Belemnitella americana*, an extinct genus of marine cephalopods, deposited in the

Pee Dee Formation (South Carolina). The standard was prepared by Harold C. Urey in his laboratory at the University of Chicago in the early 1950s (see Urey *et al.*, 1951). Since the initial material has long been exhausted, the VPDB (Vienna Pee Dee Belemnite) scale has been introduced, which is anchored by the NBS-19 calcium carbonate (National Bureau of Standards) and the L-SVEC lithium carbonate (prepared by H. Svec). This was accomplished by assigning consensus  $\delta^{13}\text{C}$  values determined relative to the PDB-standard to both, NBS-19 and L-SVEC (see e.g., Coplen *et al.*, 2006a,b; Hut, 1987; Werner & Brand, 2001).

Nitrogen stable isotope ratios are expressed as  $\delta^{15}\text{N}$  values (1.2), relative to atmospheric nitrogen (AIR: "Ambient Inhalable Reservoir"), which by convention has a  $\delta^{15}\text{N}$  value of 0.00 ‰ (for a review see e.g., Coplen *et al.*, 2002; Werner & Brand, 2001).

$$\delta^{15}\text{N} = \left( \frac{{}^{15}\text{N}/{}^{14}\text{N}_{\text{spl}} - {}^{15}\text{N}/{}^{14}\text{N}_{\text{ref}}}{{}^{15}\text{N}/{}^{14}\text{N}_{\text{ref}}} \right) \cdot 1000 \text{ ‰} \quad (1.2)$$

Atmospheric nitrogen is a reliable reference because its isotopic signature is considered to be constant on a geographical scale and does not seem to be influenced by human activity (Mariotti, 1983), whereas carbon dioxide in the atmosphere is not suitable for this purpose. The atmosphere's carbon isotopic composition is subject to variation caused by natural processes and anthropogenic influence. One example for this is the seasonal variation in the  $\delta^{13}\text{C}$  of atmospheric carbon dioxide related to plant growth (see e.g., Mook & Koopmans, 1983). Another cause of variation is fossil fuel burning, which is responsible for a slow decrease of the carbon stable isotope ratio in the atmosphere (Mook & Koopmans, 1983).

## 1.3 Isotope Effects

Isotope effects are physical phenomena that become apparent as differences in behavior of the isotopes during chemical reactions and physical processes like diffusion or the change of state of aggregation caused by the varying masses of the different isotopes (see e.g., Gannes *et al.*, 1998; Hoefs, 2004). The two main mechanisms are kinetic and equilibrium isotope effects. The less frequent mass-independent isotope effects (e.g., Farquhar *et al.*, 2000) are not discussed here. For a general introduction to isotope fractionation see e.g., Hayes (2002).

### 1.3.1 Kinetic Isotope Effects in Incomplete, Unidirectional Processes

Kinetic isotope effects occur during incomplete, unidirectional processes because of mass-dependent reaction- or transport rates (e.g., Hoefs, 2004). For example, isotope effects during chemical reactions can be described using the respective reaction rate constants. If substrate A is converted irreversibly to a product B and the substrate molecule contains an element consisting of two isotopes, then the reaction of the substrate comprising the different isotopes ( $A^{\text{L}}$ : isotopically lighter;  $A^{\text{H}}$ : isotopically



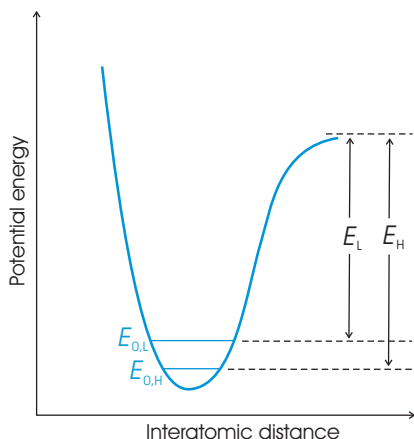
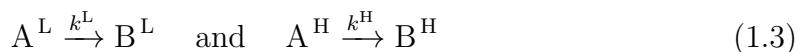


**Figure 1.1:** Schematic diagram of the potential-energy curve of a diatomic molecule, adapted from Hoefs (2004). ( $E_0$ : zero-point energy,  $E$ : dissociation energy; indexes "L" and "H" indicate the lighter and the heavier isotopologue respectively.)

heavier) can be denoted by the two equations:



Since the reaction rate constant depends on the masses of the isotopes, each of the two given conversions has its own constant,  $k^L$  refers to the conversion of the substrate containing the lighter isotope and  $k^H$  to the heavier analog. The magnitude of the kinetic isotope effect ( $\alpha_{kin}$ ) can then be denoted according to equation 1.4 (Farquhar *et al.*, 1989).

$$\alpha_{kin} = \frac{k^L}{k^H} \quad (1.4)$$

In most cases the lighter isotope containing compound reacts faster than the heavier counterpart. As a consequence, the corresponding  $\alpha_{kin}$  is greater than one, resulting in an "isotopically lighter" product (i.e., depleted in the heavier isotope) with respect to the remaining substrate, which is termed "heavier" (i.e., enriched in the heavier isotope). Such an isotope effect is called "normal", but "inverse" effects with  $\alpha_{kin} < 1$  are also found e.g., some kinetic isotope effects involving hydrogen atoms are inverse. Note that whenever all the available substrate is converted during a reaction (as it occurs under kinetic control of a reaction in closed systems), there will be no net fractionation.

The reason why molecules comprising different isotopes exhibit slightly different reaction rates, is the influence of the masses of atoms on the strength of the bonds between them. Generally, bonds including the lighter isotope are weaker and will break more readily than bonds containing the heavier isotope (e.g., O'Leary *et al.*, 1992). This effect is caused by differences in the potential energies between isotopic species. Figure 1.1 shows the schematic potential-energy curve of a diatomic molecule. The lowest possible energy for a bond – its zero-point energy – is defined as  $1/2 \cdot h\nu$ , where  $h$  is Planck's constant and  $\nu$  is the vibration frequency, which depends on the isotope masses (Wiberg, 1955). The compound containing the lighter isotope will have a higher zero-point energy,  $E_{0,L}$ , than the one with the heavier isotope,  $E_{0,H}$ . Therefore, the dissociation energy of the lighter molecule - depicted as  $E_L$  - is smaller than

## 1 Introduction

$E_H$ , the corresponding dissociation energy of the heavier analog, which explains the greater stability of the latter.

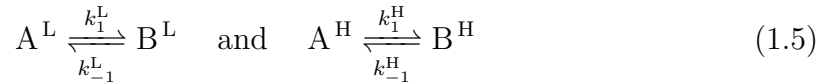
An important example for a normal kinetic isotope effect in nature is the difference between the rate constants for the reaction of  $\text{CO}_2$  containing  $^{12}\text{C}$  or  $^{13}\text{C}$  with Ru-bisco (Ribulose-1:5-bisphosphate carboxylase), the enzyme catalyzing carbon dioxide fixation in the Calvin Cycle (see Section 1.4.1).

### Isotope Fractionation during Diffusion

Another important isotope effect can for instance be observed as unequal diffusion rates of gas molecules containing different isotopes, where the molecule with the lighter isotope will often show a slightly higher rate of diffusion, since application of the same force will displace the isotopically lighter molecule faster than its heavier counterpart (e.g., Peterson & Fry, 1987). Such an isotope effect can for example be found during diffusion of carbon dioxide in air, where the  $^{12}\text{CO}_2$  molecules show a faster diffusion rate than the  $^{13}\text{CO}_2$  molecules (see e.g., Farquhar *et al.*, 1989).

### 1.3.2 Equilibrium Isotope Effects

Equilibrium isotope effects occur during isotope exchange reactions, in which an atom is exchanged between chemical substances or between different phases like they occur in evaporation/condensation processes and can be thought of a balance of two kinetic isotope effects in chemical equilibrium (Farquhar *et al.*, 1989). To generate an equilibrium condition for the case shown in Equation 1.3, the possible back-reactions have to be considered:



Index "1" refers to the respective rate constant for the forward reaction, index "-1" to the backward reaction. The equilibrium constants for the reactions ( $K^L$  and  $K^H$ ) are related to the equilibrium concentrations (denoted as  $c$ ) of the involved substances and the rate constants of the respective forward and backward reaction according to:

$$K^L = \frac{c(\text{B}^L)}{c(\text{A}^L)} = \frac{k_1^L}{k_{-1}^L} \quad \text{and} \quad K^H = \frac{c(\text{B}^H)}{c(\text{A}^H)} = \frac{k_1^H}{k_{-1}^H} \quad (1.6)$$

The magnitude of the equilibrium isotope effect, expressed as fractionation factor  $\alpha_{equ}$ , is the ratio of the respective equilibrium constants as shown in Equation 1.7.  $\alpha_{equ}$  can be linked to the kinetic isotope effect for the forward reaction divided by that of the backward reaction (Farquhar *et al.*, 1989):

$$\alpha_{equ} = \frac{K^L}{K^H} = \frac{\left(\frac{k_1^L}{k_{-1}^L}\right)}{\left(\frac{k_1^H}{k_{-1}^H}\right)} = \frac{\left(\frac{k_1^L}{k_1^H}\right)}{\left(\frac{k_{-1}^L}{k_{-1}^H}\right)} = \frac{\alpha_{kin,1}}{\alpha_{kin,-1}} \quad (1.7)$$

As a general rule of thumb for equilibrium isotope effects, the heavier isotope accumulates in the substance with the stronger bonds or the phase with the greater density (e.g., Kendall & Caldwell, 1998). In nature, a fractionation due to an equilibrium isotope effect can for instance be observed when gaseous carbon dioxide dissolves in water and forms bicarbonate  $\text{HCO}_3^-$  enriched in  $^{13}\text{C}$  (Mook *et al.*, 1974), which plays e.g., a role in the photosynthesis of green plants. Isotope fractionation occurring in the photosynthetic reactions represents a fundamental basis for diet reconstructions, which will be pointed out in the following section.

## 1.4 Stable Isotopes in Palaeodietary Reconstruction

### 1.4.1 Carbon Stable Isotope Signatures in Food Webs

Carbon enters the biosphere via autotrophic organisms, which are capable of synthesizing complex organic compounds from simple inorganic molecules. These organisms are the primary producers of the biosphere and therefore form the lowest trophic level on earth. Green plants and algae are such primary producers. Using the energy from sunlight, they are able to synthesize carbohydrates from carbon dioxide and water in a reaction-sequence called photosynthesis.

#### The Photosynthetic Pathways

In vascular plants, air containing carbon dioxide enters the leaf via pores in the epidermis, so called stomata, which lead to the mesophyll of the leaf. There, carbon fixation takes place, following one of the three different metabolic mechanisms (the  $\text{C}_3$ -cycle, the  $\text{C}_4$ -cycle and crassulacean acid metabolism, CAM).

The majority of the plants in temperate areas including trees, woody shrubs, herbs and most important cereals such as wheat, barley or rice and also root staples like potatoes etc., use the  $\text{C}_3$ -cycle (also called Calvin cycle) (e.g., Lee-Thorp, 2008; Price *et al.*, 1985). These so called " $\text{C}_3$ -plants" fix atmospheric carbon dioxide in their mesophyll cells by carboxylation of Ribulose-1:5-bisphosphate mediated by the enzyme Ribulose-1:5-bisphosphate carboxylase (Rubisco) as depicted in Figure 1.2. This first step in the cycle yields 3-phosphoglycerate, a compound containing three carbon atoms, giving rise to the denomination of this pathway as the  $\text{C}_3$ -cycle (see e.g., Elliott & Elliott, 2001).

In the mesophyll of  $\text{C}_4$ -plants, dissolved  $\text{CO}_2$  is in equilibrium with  $\text{HCO}_3^-$ , which is then used by the enzyme Phosphoenolpyruvate carboxylase (PEPc) to produce oxaloacetate (Farquhar *et al.*, 1989). The latter substance is a  $\text{C}_4$ -compound and therefore this photosynthetic pathway is referred to as the  $\text{C}_4$ -cycle. Oxaloacetate is subsequently reduced to malate, which is transported into neighboring bundle sheath cells, which are photosynthetic cells tightly arranged around the leaf-veins. There,  $\text{CO}_2$  is released, resulting in a substantially higher concentration of carbon dioxide than in the  $\text{C}_3$  photosynthetic cells. The  $\text{CO}_2$  in the bundle sheath then enters the Calvin cycle and is assimilated into carbohydrates (see Figure 1.3). Examples for

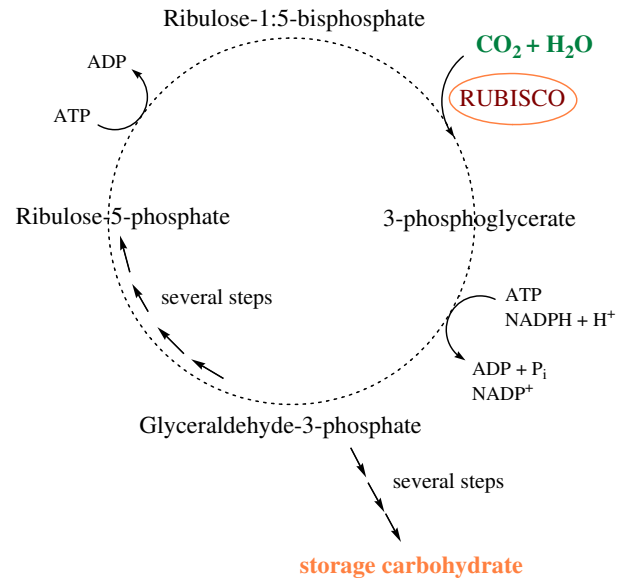


**Figure 1.2:** Simplified diagram of the Calvin Cycle adapted from Elliott & Elliott, 2001. (ADP: adenosine diphosphate; ATP: adenosine triphosphate;  $\text{NADP}^+$ : nicotinamide adenine dinucleotide phosphate; NADPH: reduced form of  $\text{NADP}^+$ ; RUBISCO: ribulose-1:5-bisphosphate carboxylase,  $\text{P}_i$ : inorganic phosphate).

$\text{C}_4$  plants are a number of tropical grasses, economically important  $\text{C}_4$  crops are for instance maize, sugar cane or millet (e.g., Lee-Thorp, 2008; Price *et al.*, 1985).

Crassulacean acid metabolism is interpreted as an adaption to arid environments (see Ting, 1985, and literature cited there). However, only few CAM plants are relevant for human nutrition, examples are pineapple or agave (e.g., DeNiro, 1987).

## Isotope Fractionation during Photosynthesis

Isotope fractionation occurs to unequal extents during the three above mentioned photosynthetic pathways. The major isotope fractionation during the  $\text{C}_3$ -cycle is caused by the enzyme Rubisco, which strongly discriminates against  $^{13}\text{C}$ . But the overall fractionation occurring in  $\text{C}_3$ -photosynthesis depends on the fractionation due to diffusion of  $\text{CO}_2$  in air through the stomata, the fractionation caused by Rubisco when fixing gaseous  $\text{CO}_2$  and the ambient and intercellular partial pressures of  $\text{CO}_2$  (Craig, 1954; Farquhar *et al.*, 1982; O'Leary, 1980; Roeske & O'Leary, 1984).

Environmental conditions like water availability, soil salinity or light intensity influence the intercellular partial pressure of  $\text{CO}_2$  (Farquhar *et al.*, 1982; O'Leary, 1981, and literature cited there) and the variability in these conditions ultimately leads to a variability in plant  $\delta^{13}\text{C}$  values.

In nature  $\delta^{13}\text{C}$ -values from around -20 ‰ to -36 ‰ have been reported for modern  $\text{C}_3$ -plants (Smith & Epstein, 1971; Troughton *et al.*, 1974; van der Merwe, 1982). However, due to human activity (e.g., burning of fossil fuels),  $\delta^{13}\text{C}$  of atmospheric carbon has decreased by  $\sim 1.5$  ‰ over the past 200 years from approximately -6.5 ‰ to -8.0 ‰ (Friedli *et al.*, 1986). Therefore the  $\delta^{13}\text{C}$  range for pre-industrial  $\text{C}_3$  plants was probably closer to -18 ‰ to -34 ‰.

In  $\text{C}_4$  plants, PEPc discriminates to a much lesser extent against  $^{13}\text{C}$  than Rubisco (e.g., O'Leary *et al.*, 1992, and literature cited there). Hence, the overall discrimination during  $\text{C}_4$  photosynthesis is numerically smaller than for the  $\text{C}_3$  pathway,

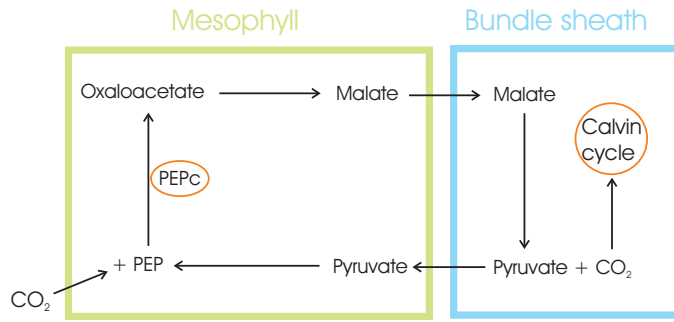


**Figure 1.3:** Schematic overview of the C<sub>4</sub> photosynthetic pathway adapted from Elliott & Elliott, 2001. (PEP: phosphoenolpyruvate; PEPC: phosphoenolpyruvate carboxylase).

leading to significantly higher  $\delta^{13}\text{C}$ -values of C<sub>4</sub> plants compared to C<sub>3</sub> plants. In nature,  $\delta^{13}\text{C}$  values from approximately -9 ‰ to -19 ‰ are found for modern C<sub>4</sub> plants (Troughton *et al.*, 1974; van der Merwe, 1982).

CAM plants show carbon isotopic compositions ranging from C<sub>3</sub>-like to C<sub>4</sub>-like, approximately from -10 ‰ to -33 ‰. This wide range is caused by variation in metabolism within this type of plants (see Ting, 1985, and literature cited there).

Apart from the isotopic difference between C<sub>3</sub> and C<sub>4</sub> plants on land, there are also characteristic differences in carbon isotopic composition between terrestrial and aquatic systems. Although most aquatic photosynthetic organisms use the C<sub>3</sub> pathway (e.g., O’Leary, 1981; Raven *et al.*, 2008, and literature cited there), the carbon isotopic composition of marine primary producers can differ substantially from those of terrestrial C<sub>3</sub> plants. Many marine plants actually show  $\delta^{13}\text{C}$  values in the range of terrestrial C<sub>4</sub> plants (e.g., DeNiro, 1987; Gannes *et al.*, 1998; Schoeninger & Moore, 1992, and literature cited there). This is partly due to the more variable  $\delta^{13}\text{C}$  values of the source inorganic carbon in aquatic systems compared to the atmosphere (e.g., Raven *et al.*, 2008) and there are several other factors influencing the  $\delta^{13}\text{C}$  of phytoplankton like temperature, light intensity, nutrient availability, pH and physiological features (e.g., Hoefs, 2004, p. 47).

In freshwater plants, the  $\delta^{13}\text{C}$  values vary depending on the relative contributions of different carbon reservoirs. The dissolved CO<sub>2</sub> used for photosynthesis may originate from the atmosphere, from carbonate rock weathering, from mineral springs or from degraded organic matter (Peterson & Fry, 1987; Schoeninger & Moore, 1992, and literature cited there).

### Carbon Isotope Fractionation in the Food Web

In the next trophic level, the primary consumers feed on the different types of plants and in the course of metabolism, isotope fractionation occurs, leading to different isotopic compositions of distinct tissues or biochemical compounds in the body. DeNiro & Epstein (1978) showed that the whole body of an animal reflected the isotopic composition of its diet. However, the body of the animal was slightly enriched (by ~ 1 ‰) in <sup>13</sup>C compared to the diet, which is due to respiration of depleted CO<sub>2</sub>. Isotopic compositions of proteins like collagen and keratin and inorganic components of the body like bone carbonate were also found to be related to diet, but they were more enriched than the whole body of the animal. For instance, the  $\delta^{13}\text{C}$  difference

## 1 Introduction

( $\Delta^{13}\text{C}_{\text{d-c}}$ ) between the plant diet and the bone collagen of wild herbivores is widely suggested to be around +5 ‰ (Ambrose & Norr, 1993; Sullivan & Krueger, 1981; van der Merwe, 1989; Vogel, 1978). In turn, lipids in animals and also plants are generally depleted in  $\delta^{13}\text{C}$  with respect to proteins and carbohydrate, so that isotope mass balance of the organism is maintained (DeNiro & Epstein, 1978).

In the case of a herbivore, who exclusively consumes  $\text{C}_3$  plants with a mean  $\delta^{13}\text{C}$  value of -26.5 ‰, the bone collagen of the animal would exhibit a  $\delta^{13}\text{C}$  of -21.5 ‰ (e.g., Krueger & Sullivan, 1984). On the other hand, the collagen  $\delta^{13}\text{C}$  of exclusive  $\text{C}_4$  plant consumers would range around -7.5 ‰, since the mean  $\delta^{13}\text{C}$  of  $\text{C}_4$  plants is found around -12.5 ‰. Hence, the  $\delta^{13}\text{C}$  spacing between  $\text{C}_3$  and  $\text{C}_4$  plants is passed on to the next trophic level, which can be used to distinguish between the consumers of  $\text{C}_3$  and  $\text{C}_4$  plants (e.g., Cerling *et al.*, 1999).

This difference between  $\text{C}_3$  and  $\text{C}_4$  plant feeders is also reflected in the body of a secondary consumer. There is a relatively small offset between the  $\delta^{13}\text{C}$  in the collagen of an exclusive carnivore and that of its prey of approximately +1 to +2 ‰ (Bocherens & Drucker, 2003; Lee-Thorp, 2008). In the case of omnivorous species it is more complicated to comprehend how the isotopic composition of the overall nutrition is composed because their diet comprises all three macronutrients originating from different diet sources, carbohydrates (mainly from plants), protein and lipids (mainly from animal foods).

The collagen formed in the body of a consumer, is predominantly composed of non-essential amino acids (the three prevalent AAs in collagen – glycine, proline and alanine – comprise over 50 % of the AA-residues in collagen). Non-essential AAs can in principal be synthesized by the body using dietary fractions other than protein. To a smaller extent, collagen is composed of essential amino acids, which have to be obtained from dietary protein and account for 18 % of the carbon in collagen (Ambrose & Norr, 1993; Schoeninger *et al.*, 1989, also see Section 1.4.3). However, the  $\delta^{13}\text{C}$  in collagen is known to reflect mainly the isotopic composition of the protein fraction in the diet (Ambrose & Norr, 1993; Tieszen & Fagre, 1993). This is because carbon is preferentially routed from dietary protein to collagen. Ambrose & Norr (1993) for instance, found that even for diets with a protein content as low as 5 %, carbohydrates and lipids contributed only 49 to 58 % of the carbon in collagen and concluded that the isotopic composition of the non-protein portion in the diet was substantially underestimated in collagen  $\delta^{13}\text{C}$  values. Hence, small contributions of low-protein foods e.g., a small  $\text{C}_4$  plant portion in an omnivorous  $\text{C}_3$  diet, might not be detectable via collagen  $\delta^{13}\text{C}$  values (e.g., Ambrose & Krigbaum, 2003). Nevertheless,  $\delta^{13}\text{C}$  can be used to distinguish between diets mainly based on  $\text{C}_3$  or  $\text{C}_4$  resources and in case that herbivores feeding on  $\text{C}_4$  plants are consumed by the examined omnivores, a  $\text{C}_4$  signal should be visible in their collagen even when the contribution was small.

However, the input of marine resources into the diet causes the  $\delta^{13}\text{C}$  of a consumer to increase in a similar way than a  $\text{C}_4$  component would. This can be understood by the frequently higher  $\delta^{13}\text{C}$  values of marine primary producers with respect to terrestrial  $\text{C}_3$  plants, which are passed on to marine organisms consuming them. For example, in a detailed survey of carbon and nitrogen isotopic compositions in animals

Schoeninger & DeNiro (1984) determined a mean  $\delta^{13}\text{C}$  of  $(13.5 \pm 2.1) \text{‰}$  in marine animals (fish, mammals and birds). Because of their high protein content, marine animal products will be prominently reflected in the consumer collagen.

Hence, there are several reasons for a change in  $\delta^{13}\text{C}$  values.  $\text{C}_4$  resources in the diet cause the  $\delta^{13}\text{C}$  value to rise. A similar effect is observed when marine foods are consumed and furthermore, an increase in trophic level can lead to a slight elevation of  $\delta^{13}\text{C}$  values. It cannot be distinguished between these causes solely by the  $\delta^{13}\text{C}$  value of a consumer. If none of the possible reasons for elevated collagen  $\delta^{13}\text{C}$  values can be ruled out e.g., due to an inland situation or the absence of  $\text{C}_4$  plants in a certain region, the nitrogen isotopic composition of bone collagen can help to identify the respective input as marine or  $\text{C}_4$ .

### 1.4.2 Nitrogen Stable Isotope Signatures in Food Webs

The biggest reservoir of nitrogen on earth is the atmosphere, which consists to a large extent of gaseous  $\text{N}_2$  with a constant isotopic composition ( $\delta^{15}\text{N} = 0 \text{‰}$  per definition) (Mariotti *et al.*, 1981). This reservoir serves as the the nitrogen source for plants capable of nitrogen fixation. The majority of nitrogen-fixing plants are members of the legume family e.g., clover, peas or beans. Such plants coexist in symbiosis with bacteria capable of reducing atmospheric  $\text{N}_2$  to  $\text{NH}_4^+$ , so called rhizobia, which are hosted in the root nodules of the plant. Generally, the supply with nitrogen is the limiting factor in the fixation reaction, so that almost all available nitrogen is converted, leading to rather small net fractionations (e.g., Peterson & Fry, 1987). Hence, nitrogen-fixing plants exhibit  $\delta^{15}\text{N}$  values around  $0 \text{‰}$  similar to nitrogen in the atmosphere (e.g., Delwiche & Steyn, 1970). Terrestrial plants that cannot fix nitrogen have to obtain the nitrogen necessary for protein synthesis by  $\text{NO}_3^-$  and  $\text{NH}_4^+$  from the soil. Therefore, their nitrogen isotopic composition is usually closer to that of total soil-nitrogen (e.g., Peterson & Fry, 1987), which is frequently more positive than atmospheric nitrogen (Delwiche & Steyn, 1970; Rennie *et al.*, 1976). Variation in  $\delta^{15}\text{N}$  of soils and plants occurs due to dependence on environmental conditions like e.g., water availability or salinity (e.g, Handley *et al.*, 1999; Karamanos *et al.*, 1981).

In a compilation of published  $\delta^{15}\text{N}$  values in plant organic matter, Schoeninger & DeNiro (1984) determined a mean value close to  $(1 \pm 2) \text{‰}$  and  $(3 \pm 3) \text{‰}$  for terrestrial  $\text{N}_2$  fixers and non- $\text{N}_2$  fixing plants respectively. Values for marine algae and phytoplankton were significantly more enriched in  $^{15}\text{N}$  and scattered around a mean of  $(7 \pm 2) \text{‰}$ . This is due to the large net fractionations associated with nitrification and denitrification processes in the oceans (Peterson & Fry, 1987; Price *et al.*, 1985, and literature cited there).

Plant  $\delta^{15}\text{N}$  values are, however, influenced by the application of manure or mineral fertilizers for the cultivation of crops. Animal manure shows significantly higher  $\delta^{15}\text{N}$  values than atmospheric  $\text{N}_2$ , whereas nitrogen in mineral fertilizers exhibits  $\delta^{15}\text{N}$  values closer to atmospheric nitrogen. Therefore, substantial differences can be found between  $\delta^{15}\text{N}$  values of plants grown on manured land and plants from soils treated with mineral fertilizers or from unfertilized areas (see e.g., Bogaard *et al.*,

2007; Bol *et al.*, 2005; Senbayram *et al.*, 2008; Watzka *et al.*, 2006).

Experiments with animals raised under controlled conditions, confirmed that the nitrogen in the body tissue of a consumer is correlated to the nitrogen isotopic composition of the respective diet (DeNiro & Epstein, 1981). The nitrogen for the synthesis of body protein (e.g., collagen) in a consumer has to be derived from food protein, since carbohydrates and lipids do not contain any nitrogen. However, with every trophic level (from primary producers to primary consumers and secondary consumers) there is an increase of +3 to +5 ‰ of collagen  $\delta^{15}\text{N}$ , in terrestrial as well as in marine ecosystems (Bocherens & Drucker, 2003; Minagawa & Wada, 1984; Schoeninger & DeNiro, 1984). This so called "trophic level effect" originates from the discrimination against  $^{15}\text{N}$  during urea synthesis. While the depleted urinary nitrogen is excreted, other nitrogen pools in the body have to be  $^{15}\text{N}$  enriched compared to the diet (Minagawa & Wada, 1984; Steele & Daniel, 1978).

Hence, the  $\delta^{15}\text{N}$  can be used to distinguish between organisms from different trophic levels like primary consumers and secondary consumers within a food web (e.g., Bocherens & Drucker, 2003). It is however difficult to compare isolated values from different geographical regions, since  $\delta^{15}\text{N}$  also depends on climatic factors. There is a tendency of higher  $\delta^{15}\text{N}$  values for food webs in hot, arid areas compared to cool, wet ones (see the discussion in Ambrose, 1991).

In aquatic food webs (marine and freshwater), higher  $\delta^{15}\text{N}$  values can generally be observed compared to terrestrial situations. One reason for this is the  $^{15}\text{N}$  enriched source nitrogen of the marine primary producers, which is passed on to the consumers. Furthermore, the food chains in aquatic systems are longer (there is at least one additional trophic level) compared to terrestrial ecosystems (Schoeninger & DeNiro, 1984). Thus, nitrogen isotopic composition can be used to identify the utilization of marine foods by consumers, especially in combination with elevated  $\delta^{13}\text{C}$  values as demonstrated e.g., by Fischer *et al.* (2007); Keenleyside *et al.* (2009); Müldner & Richards (2007b); Richards & Hedges (1999).

Since the  $\delta^{15}\text{N}$  value offers information about the trophic level of an organism, an obvious thought is to use it for the quantification of the amount of animal protein<sup>1</sup> in human diets. But this is complicated by several factors, which were discussed in detail by Hedges & Reynard (2007). Important issues covered by this paper, are uncertainties in the  $^{15}\text{N}$  enrichment in humans with respect to their diet and whether this value varies with the type of diet (high protein vs. low protein diets). Also, humans and the local herbivores might have eaten different plants with differing  $\delta^{15}\text{N}$  values, so that  $\delta^{15}\text{N}$  values of humans consuming pure plant diets could deviate from those of the herbivorous animals. Furthermore,  $\delta^{15}\text{N}$  values could have been elevated by manuring or the consumption of freshwater fish. Due to such uncertainties, there is – today – no validated model for the quantitative assessment of animal versus plant foods in human nutrition. However, Ambrose & Krigbaum (2003) pointed out that a higher  $\delta^{15}\text{N}$  value most likely indicated a higher consumption of animal foods, when individuals from a similar context (e.g., from the same population of an archaeological site) are compared with each other. The comparison of  $\delta^{15}\text{N}$  values within a

---

<sup>1</sup>Meat, egg and milk protein are similar in  $\delta^{15}\text{N}$  (Minagawa, 1992).



population is therefore an approach frequently chosen to investigate differentiation into population subgroups due to cultural, social or gender-related factors as mentioned before. Another application, where the  $\delta^{15}\text{N}$  values are compared (sometimes of individuals differing in age, sometimes the values of one individual determined in tissues representing different time scales), is the assessment of weaning age in infants. This method is based on the elevated  $\delta^{15}\text{N}$  value of a breast-fed child with respect to its mother, which subsequently decreases to "adult-like" values after completion of the weaning (e.g., Fuller *et al.*, 2003; Richards *et al.*, 2002; Schurr & Powell, 2005).

### 1.4.3 The Sample Material: Bone Collagen

When  $\delta^{13}\text{C}$  and  $\delta^{15}\text{N}$  values are to be determined in human and animal remains from archaeological contexts, this is usually done in bone collagen. Apart from special cases like e.g., mummies, other body tissues than bone are usually not preserved during burial due to taphonomic changes and collagen is well suited as material for palaeodietary reconstructions for several reasons, which become clear when the complex composition of bone and collagen is studied.

Bone is a mineralized connective tissue consisting to a major extent of bone matrix composed of inorganic and organic compounds and to a smaller extent of bone cells (osteoprogenitor cells, osteoblasts, osteocytes, bone lining cells and osteoclasts). The cells responsible for the formation of the bone matrix are the osteoblasts. They descend from osteoprogenitor cells and later become osteocytes when they are completely surrounded by the matrix, which they have produced. Bone lining cells are inactive osteoblasts covering the bone surface and osteoclasts are responsible for bone resorption. The major constituents of bone are mineral substances, collagen is the second most abundant component (25 %wt.), water accounts for 5-10 % of the bone weight, noncollagenous proteins make up around 5 % of the dry bone weight and there are small proportions accounted for by lipids, vascular elements and cells. During bone formation, the organic part of the matrix (osteoid) is secreted first and subsequently mineralized. Osteoid mainly consists of collagen (90-95 %wt.), the rest is composed of non-collagenous proteins like osteonectin or osteocalcin, glycosaminoglycans and a small amount of lipoproteins. The major part of the inorganic matrix consists of a calcium phosphate similar to hydroxyapatite  $\text{Ca}_{10}(\text{PO}_4)_6(\text{OH})_2$  and is often referred to as bone apatite. Bone apatite contains many impurities like for example  $\text{CO}_3^{2-}$ ,  $\text{Mg}^{2+}$ ,  $\text{K}^+$  and  $\text{F}^+$ . (See e.g., Boskey, 1999; Junqueira & Carneiro, 1996; Ortner, 2003; Schoeninger & Moore, 1992, .)

Collagens are the most abundant proteins in the human body constituting a main part of connective tissues and are responsible for the flexibility of these tissues. They can be grouped into seven families according to their supramolecular assembly. In cartilage and bone the family of the fibril-forming or fibrillar collagens is dominant. Five types of collagen differing in their molecular composition are members of the fibrillar collagen family (type I, II, III, V and XI). But the key feature of all collagens is the structure of a right handed triple-helix composed of three polypeptide chains. The structural requirement for the formation of the triple-helix is the repeating amino acid sequence Gly-X-Y in each polypeptide chain. Therefore, a Glycine (Gly) residue

occupies every third position. X and Y are often proline and/or hydroxyproline, whose additional OH-group is essential for the formation of intramolecular hydrogen bonds. Within the collagen molecule, there are also non-collagenous domains, which are not assembled to a triple-helical structure. But in fibrillar collagens, the major part of the molecule is arranged in a triple-helical structure. Bone collagen mainly consists of type I and type V heterofibrils, but also other collagens like types VI or XIV are found to a minor extent. For more detailed information see e.g., Brinckmann (2005); Engel & Bächinger (2005); von der Mark (1999).

The advantages of collagen as a sample material for palaeodietary studies are thus, its high abundance in bone and its good stability and low solubility in water, which is why it is likely to be preserved in ancient bones. As a protein, it contains both, carbon and nitrogen, in sufficient amounts to allow the determination of  $\delta^{13}\text{C}$  and  $\delta^{15}\text{N}$  values (e.g., Schoeninger & Moore, 1992).

Another component of bone occasionally used in diet reconstructions is the carbonate in the mineral fraction.  $\delta^{13}\text{C}$  values of carbonate in bone apatite were found to reflect the isotopic composition of the whole diet including carbohydrates, lipids and protein, whereas carbon in collagen is mainly routed from dietary protein (Ambrose & Norr, 1993; Tieszen & Fagre, 1993). Bone carbonate is however vulnerable to diagenetic alterations, since recrystallization may lead to the inclusion of foreign ions like e.g., carbonates from the surrounding environment (Lee-Thorp, 2008).

Even though collagen is a very stable molecule it can be degraded depending on the environmental conditions like pH, temperature or moisture, during burial or storage of the bone. During this time, the bone may also take up organic contaminants like humic acids from the soil. These substances are, however, effectively removed by suitable sample preparation techniques (See Section 4.1). The process of bone diagenesis often starts with the partial dissolution of the mineral phase, which is protecting the collagen. In a more porous bone, collagen will be exposed to microbial attack. This process, also called biodegradation, is the most frequent cause for bone deterioration and takes place at the highest rate when the environmental pH is near neutral. Dissolution of bone mineral is accelerated by low pH and high water availability. Under such conditions collagen can also be lost due to chemical mechanisms, since exposure to acid will lead to hydrolysis and the solubilization of collagen. High temperatures will furthermore increase the loss of collagen (see e.g., Collins *et al.*, 2002; Hedges, 2002; Lee-Thorp, 2008, and literature cited there).

Frequently, collagen molecules seem to remain structurally intact until only a small amount of collagen is left in the bone (Ambrose, 1990; van Klinken, 1999). It is however important to assess the state of preservation of a bone sample prior to dietary studies in order to avoid the inclusion of samples that have not retained the original isotopic composition. Therefore several quality parameters for collagen extracted from archaeological bone samples are now generally accepted. These parameters are the collagen yield of the extraction procedure, the carbon and nitrogen content of the extracted collagen and its atomic carbon to nitrogen ratio. It is recommended to reject samples that yielded less than 1 %wt. of collagen from further analysis (van Klinken, 1999). DeNiro (1985) suggested to consider only collagen samples with atomic C/N ratios within the range of 2.9 and 3.6, since this range encompasses the

values found in a large variety of modern animal and human samples. Schoeninger *et al.* (1989) found that gelatin samples with C/N ratios between 2.6 and 3.4 had amino acid profiles similar to a collagen standard. According to van Klinken (1999), intact collagen samples should exhibit carbon contents around  $(35 \pm 9) \%$ wt. and nitrogen contents between 11 and 16 %wt., Ambrose (1990) found C and N contents of 15.3 to 47.0 %wt. and 5.5 to 17.3 %wt., respectively, in modern animals. The low values are most likely due to the presence of inorganic salts (remnants of the extraction procedure). Usually all of the mentioned quality parameters are determined after the collagen extraction and in the course of the EA-IRMS measurement of a collagen sample (see Section 3.2.2).

When diet interpretations are made, it is also important to know the turnover rate of the analyzed material and thus the time frame in the life of an organism, for which the diet information is recorded. Carbon and nitrogen isotopic compositions in collagen from human bone reflect the diet information gathered over a long period of an individual's life (at least the last 10 years before death), since the mean turnover rate of the whole adult skeleton was estimated (using activity rates of the basic multicellular unit<sup>2</sup>) to be  $\sim 10 \%$  per year (Manolagas, 2000; Parfitt, 1994). This is an averaged value derived from the turnover rates of cortical bone ( $\sim 4 \%$  per year) and trabecular bone ( $\sim 28 \%$  per year), which represent approximately 25 % (cortical bone) and 75 % (trabecular bone) of the entire skeleton.

Turnover rates have also been investigated by the measurement of  $^{14}\text{C}$  contents in human bone collagen (Hedges *et al.*, 2007; Libby *et al.*, 1964; Stenhouse & Baxter, 1979; Wild *et al.*, 2000). These studies confirm long turnover times for human bone collagen. For example, Hedges *et al.* (2007) found age dependent rates of 3 to 4 % in femoral bone from adult females and of 1.5 to 3 % for adult males, during adolescence turnover rates were however substantially higher. They concluded that femoral collagen represented material synthesized over a period longer than 10 years and even included a portion from adolescence.

Collagen can also be extracted from tooth dentin, which is a biologically static tissue that is not remodeled once it is laid down (Borggreven *et al.*, 1979; Dupras & Tocheri, 2007; Richards *et al.*, 2002). Since the formation periods of the single teeth are well established (e.g., Smith, 1991a), diet information from different time periods in the early life of an individual is accessible via the analysis of collagen from different teeth (see also Section 4.3.2). After the growth period of a tooth, in which the primary dentin is formed, smaller amounts of secondary and tertiary dentin are deposited (Cook *et al.*, 2006). Furthermore, tooth cementum is deposited throughout life, but it is easily removed prior to collagen extraction, since it constitutes the outermost layer of the root. Therefore the isotopic composition of tooth collagen is mainly determined by that of primary dentin (Schoeninger & Moore, 1992).

---

<sup>2</sup>The basic multicellular unit (BMU) is responsible for the bone replacement process known as "remodeling". It consists of osteoclasts and osteoblasts as well as connective tissue, blood vessels and nerves. Its dimensions are 1 to 2 mm in length and 0.2 to 0.4 mm in width and about 1 million BMUs are operating in a human adult at any moment (see e.g., Manolagas, 2000; Parfitt, 1994).



## 2 Materials

Bone samples from animals and human individuals originating from the prehistoric necropolis in Gemeinlebarn and from the burial grounds of the Early Medieval settlement of Thunau/Gars am Kamp were analyzed in the course of the present work. In the following, a brief overview of the archaeological sites will be given and the process of sample selection is described.

### 2.1 Gemeinlebarn

The municipality of Gemeinlebarn is situated in the province of Lower Austria, 4.5 km east of the city Traismauer and approximately the same distance south of the river Danube. Its location is ~45 km west of the Austrian capital Vienna (Wien) and ~20 km north-east of the province capital St. Pölten. See Figure 2.1 for a map of the area.

#### 2.1.1 The Archaeological Site of Gemeinlebarn

The region between Traismauer and St. Pölten along the river Traisen is an important area for the investigation of central European prehistory due to its great number of archaeological finds. They document human activity in this area from the Upper Palaeolithic until the Roman Empire time period. Especially the period of the Early Bronze Age (around 2300 to 1600 BC in the region of Austria) is prominently represented by several grave fields, of which almost 2800 burials were discovered by 1994 (see e.g., Neugebauer, 1991; Neugebauer *et al.*, 1987, 1994).

In Gemeinlebarn, already in the late 19<sup>th</sup> and the beginning of the 20<sup>th</sup> century a large number of prehistoric burials located at several find spots (numerated from A to E) was examined in systematic excavations (e.g., Szombathy, 1929). In 1973, further inhumations were discovered in a gravel pit only 300 m distant from find spot A. In this area, which was named the "Necropolis F", a total of 257 inhumation graves and one cremation burial were recovered between 1973 and 1981 (see Neugebauer, 1991, p. 1-2,7). Samples of the human remains from this burial ground, dated to the late phase of the Early Bronze Age, were subjected to the palaeodietary investigations presented here.

#### 2.1.2 The Investigated Bone Samples from Gemeinlebarn F

In the course of the archaeological and anthropological examinations of the skeletal material recovered from Gemeinlebarn F, aspects of social and socio-biological differ-



**Figure 2.1:** Geographical situation of Gemeinlebarn.

entiation were studied (Heinrich & Teschler-Nicola, 1991; Teschler-Nicola, 1989). For this, a classification into social categories was adopted from the statistical evaluation of the data using cluster analysis, which was undertaken by Stadler (1991). Cluster analysis comprises a range of multivariate, statistical procedures for data analysis, with the purpose of grouping data points with similar "properties" together (see e.g., Backhaus *et al.*, 2006; Härdle & Simar, 2007). In the investigated case, the data points were the 258 buried individuals and the considered properties were the character and abundance of associated grave goods, the grave dimensions and the degree of deprivation in prehistoric times as well as sex and age of each individual. The optimal number of clusters was calculated as 11, and the formation of these groups was interpreted as an initial grouping into the large categories of males (clusters 1,2,6 and 7), females (clusters 3,4,5 and 11) and children (clusters 8,9 and 10), which were then further split into subgroups mainly caused by social differences.<sup>1</sup> Clusters 1 and 7 comprise mostly male individuals of high social status, whereas the males assigned to cluster 2 had almost no associated burial objects and the grave dimensions were clearly smaller than for clusters 1 and 7. A less pronounced differentiation into rich and poor was observed for the females. Still, members of clusters 3 and 5 could be characterized as more wealthy than those of clusters 4 and 11. In total, the majority of the individuals of Gemeinlebarn F was categorized as poor (55 females and 54 males). According to the cluster analysis, approximately 35% of the investigated burials belonged to wealthier individuals (35 females and 25 males).

Based on this categorization into social strata, the anthropological examination revealed a statistically significant correlation between the social status and the body height as well as other measurements of the post cranium of the male individuals (Teschler-Nicola, 1989). As possible reasons for these effects, of which the mean difference in body height of  $\sim 3$  cm between the rich group ( $\bar{x} = 169.2$  cm) and the poor group ( $\bar{x} = 166.4$  cm) was the most obvious, social selection mechanisms and envi-

<sup>1</sup>This is only applicable to the adults. For the children, the sub groups were generated according to sex and age.

ronmental modification like for instance, a more favorable nutrition for the wealthier individuals are given.

For the females, there was less substantive evidence for socio-biological differentiation in the collected anthropological data. Although two measures of the post cranium were significantly larger for the wealthy women, no significant difference in body height was observed between the rich and the poor females.

These results led to the hypothesis, that the differences between the social groups – if they were caused by variation in nutrition – could also be reflected in the bone collagen  $\delta^{13}\text{C}$  and/or  $\delta^{15}\text{N}$  values of the individuals. Therefore, a major purpose of the palaeodietary investigations was to test for this hypothesis. Hence, a suitable sample set for this investigation comprising 7 rich males and 9 rich females as well as 21 poor males and 22 poor females was selected depending on the availability of the specimen (see Table 4.11). In total, this number of samples represents 35 % of the adults of the Necropolis F, for whom the sex could be determined (169 individuals). One specimen within the selection belonged to an individual with indeterminate sex (sample ID 5).

Whenever possible, rib samples were chosen for the collagen extraction. In two cases, long bone fragments were taken and in three cases, finger bones had to be used.

At the necropolis F of Gemeinlebarn, only a very small number of animal bones was recovered during the excavations (Neugebauer, 1991, p. 45). Therefore, the animal samples for the palaeodietary reconstruction were taken from contemporaneously used sites in the vicinity of Gemeinlebarn i.e., the Early Bronze Age cemeteries of Pottenbrunn and Franzhausen I. The location of both sites is plotted in Figure 2.1. But still, the number of recovered animal remains was small. In total, 10 samples of animal bones could be obtained for the carbon and nitrogen stable isotope analysis, comprising 5 different species (cattle, goat/sheep, pig, a dog and presumably a fox). All animal and human bone samples were kindly provided by the Natural History Museum of Vienna.

## 2.2 Thunau/Gars am Kamp

The second archaeological site, from which bone samples were examined, is the fortified hill-top settlement of Thunau/Gars am Kamp. It is located at the river Kamp in the northern part of the province Lower Austria, approximately 90 km north-west of the Austrian capital Vienna and around 30 km north of the river Danube. Figure 2.2 shows a map of the region around Gars am Kamp.

### 2.2.1 The Archaeological Site of Thunau

The archaeological find spot of Thunau is known since the late 19<sup>th</sup> century. But only in 1965, extended excavations were started under the supervision of Herwig Friesinger and later, from 1993 onward, were continued under the direction of Erik Szameit (both Department for Prehistoric and Medieval Archaeology, University of Vienna) (e.g., Friesinger & Friesinger, 1975; Szameit, 1995).

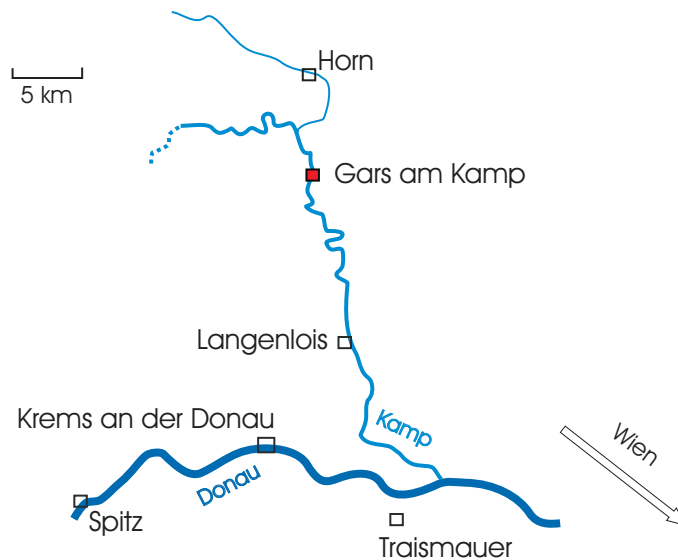


**Figure 2.2:** Geographical situation of Thunau/Gars am Kamp.

A general description of the Schanzberg (in German language) can e.g., be found in Friesinger & Friesinger (1991). There, the earliest settlement traces at the site, which originate from the Late Neolithic, are described. Further finds suggest a discontinuous occupation of the site from the Late Bronze Age to the Roman Empire. However, the majority of the finds belong to the Early Medieval settlement (human bone samples from this settlement were dated to a time period between the 7<sup>th</sup> and the 11<sup>th</sup> century AD by <sup>14</sup>C dating at VERA, **V**ienna **E**nvironmental **R**esearch **A**ccelerator). A detailed description of the settlement chronology and structure during Early Medieval times is given by Herold (2008). In Nowotny (2011), the "Obere Holzwiese" (see below) is investigated in detail.

The archaeological site comprises the fortified hill-top settlement with a manor house and a grave field as well as several isolated burials, herein after referred to as



the "Schanzberg", and remains of a riverine settlement including numerous burials in the valley of the Kamp. In the valley area, clear evidence for large-scale handicraft (forging, pottery or textile processing) and agricultural activities was documented (Obenaus *et al.*, 2005). The current view is therefore that this production orientated area provided the supply of the fortified hill-top settlement with necessary goods (Obenaus & Eichert, 2009). It might thus be possible, that the inhabitants of these two separated areas represent different social strata. Hence, a major goal of this work was to study carbon and nitrogen stable isotope ratios in bones from these locations in order to identify a purported social stratification reflected in diet. Another motivation was to examine whether differences in the subsistence between males and females existed.

### 2.2.2 The Investigated Bone Samples from Thunau

A total of 41 human bone samples and 27 animal samples assigned to the Early Medieval period in Thunau were investigated using carbon and nitrogen stable isotope analysis. The complete list of all samples is given in Tables 4.8 and 4.9 in Section 4.3. 20 bone specimen originated from burials recovered at the Schanzberg and 19 were obtained from the excavation in the valley settlement. Within the Schanzberg area, several find spots can be distinguished. Bone samples found at the "Herrenhof" (the manor house area), "obere Holzweise", "untere Holzweise", "Schanze" and "Saugrube" were analyzed. The location of the individual find spots of the Schanzberg area is shown in Figure 2.3. Samples specified as originating from "Goldberggasse", "Schimmelsprunggasse" and "Asenbaumacker" in Table 4.9 are attributed to the valley settlement. The human samples were selected from the recovered skeletal remains of 373 individuals and comprise 21 males, 18 females and 2 children.

Where possible, ribs were sampled. When these were not preserved (in three cases), cranial, metatarsal or finger bones were used instead. In addition, permanent teeth of two individuals were analyzed.

A large number of animal remains was excavated at the site and a part of this material was investigated archaeozoologically by Kanelutti (1990). According to this examination, cattle (*Bos taurus*) was the most frequent domesticated animal species followed by pigs (*Sus scrofa domestica*). In the Medieval period, sheep (*Ovis orientalis aries*) and goat (*Capra aegagrus hircus*) were mainly kept for their milk and wool. The meat of horses (*Equus ferus caballus*), which were kept as mounts and draft animals, was usually not consumed. Wild animals like red deer (*Cervus elaphus*), wild boar (*Sus scrofa*) and roe deer (*Capreolus capreolus*) were frequently hunted and also several remains of brown bears (*Ursus arctos*) were found.

A broad range of animal species (depending on the availability of bone samples) was included in the palaeodiet investigation (see Table 4.8) and it was taken care to select domesticated as well as wild animals in order to get a realistic basis for the human diet interpretation. Apart from one sample (sample ID 33 in Table 4.8), which originates from the valley area, all animal bones were recovered at the Schanzberg (personal communication Hajnalka Herold, Institute for Prehistoric and Medieval Archaeology, University of Vienna). The samples were selected from find spots with

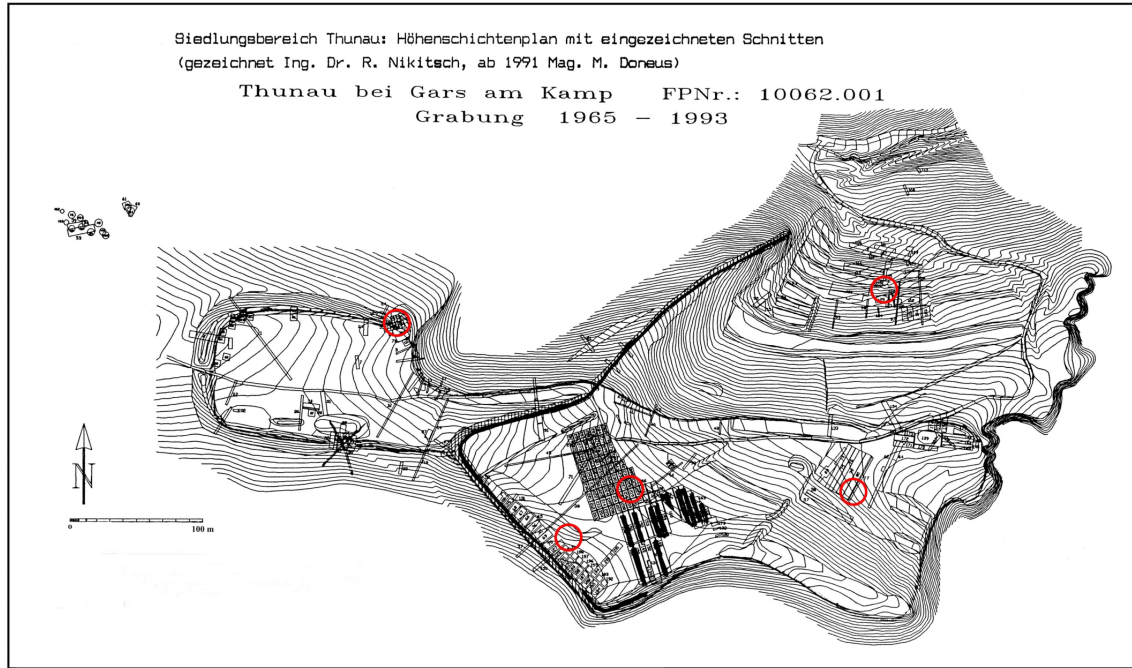


**Figure 2.3:** Map of the Early Medieval hill-top settlement in Thunau/Gars am Kamp. The red circles indicate the different find spots (from left to right: Schanze, Saugrube, Herrenhof/obere Holzweise, Kirche, untere Holzweise).

a clear Early Medieval context. However, it cannot completely be ruled out that in isolated cases a sample from the Bronze Age was included in the analysis. But it is assumed that the carbon and nitrogen stable isotope ratios of animal bone collagen from the Bronze Age and Early Medieval times are not significantly different. The animal samples with IDs from 109 to 127 in Table 4.8 were kindly provided by the Institute for Prehistoric and Medieval Archaeology, University of Vienna. All other animal and human samples originate from the Natural History Museum of Vienna.

## 3 Methods

### 3.1 Bone Collagen Preparation

Several procedures for the extraction of collagen from archaeological bone material have been published to date. Most of them are based on the method introduced by Longin (1971), who treated cleaned bone powder with diluted hydrochloric acid to eliminate most inorganic substances ("demineralization"). Another effect of this treatment is the hydrolysis of some collagen cross links, which facilitates collagen dissolution in the next step (e.g., Babel, 1996). The acid treatment leaves a residue containing organic compounds, from which collagen is extracted by heating in acidified water ("solubilization" or "gelatinization"). During the solubilization step the collagen is denatured and hydrolyzed to some extent and thus becomes soluble (e.g., Chisholm *et al.*, 1983). The dissolved collagen can be recovered by drying in an oven at temperatures up to 95°C or freeze drying. In a strict sense, the extracted material is probably a mixture of polypeptide chains with different lengths originating from collagen (Semal & Orban, 1995), but may also contain smaller amounts of non-collagenous proteins (Schoeninger *et al.*, 1989) and other organic and inorganic substances (Ambrose, 1990). Still, in the literature the term "collagen" is commonly used in this context. Alternatively, the extract is often referred to as "gelatin", which is a denatured and partially hydrolyzed form of collagen (e.g., Djagny *et al.*, 2001; Nicolas-Simonnot *et al.*, 1997).

A common modification of the Longin method is a treatment step with NaOH solution after the demineralization in order to remove humic acids (e.g. DeNiro & Epstein, 1981) and some lipids (Ambrose, 1990), since triacylglycerides are saponified by NaOH yielding water soluble glycerol and fatty acid salts. Both, humic acids and bone lipids, have  $\delta^{13}\text{C}$  values more negative than collagen (e.g., Ambrose, 1990; Liden *et al.*, 1995) and thus should be removed during extraction. Schoeninger *et al.* (1989) extracted collagen from archaeological bone samples using a method with a NaOH step and compared the amino acid profile of the extract with that of a commercially available bovine collagen standard. The standard and the extract had almost identical profiles with a glycine content of approximately 30 % and a hydroxyproline to proline ratio of  $\sim 0.6$ . These features are characteristic for collagen.

Concerns have been expressed about possible alteration of the isotopic composition of collagen and reduction of the extraction yield by NaOH (e.g., Chisholm *et al.*, 1983). An alternative to the NaOH treatment was suggested by Brown *et al.* (1988). This method comprises an ultrafiltration step after the solubilization, where molecules larger than 30 kDa<sup>1</sup> are selected using filter tubes with a special membrane.

---

<sup>1</sup>The unit Dalton (Da) is equivalent to the unified atomic mass unit (u).

The membrane has pores with well defined sizes and therefore the sample molecules can be separated into two fractions (higher and lower than 30 kDa) when the sample solution is driven through the membrane (e.g., by centrifugation). The aim of this procedure is to get rid of lower molecular weight contaminants like humic acids and to extract only the larger peptides, which are more likely to represent intact collagen.

In a comparison of the ultrafiltration method with three other methods containing NaOH steps, Liden *et al.* (1995) investigated the effect of NaOH treatment on the composition of the extract. They found NaOH to decrease the yield and to change the amino acid composition of the extracted collagen, although this did not alter the  $\delta^{13}\text{C}$  value. Also, they concluded that NaOH did not sufficiently remove lipids.

In a similar study Jørkov *et al.* (2007) examined three extraction methods, a modified Longin protocol with a NaOH step, a method applying ultrafiltration and a variation of the second method, where the ultrafiltration step was left out. They found slightly differing  $\delta^{13}\text{C}$  values between the three methods, whereas the  $\delta^{15}\text{N}$  values were not affected. Ultrafiltration resulted in a substantial yield reduction, since the fraction containing the molecules smaller than 30 kDa was rejected. Contrary to the results of Liden *et al.* (1995), NaOH did not have a yield reducing effect.

In view of these findings, an investigation of several selected collagen extraction methods was considered necessary to find a suitable method for the preparation of collagen samples. The chosen approach is pointed out below.

#### 3.1.1 Comparison of Collagen Extraction Methods

In order to establish a sample preparation method for archaeological bone specimen, several collagen extraction procedures based on published methods were compared with each other. Thereby it was investigated, if different preparation steps affected the quality of the extracted material or its  $\delta^{13}\text{C}$  and  $\delta^{15}\text{N}$  values. Collagen was extracted from a  $\sim 5800$  year old cattle bone (Radius), with the different extraction methods given in Table 3.1. Prior to the extraction, the bone was mechanically cleaned by scraping its surface with a scalpel and then ground to a coarse powder using mortar and pestle. Approximately 500 mg of the bone powder were used for one extraction.

The starting point for the comparison (**Method 1** described in Table 3.1) was a method adopted from the sample preparation laboratory of the Accelerator Mass Spectrometry (AMS) facility "VERA" (Vienna Environmental Research Accelerator, University of Vienna, Faculty of Physics). It is in essence the laboratory's standard extraction method for the  $^{14}\text{C}$  dating of bone (see e.g., Wild *et al.*, 2007, 2010) and is a modified form of Longin's collagen extraction method with a NaOH step followed by an additional treatment with acid to remove potentially present bicarbonates and carbonates formed by the reaction of NaOH with atmospheric  $\text{CO}_2$ .

**Table 3.1:** Preparation steps of the seven collagen extraction methods investigated in the method comparison. (Abbreviations: o.n.=overnight, h=hour(s), d=day(s), sol.=solution, MWCO=molecular weight cut off)

Preparation Step	Method 1	Method 2	Method 3	Method 4
Deminerallization	1 M HCl, o.n.	1 M HCL, o.n.	0.5 M HCL, o.n.	1 M HCl, 20min
NaOH	0.1 M NaOH, 1-2 h	0.1 M NaOH, 1-2 h	-	0.125 M NaOH, 20 h
HCl	1 M HCl, 10 min	-	-	-
Solubilization	pH=3 sol., 90-95°C, 2 d	pH=3 sol., 90-95°C, 2 d	pH=3 sol., 70-75°C, 20 h	pH=3 sol., 90-95°C, 10 h
Ultrafiltration	-	-	-	-
Drying	90-95°C	90-95°C	90-95°C	90-95°C
Preparation Step	Method 5	Method 6	Method 7	
Deminerallization	0.5 M HCl, o.n.	0.5 M HCL, o.n.	0.5 M HCL, o.n.	
NaOH	-	0.1 M NaOH, 2 h	0.1 M NaOH, 2 h	
HCl	-	-	-	
Solubilization	pH=3 sol., 70-75°C, 20 h	pH=3 sol., 70-75°C, 20 h	pH=3 sol., 70-75°C, 20 h	
Ultrafiltration	MWCO 30 kDa	MWCO 30 kDa	-	
Drying	90-95°C	90-95°C	90-95°C	

### 3 Methods

After each acid or base treatment the residue was rinsed with ultra-pure water (*Gen-Pure* ultra-pure water system, *TKA Wasseraufbereitungssysteme*) until the supernatant, obtained by centrifugation, reached an almost neutral pH-value. Solubilization was accomplished by heating the residue in water, acidified with HCl to pH=3, for two days. Collagen was then recovered from the supernatant by evaporation at  $\sim 90^\circ\text{C}$ .

**Method 2** is a modified version of Method 1, where the second HCl step was left out and all centrifugation steps were replaced by filtration using sintered glass frit filter funnels (pore sizes: 16-40  $\mu\text{m}$  and 10-16  $\mu\text{m}$ ) with Teflon stopcocks and vacuum flasks as specified in Schoeninger & DeNiro (1984) and Ambrose (1990). These filter funnels were used in all subsequently described extraction methods.

**Method 3** comprises the main steps of Longin's method. The concentrations of the used solutions and timings for the steps etc. are again given in Table 3.1.

**Method 4** was carried out according to specifications by Ambrose (1990), who in principal adopted a method described by DeNiro & Epstein (1981) and Schoeninger & DeNiro (1984).

In **Method 5**, which is based on a procedure given in Müldner & Richards (2005), an ultrafiltration step is performed as described by Brown *et al.* (1988). The ultrafiltration tubes (*Vivaspin 15*, 30 kDa MWCO) were cleaned according to Bronk Ramsey *et al.* (2004) in order to remove the humectant coating the filter membrane. After demineralization and solubilization, the solution containing collagen was filtered through PTFE-filters with a pore size of 25  $\mu\text{m}$ . The obtained filtrate was subjected to ultrafiltration yielding two fractions ( $> 30$  kDa and  $< 30$  kDa), both of which were collected and evaporated to dryness. However, evaporation of the  $< 30$  kDa fractions did not yield enough material for measurement.

**Method 6** builds on Method 5 with the addition of a NaOH treatment after the demineralization. **Method 7** is in principle Method 6 with the ultrafiltration omitted.

The necessary amount of acid for the demineralization of the bone powder was estimated by the following considerations: 10 moles of hydrochloric acid are needed to dissolve one mole of hydroxyapatite (see Equation 3.1). Typically,  $\sim 500$  mg of bone powder were used for one extraction. Even if the whole amount of bone powder was assumed to be hydroxyapatite, it would equal approximately 1 mmol of hydroxyapatite. Thus, 10 mmol of HCl would be necessary to dissolve this quantity of hydroxyapatite. This amount corresponds to 10 mL of 1 M  $\text{HCl}_{(\text{aq})}$ . In order to ensure complete demineralization HCl was added in excess (usually  $\sim 50$  mL).



To test for the completeness of demineralization a complexometric analysis method for  $\text{Ca}^{2+}$  ions, using calconcarboxylic acid was applied. This acid is an azo compound, which forms a red colored chelate complex with calcium ions. It is frequently used as an indicator for the complexometric titration of calcium. The titration method with calconcarboxylic acid described in a brochure by Merck (1963) was modified, so that calcium ions could be detected qualitatively as specified below.

After demineralization, the bone sample is washed with ultra pure water and once again soaked in 1 M  $\text{HCl}_{(\text{aq})}$  for around one hour. The resulting solution is then tested for calcium ions in order to see if any more hydroxyapatite dissolved in the acid solution. Therefore the pH of an aliquot is adjusted to approximately 12 with 1 M  $\text{NaOH}_{(\text{aq})}$  solution in order to remove present magnesium by precipitation, which would otherwise disturb the test. Subsequently a few drops of the test solution (calcancarboxylic acid in methanol) are added to the sample solution. An appearing red color indicates a positive test for calcium ions. Note that also barium and strontium ions are detected in this way. When the solution is colored blue, the test is considered negative.

The sensitivity of this test was determined by applying it to a dilution series containing known amounts of a calcium salt ( $\text{Ca}(\text{NO}_3)_2 \cdot 4 \text{H}_2\text{O}$ ). The solution with the smallest concentration of calcium ions that was tested positive contained 0.01 g/L. Therefore, assuming that in the first step of the test, the demineralized residue is soaked in 25 mL of 1 M  $\text{HCl}$  (the usual procedure), a total amount of approximately 0.25 mg of calcium ions corresponding to 0.63 mg of hydroxyapatite can remain undetected in this volume. This corresponds to  $\sim 0.1\%$  of the amount of bone powder used for the extraction (i.e.,  $\sim 500$  mg). Thus, the sensitivity of the test was considered sufficient to check for the completeness of demineralization.

All of the used demineralization methods were controlled via the test procedure stated above. None of the methods left detectable amounts of calcium ions in the demineralized samples.

Three subsamples of each collagen sample obtained using one of the extraction methods listed in Table 3.1 were measured (each subsample in a separate measurement run) by EA-IRMS, where carbon and nitrogen contents and isotope ratios were determined in one single sample using the "peak jump" mode of the mass spectrometer (see Section 3.3.1). All  $\delta$ -values are reported as mean values of these 3 determinations. The results of the method comparison are presented in detail and discussed in Section 4.1. Briefly, they do not indicate any differences in  $\delta^{13}\text{C}$  and  $\delta^{15}\text{N}$  values of the gelatin extracts produced using the different methods. Furthermore, the collagen quality indicators were within the accepted ranges (given in Section 1.4.3) for all samples. Together, these results show the suitability of all tested methods for the extraction of collagen from bone samples for carbon and nitrogen stable isotope analysis.

As no significant differences between the methods could be found, method 2 was chosen for the manual processing of bone samples, because the glass frit filters used in this method, have been found to be very effective and convenient for the treatment of up to 10 bone samples in parallel.

Since over 140 collagen samples had to be prepared, a semi-automated bone pretreatment system as described by Law & Hedges (1989) was provided by the the VERA laboratory, which allows the processing of up to 24 samples in parallel. For the treatment, each sample is placed in one of the 24 flow-cells closed with PTFE filters (25  $\mu\text{m}$  pore size), through which the different solutions (acid and alkali) are pumped in subsequent steps. The extraction is conducted according to the steps of method 1 with adjusted durations (acid: 8 h; alkali: 2-3 h; acid: 30 min).

The steps of the semi-automated method and the "manual" method 2 are very similar. Therefore, any altering effects of the two methods on the  $\delta$ -values of the treated samples is highly improbable. Still, the automated method was checked for its suitability in the preparation of collagen for palaeodiet studies, even though the system was already established for the preparation of samples for  $^{14}\text{C}$ -dating at the VERA laboratory. This check also served to assure reproducibility of the  $\delta$ -values of the extracted material.

Several bone samples were treated in parallel with both methods. Each sample was separated into aliquots, one of which was treated with the automated method, a second one was processed using method 2. The manual method was repeated with a 3<sup>rd</sup> aliquot in order to get information on the reproducibility of the  $\delta$ -values within a method. Both collagen  $\delta^{13}\text{C}$  and  $\delta^{15}\text{N}$  values of each sample pair (or triple) matched well within their uncertainties. It was therefore assumed, that both methods produced collagen with comparable  $\delta$ -values from one bone specimen.

In the course of this work, the stable isotope laboratory was equipped with a freeze dryer (*Zirbus technology VaCo2* operated with a *BOC Edwards XDS 5* dry scroll pump), since lyophilized collagen, a fluffy voluminous substance, is much easier to handle than the amorphous evaporation product. A small test series with seven collagen samples was performed in order to exclude any contamination sources originating from the new lyophilization equipment and to confirm the better handling of the freeze dried samples (in terms of minimized product loss e.g., due to electrostatically charged product). For this, the seven bone samples were divided into 2 aliquots and processed using method 2. After the solubilization, one aliquot was freeze dried, the other one was evaporated to isolate the collagen. Also here, the  $\delta^{13}\text{C}$  and  $\delta^{15}\text{N}$  values of each sample pair were in agreement within their uncertainties. Hence it was assumed, that  $\delta$ -values of lyophilized collagen samples can be compared with those of samples dried by evaporation (see Section 4.1 for further details).

#### 3.1.2 Sample Preparation for Archaeological Bone

All archaeological bone samples were cleaned mechanically by scraping their surface with a scalpel. When necessary e.g., when soil was adhering to the bones, they were ultrasonicated in ultra pure water. Trabecular bone was removed with a scalpel, only compact bone was subjected to the extraction. The dry bone samples were crushed to small chunks and  $\sim 500$  mg of these chunks were used for each collagen extraction. Two selected teeth (Thunau), which were also processed in the course of this work, were separated into the crowns and the roots. After removing the tooth cement with a scalpel, the roots were crushed into small pieces, which were then used for the extraction.

Most of the samples from Gemeinlebarn and Thunau were treated using the semi-automated collagen extraction device. A smaller number of collagen extracts (including those of the human teeth) were generated "manually" using method 2.

For the majority of the samples, the solubilized collagen was freeze dried. However, some samples were prepared before the freeze dryer was available, therefore the collagen containing solutions were evaporated to dryness in an oven at  $\sim 90^\circ\text{C}$ .



Several of the human bone samples from Thunau chosen for the stable isotope analysis, were also  $^{14}\text{C}$ -dated at VERA. Thus, collagen had already been extracted at the VERA sample preparation laboratory by Method 1. Aliquots of these collagen samples were provided for the IRMS measurements.

The sample material was weighed into small tin capsules ( $5 \times 9$  mm) using a *Sartorius M5P* micro balance with a measurement precision of  $\leq \pm 0.001$  mg (one standard deviation). In order to avoid any contamination, unpowdered latex-gloves were worn during sample handling and every sample capsule was prepared on a fresh piece of aluminum foil. Tweezers and spatulas were thoroughly cleaned after each sample. It is crucial to tightly fold the capsules after filling in the sample material, to remove any residual air in the sample, which might interfere with the nitrogen measurement.

## 3.2 Instrumentation: EA-IRMS

There are several papers and textbooks reviewing the development and the underlying principles of isotope ratio mass spectrometry (e.g., Brand, 2004; Brenna *et al.*, 1997; Matthey, 1997; Platzner, 1997). To provide the necessary technical background for the presented work, an overview based on the references cited above and the operation manuals of the employed analytical instruments is given here. It describes the measurement system and methods used in this palaeodiet study.

### 3.2.1 System Configuration

The stable isotope ratios given in this thesis were determined by elemental analyzer - isotope ratio mass spectrometry (EA-IRMS). The measurements were performed with a *CE-Instruments NC2500* elemental analyzer coupled to a *Micromass Optima* IRMS at the Faculty of Physics/Isotope Research. Figure 3.1 shows a schematic diagram of such a system.

The *NC2500* elemental analyzer is equipped with an autosampler, which is mounted on top of the oxidation reactor. This reactor consists of a vertically positioned quartz tube (45 cm length, 18 mm diameter) heated to  $1030^\circ\text{C}$ , which is filled with a 12 cm layer of chromium(III) oxide ( $\text{Cr}_2\text{O}_3$ ) on top and a 6 cm layer of silvered cobalt(II,III) oxide ( $\text{Co}_3\text{O}_4$ ), separated by a 1 cm layer of quartz wool. Quartz wool is also used to close the tube (4 cm on the bottom and 1 cm on top of the filling). The reduction reactor is the same kind of quartz tube completely filled with short copper rods closed by quartz wool (3 cm on the bottom and 2 cm on top of the tube). In operation mode it is heated to  $650^\circ\text{C}$ . A water absorption trap containing magnesium perchlorate is mounted after the reduction reactor. All chemicals and consumable supplies for elemental analysis were obtained from *HEKAtech*, Germany. After the water trap, the GC (gas chromatography) oven is placed, which is kept at a temperature of  $50^\circ\text{C}$ . It houses a packed GC column of 2 m length (column packing material: *Porapak PQS*) and a thermoconductivity detector (TCD). The EA-IRMS system was operated in continuous flow (CF) mode, in which a constant stream of high purity helium ( $\geq 99.9999\%$  Vol.) transports the sample gas through the elemental analyzer

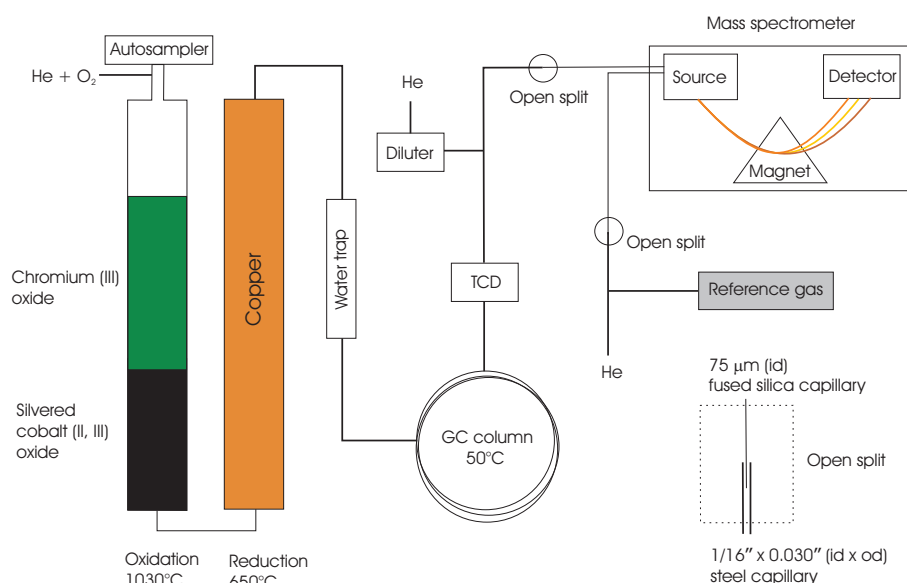


**Figure 3.1:** Schematic diagram of an elemental analyzer - isotope ratio mass spectrometry system, adapted from Matthey (1997). (id: inner diameter, od: outer diameter)

and subsequently into the mass spectrometer via an open split coupling consisting of a fused silica capillary (mounted to the ion source inlet of the MS) inserted in a larger diameter stainless steel capillary as shown in Figure 3.1. Carbon dioxide and nitrogen reference gas are admitted to the mass spectrometer as discrete pulses introduced into the helium stream in a separate reference gas line, which reaches the mass spectrometer through another open split coupling.

Directly after the elemental analyzer, an automatic dilution system ("diluter") is mounted, which can reduce the amount of sample gas admitted to the MS. Therefore, a portion of the He and sample gas mixture (arriving from the EA) is split off and introduced into a He stream, which is then fed into the MS. This becomes necessary whenever the linear measuring range of the detector, which is between 1 nA and 10 nA, is not sufficiently wide e.g., when carbon and nitrogen stable isotope ratios are measured in a single sample with high C/N ratios so that the major nitrogen current would be at the lower limit of the linear range and the major carbon dioxide current would be out of range.

The mass spectrometer comprises an electron impact (EI) ion source at high electric potential, a flight tube which passes through the field of an electromagnet and an ion collector assembly with three Faraday cups, allowing the simultaneous detection of three different ion currents. (See the next section for a more detailed description.)

It is necessary to maintain a high vacuum in the range of  $10^{-6}$  mbar within the mass spectrometer, in order to avoid ion beam scattering due to collision with residual gas molecules. This is accomplished by permanent pumping with a turbomolecular pump (*Edwards*, 250 l/s) backed by an *Edwards RV5* rotary vane pump, which reduces the pressure to around  $10^{-3}$  mbar. Only at pressures as low as this, the turbomolecular pump can be switched on. High pumping capacities are here crucial to deal with the

large throughput of helium carrier gas.

### 3.2.2 Processes during a Measurement

#### Combustion

When a measurement sequence is started, the tin capsule with the sample is dropped from the autosampler carousel into the oxidation reactor. There, flash combustion of the sample is induced by a pulse of pure oxygen ( $\geq 99.995\%$  Vol.) introduced into the helium carrier gas, which is set to a flow rate of 90 mL/s. During the combustion, temperatures of up to 1800°C are generated due to the exothermic oxidation of the tin. When a collagen sample is combusted in the reactor, the main products are gaseous  $\text{CO}_2$ ,  $\text{NO}_x$  and  $\text{H}_2\text{O}$ . To ensure complete oxidation, the gas mixture emerging from the flash combustion is passed over the layers of  $\text{Cr}_2\text{O}_3$  and  $\text{Co}_3\text{O}_4$ . Halogens and oxides of sulphur, which might be present in the sample gas in minor amounts, are eliminated by the silver contained in the  $\text{Co}_3\text{O}_4$  layer. The carrier gas stream transports the gas mixture into the reduction reactor, where nitrogen oxides are reduced to nitrogen and excess oxygen is bound as cupric oxide ( $\text{CuO}$ ). After the reduction step, water vapor is absorbed in the water trap. The gas mixture is subsequently carried into the GC-column, where nitrogen and carbon dioxide are separated. After the separation the gas peaks are detected in the TCD (see e.g., Pella & Colombo, 1973). The sample gas reaches the ion source via the open split (see above), which admits approximately 0.3 % of the gas stream consisting of helium and the sample gas to the ion source, the majority of the gas mixture is vented to the atmosphere.

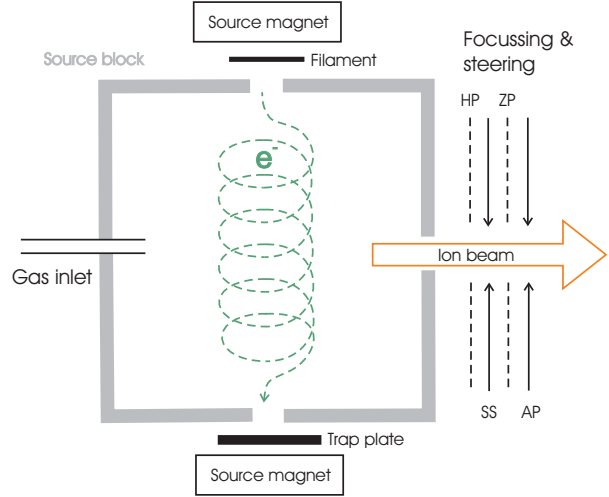
#### Ionization

In the ion source, depicted schematically in Figure 3.2, electrons are emitted from a hot filament coated with thorium oxide and then accelerated by a small voltage between the filament and the source block of around 100 V. The electrons are brought onto a helical trajectory by the magnetic field of the source magnets, two small permanent magnets, in order to increase the ionization efficiency. When the gaseous sample molecules enter the source, they are ionized by collisions with the electrons. The most important effect is the formation of singly charged cations, which is shown in Equation 3.2, where M stands for a sample molecule,  $e^-$  is an electron and  $M^+$  is the generated cation.



Electrons not involved in the ionization process are collected at an anode mounted across the source chamber, the "trap plate", and measured as trap current. Via the trap current, the sensitivity of the mass spectrometer can be adjusted (the higher the trap current, the higher the sensitivity). The generated ions are extracted from the ionization region by a potential difference between the source block and the half plates located outside the block. An acceleration voltage of up to 5 kV may be applied to the source block and the "extraction voltage", which is typically  $\sim 80\%$

**Figure 3.2:** Schematic diagram of an electron impact ion source, based on (Mattey, 1997). (HP: half plates, SS: source slit, ZP: z-plates, AP: alpha plate)



of the acceleration voltage, is applied to the half plates. In addition, the ions in the source are pushed out of the ionization region by an electrode called the "ion repeller", which is mounted at the back of the source block, opposite the ion exit slit. However, this electrode only acts as a repeller in hydrogen measurements. For the measurement of all other gas species, a negative voltage is applied to it causing a short retention of the positive ions in the source. After the extraction, the ions are further accelerated by the potential drop along their path.

Beam steering is accomplished by adjustable voltages between the two half plates (horizontal steering) and the two z-plates (vertical steering) respectively. The assembly of the ion source construction (source block, half plates and source slit together) also provides a focusing effect on the ions. Scattered ions are collected at the source slit held at ground potential. When the ions enter the flight tube through the slit in the alpha plate, which is kept at ground potential, they finally have reached an energy related to the applied acceleration voltage.

### Mass Separation

In the magnetic field of the analyzer magnet, the ions are deflected perpendicular to their flight direction and to the magnetic field due to the Lorentz force. Generally, ions moving in a homogeneous magnetic field describe a circular path with a radius  $r$  defined by their momentum ( $p = \sqrt{2mE}$ ) over charge:

$$B \cdot r = \frac{\sqrt{2mE}}{q} \quad (3.3)$$

where  $B$  is the magnetic field,  $m$  the mass,  $E$  the kinetic energy and  $q$  the charge of the ion. Substituting the kinetic Energy  $E$  in Equation 3.3 by  $U \cdot q$  and solving the equation for  $m/q$  gives:

$$\frac{m}{q} = \frac{B^2 \cdot r^2}{2U} \quad (3.4)$$

When regarding Equation 3.4, it can be understood clearly that the mass spectrometer separates ions according to their mass to charge ratio (in practice, the dimensionless notation  $m/z$  with  $m$ , the mass number and  $z$ , the charge number of the ion is used (see e.g., Budzikiewicz, 1998)). In principle, molecules with a mass number between 1 and 70 are amenable for analysis in the *Optima* MS. Its mass resolution is  $R = m/\Delta m = 100$  (10 % valley definition).

### **Ion Current Detection**

The collector assembly consisting of three Faraday cups is mounted at a fixed position along the focal plane of the mass spectrometer. Therefore three ion currents (of ions with different  $m/z$ ) can be registered simultaneously and are then converted to amplified electric currents proportional to their respective intensities. When measuring  $N_2$  gas, the ion currents of two isotopologues<sup>2</sup> ( $^{14}N^{14}N^+$  with  $m/z$  28 and  $^{15}N^{14}N^+$  with  $m/z$  29) have to be registered in order to obtain the necessary information to calculate the  $^{15}N/^{14}N$  ratio. In the case of  $CO_2$  measurements, the predominant isotopologue  $^{12}C^{16}O^{16}O^+$  is collected in the  $m/z$  44 Faraday cup as the "major beam". The "minor 1" beam ( $m/z$  45) comprises mainly  $^{13}C^{16}O^{16}O^+$  but also a significant contribution by  $^{12}C^{16}O^{17}O^+$ . The major constituent of the  $m/z$  46 ("minor 2") beam is  $^{12}C^{16}O^{18}O^+$ . In  $CO_2$  from natural terrestrial samples, the contribution of the isotopologue containing one  $^{17}O$  constitutes around 6 % of the  $m/z$  45 beam and thus has to be accounted for (see e.g., Matthey, 1997). This is accomplished using a correction procedure implemented in the *Optima* operation software, which follows the algorithm described by Craig (1957). The corrected  $\delta^{13}C$  value of a sample (index "spl") can be calculated according to:

$$\delta^{13}C_{spl} = 1.0676 \cdot \delta 45 - 0.0338 \cdot \delta^{18}O_g \quad (3.5)$$

$$\delta 45 = \left( \frac{R45_{spl}}{R45_{std}} - 1 \right) \cdot 1000 \text{‰} \quad (3.6)$$

with  $\delta 45$  the measured  $\delta^{13}C$  value of the sample determined from the registered  $m/z$  45 to  $m/z$  44 ratios of the sample and the standard ( $R45_{spl}$  and  $R45_{std}$  respectively) as shown in Equation 3.6. The numerical coefficients in Equation 3.5 were derived by Craig from the absolute carbon and oxygen stable isotope ratios of the original PDB reference material (see Craig, 1957). The oxygen stable isotope ratio of the measured sample gas ( $\delta^{18}O_g$ ) is calculated as follows:

$$\delta^{18}O_g = 1.0010 \cdot \delta 46 - 0.0021 \cdot \delta^{13}C_{spl} \quad (3.7)$$

$$\delta 46 = \left( \frac{R46_g}{R46_{std}} - 1 \right) \cdot 1000 \text{‰} \quad (3.8)$$

---

<sup>2</sup>According to the definition by IUPAC (International Union of Pure and Applied Chemistry), isotopologues are molecules that differ only in their isotopic composition. For example  $^{12}C^{16}O^{16}O$  and  $^{13}C^{16}O^{16}O$  are isotopologues.

### 3 Methods

with  $\delta 46$  the measured  $\delta^{18}\text{O}$  value of the sample gas determined from the registered  $m/z$  46 to  $m/z$  44 ratios as given in Equation 3.8.  $\delta^{18}\text{O}_g$  in Equation 3.5 can thus be substituted as given in Equation 3.7 and  $\delta^{13}\text{C}_{spl}$  is then:

$$\delta^{13}\text{C}_{spl} = \frac{1.067 \cdot \delta 45 - 0.0338 \cdot 1.0010 \cdot \delta 46}{1 - 0.0338 \cdot 0.0021} \quad (3.9)$$

### Data Processing

Since the sample gas is gas-chromatographically separated before entering the MS, the ion currents detected during a measurement give the typical shape of a chromatogram. Figure 3.3 shows such a chromatogram as it was recorded in a  $\text{CO}_2$  measurement. At the beginning of the measurement sequence the rectangular reference gas peak is visible, after about 190 seconds the peak of the  $\text{CO}_2$  sample gas appears. The operating software calculates the  $^{13}\text{C}/^{12}\text{C}$  ratio from the ratio of the background corrected  $m/z$  45 to  $m/z$  44 peak areas ( $m/z$  28 and  $m/z$  29 areas when measuring  $^{15}\text{N}/^{14}\text{N}$  ratios). By comparison with the reference gas, whose  $\delta^{13}\text{C}$  on the VPDB scale (or  $\delta^{15}\text{N}$  relative to AIR) has been determined before, the  $\delta^{13}\text{C}$  (or  $\delta^{15}\text{N}$ ) for the sample can be calculated (accounting for the Craig correction described above in the case of  $\delta^{13}\text{C}$  measurements). Alternatively, the  $\delta$ -value of the sample can be calculated with respect to a standard material instead of the reference gas. In this case, the standard is combusted in the elemental analyzer in the same way as the sample. The latter is consistent with the "identical treatment (IT) principle", which recommends the same reaction conditions for a sample and the standard during gas generation, so that possible isotope fractionations due to this process cancel

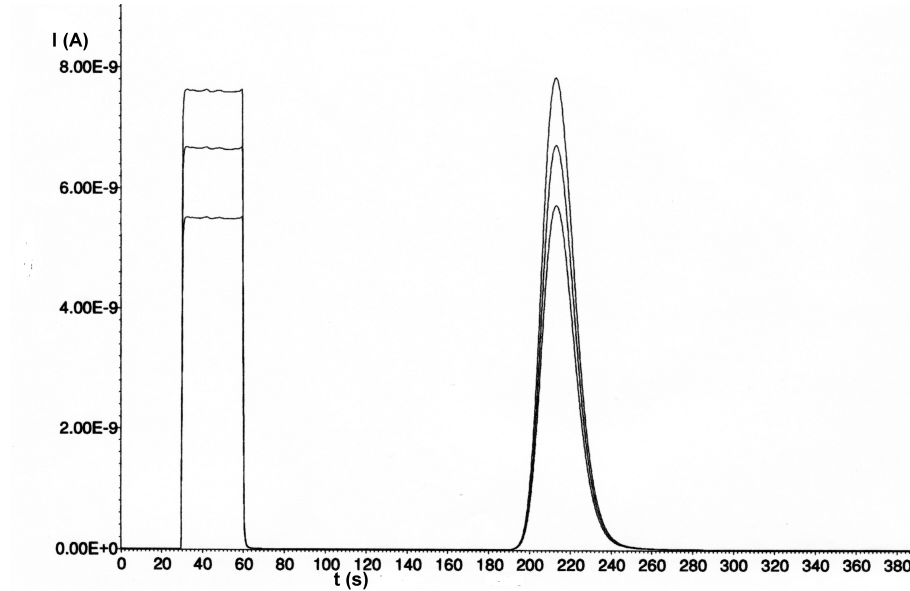


**Figure 3.3:** Printout of a chromatogram registered during a  $\text{CO}_2$  measurement. On the x-axis the time in seconds is plotted, on the y-axis the ion current of the major beam ( $m/z$  44) is indicated in Amperes.

out (Werner & Brand, 2001). To fulfill this principle, all  $\delta$ -values presented in this work were evaluated with respect to an isotope standard, which was combusted in the EA. In the measurements of the archaeological samples, the laboratory standard L-alanine was used for this purpose (see Section 3.3.2).

A  $\delta$ -value determined with respect to an arbitrary isotope standard, can be converted to a  $\delta$ -value relative to VPDB according to Equation 3.10, in which the indexes  $(x,S)$  and  $(x,VPDB)$  refer to a  $\delta$ -value of a sample  $x$  determined relative to a standard  $S$  and VPDB respectively,  $(S,VPDB)$  denotes the standard's value reported relative to VPDB (see Craig, 1957).

$$\delta_{(x,VPDB)} = \delta_{(x,S)} + \delta_{(S,VPDB)} + \frac{1}{1000} \cdot \delta_{(x,S)} \cdot \delta_{(S,VPDB)} \quad (3.10)$$

The carbon and nitrogen contents of a sample can be evaluated using the peak areas calculated from the MS- or the TCD-recordings and the weighed amounts of the sample and an elemental standard with known C- and N-content. The evaluation from the MS-signal was chosen as a default, nevertheless the results of the TCD registrations were also computed and used to check the MS evaluation. Equation 3.11 shows how the elemental content can be calculated,

$$\%wt.E_x = \left( \frac{a_x \cdot w_s \cdot \%wt.E_s}{a_s \cdot w_x} \right) \quad (3.11)$$

with  $\%wt.E$  the respective elemental content (carbon or nitrogen),  $a$  the measured peak area and  $w$  the weighed amount. The subscripts  $x$  and  $s$  refer to a sample or a standard respectively. From the obtained carbon and nitrogen contents, the atomic C/N ratio is calculated according to:

$$C/N = \frac{\%wt.C}{\%wt.N} \cdot \frac{A_r(N)}{A_r(C)} \quad (3.12)$$

with  $A_r$  the relative atomic mass of the respective element.

### 3.2.3 Tuning of the Mass Spectrometer

When the mass spectrometer is properly tuned so that all three beams are focused into their respective collector, the ion beam width is narrower than the collector slit (at the entrance to the Faraday cup). Consequently, the registered ion current gives a flat topped peak, when the ion beam is scanned across the collector (shown in Figure 3.4). Such a scan is accomplished by alteration of the acceleration voltage, which causes the beam to move across the collector. As the beam enters the cup, the current rises until the whole beam strikes the collector surface, then stays constant until the beam leaves the cup on the other side. Before a measurement is performed, the acceleration voltage has to be adjusted to a value in the middle of the flat topped peak. In doing so, the detected signal remains stable in case small drifts in ion beam position (e.g., due to fluctuations of the acceleration voltage) occur. Appropriate currents of the solenoid magnet (possible range: 0-5 A) were adjusted for

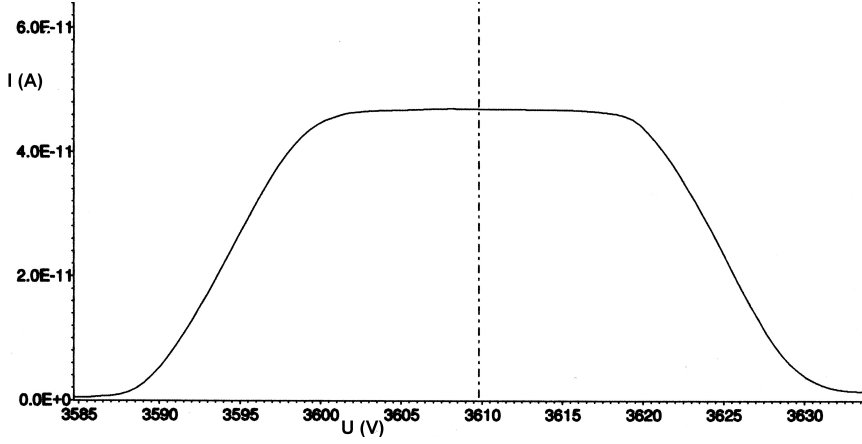


**Figure 3.4:** Flat topped peak generated by scanning the  $m/z$  45 ion beam across its collector. On the x-axis the acceleration voltage  $U$  is plotted, on the y-axis the ion current of the  $m/z$  45 ion beam is indicated.

each gas species of interest ( $N_2$  and  $CO_2$ ) to direct the beams into their corresponding collectors in the course of the initial setup of the IRMS-system. Usually the respective current for a gas species does not have to be altered during every day tuning, since the fine tuning can be done by changing the acceleration voltage (possible range: 0-5 kV).

**Table 3.2:** Source tuning parameters and their possible ranges according to the manual of the *Micromass Optima*. "EX" is the extraction voltage given as a percentage of the acceleration voltage, "HP" is the potential difference between the two half plates, "ZP" is the potential difference between the two z-plates, "EV" is the potential difference between the source block and the filament (by this potential difference the electrons emitted from the filament are accelerated to energies in the range of 50 eV to 100 eV), "IR" is the ion repeller voltage.

Parameter	Possible Range
EX	0 to 100 %
HP	-150 to +150 V
ZP	-225 to +225 V
EV	50 to 100 V
IR	-15 to +50 V

Via the trap current the degree of sensitivity of the mass spectrometer is selected. It is variable in several steps between 0 and 1000  $\mu A$ , but in practice 200 or 400  $\mu A$  were chosen. The source parameters given in Table 3.2 have then to be tuned to give the highest achievable signal intensity, stability and linearity (i.e. a constant isotope-ratio with varying ion beam intensity). The tuning strategy is a matter of experience, but one possible approach is to set the steering plates and EV to give maximum current reading in the faraday cups, whereas EX is chosen to give the



best peak shape (with the largest plateau). The better the ion beam is focused, the larger plateau can be obtained. Adjusting IR often enhances linearity. Source tuning is an iterative process, because changing one electric field influences the others and there might be several sets of parameter values, which produce satisfactory peak shapes. Subsequently the stability of the instrument is checked by measuring the minor1/major current ratio of 10 consecutive reference gas peaks of constant peak height (identical gas pressure). Also the linear behavior of the system has to be controlled. This procedure is similar to the stability test, but here the heights of the reference gas pulses have to be randomly altered to give a major beam signal between 1 nA and 10 nA, which corresponds to the linear measuring range of the *Optima* MS. As a rule of thumb, the system is considered sufficiently stable and linear respectively, when the relative difference of the highest minor1/major ratio output from that of the smallest ratio of each test is equal or smaller than 0.5 ‰. The tuning of the instrument is adjusted for every gas species of interest prior to each measurement. On a daily basis, usually only the extraction voltage has to be altered slightly and the acceleration voltage is set to the middle of the flat topped peak ("peak centering") before a stability and linearity check can be performed. When the stability and linearity requirements are met, the parameter values are saved as a tune file for the respective gas species.

### 3.3 IRMS-measurement of Bone Collagen

#### 3.3.1 Developing a Standard Measurement Procedure for Collagen Samples

The determination of  $\delta^{13}\text{C}$  and  $\delta^{15}\text{N}$  values of a sample including the carbon and nitrogen contents can be accomplished in two separate measurements of two subsamples, where only one gas species is measured at a time. Alternatively, both  $\delta$ -values and elemental contents can be determined in one sample, where  $\text{N}_2$  and  $\text{CO}_2$  data are registered in sequence. Apart from a higher efficiency concerning analysis time and resources consumption, a major advantage of the determination in the same sample is the cancellation of the sample and standard weights in the calculation of the C/N ratio (see Equations 3.11 and 3.12). Therefore uncertainties of the weights do not influence the final results.

A necessary prerequisite for the measurement of  $\text{CO}_2$  and  $\text{N}_2$  in one sample is a sufficient GC separation of both gas peaks in order to have enough time to switch the mass spectrometer from nitrogen to carbon dioxide measurement ("peak jumping"). Furthermore, the method has to be selected depending on the atomic C/N ratio of the sample material. If e.g., C and N shall be measured in one sample using the peak-jump method, the major ion currents of both gas species have to be within the linear range of the detection system. In materials with a high atomic C/N ratio, as for instance collagen, this can be accomplished by reducing the  $\text{CO}_2$  amount using the diluter and/or by selecting different instrument sensitivities for each gas species via the trap current. Both methods, the measurement of a single gas species and the

measurement of carbon and nitrogen isotope ratios by the peak-jump method, were applied for the sample measurements in the course of this work and are described below.

#### Measurement of a Single Gas Species

Of crucial importance during a measurement run are the timing of the background readings, admittance of the reference gas pulses and the sample window, which is the interval of the chromatogram that fully includes the sample peak. The background values are usually registered directly at the beginning of a chromatogram and also at the end. For this, it is important to wait until the signal has reached the true background level. When measuring a single gas species, the respective reference gas pulse is introduced after the first background reading. In all measurements performed in the course of this work, the nitrogen peak usually started after  $\sim 110$  seconds of a sample run and reached its maximum at  $\sim 130$  seconds as can be seen in Figure 3.5. In the case of the  $\text{CO}_2$  measurements, the peak arrived after  $\sim 190$  s and the maximum peak height was reached after  $\sim 210$  s (see Figure 3.3). However, the peak timing can somewhat vary in the course of time, for example after the replacement of the EA reactors. Then the respective sample windows have to be adjusted accordingly.

The parameters described above are saved in so called "method files", which contain all information needed for a specific measurement method like the gas species to be registered, specifications of the reference gases, timing of all valve operations, details for the peak-jump (if applied), which tune files to be used, instructions for data acquisition and analysis etc. These method files are accessed, when a measurement sequence is started and the necessary commands are communicated to the system components (MS, EA, diluter, reference gas box) via the system controller, which is basically a microcomputer that allows the synchronized operation of all components by the operation software.

An important point to consider for a measurement is that organic samples often show a carbon content significantly higher than the nitrogen content. For example collagen has a atomic C/N ratio of  $\sim 3$ . In order to get a feasible major peak height (ideally around 5 nA of  $^{14}\text{N}_2^+$  current) in nitrogen measurements, higher sample amounts than for carbon dioxide measurements have to be weighed. Nitrogen measurements in the single gas mode are usually performed at a trap current of 400  $\mu\text{A}$ , whereas carbon dioxide measurements at 200  $\mu\text{A}$  due to the lower sensitivity of the MS for  $\text{N}_2$  in comparison to  $\text{CO}_2$ . Collagen amounts of  $\sim 400 \mu\text{g}$  were used, which corresponds to approximately  $60 \mu\text{g} \approx 4.3 \mu\text{mol}$  of nitrogen, since the nitrogen content of bone collagen is  $\sim 15\%$ wt. Table 3.3 shows an example for a nitrogen tune file as it was applied in the measurements. In this way a  $^{14}\text{N}_2^+$ -current of around 8 nA could be obtained.

As stated above, separate  $\text{CO}_2$  measurements were performed with a trap current of 200  $\mu\text{A}$ . A typical  $\text{CO}_2$  tune file is given in Table 3.4. Sample sizes were around 120  $\mu\text{g}$  (containing approximately  $50 \mu\text{g} \approx 4.2 \mu\text{mol}$  of carbon) and generated peak heights of  $\sim 7$  nA for the  $m/z$  44 beam.

According to the manufacturer of the IRMS, the measurement precisions for  $\delta^{13}\text{C}$

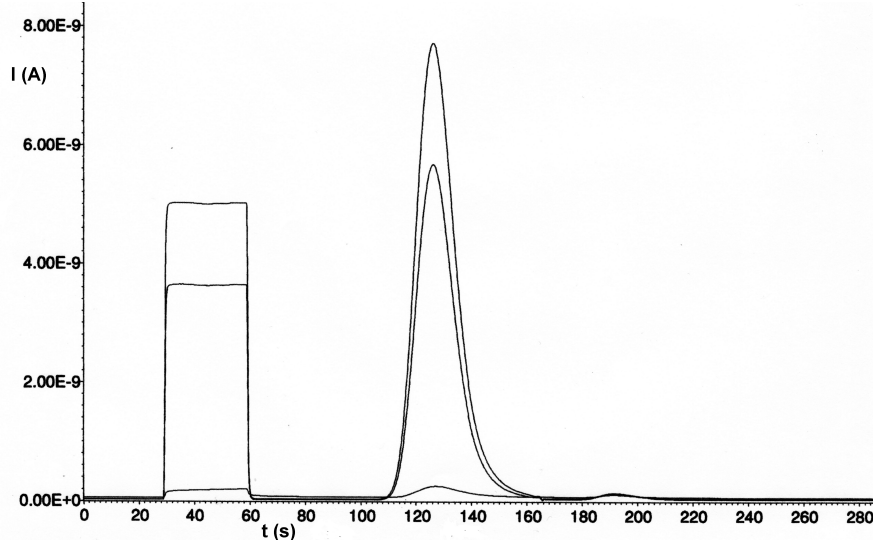


**Figure 3.5:** Chromatogram registered during a N<sub>2</sub> measurement. On the x-axis the time in seconds is plotted, on the y-axis the ion current of the major beam is indicated.

**Table 3.3:** Typical tuning parameters for a N<sub>2</sub> measurement. (AV: acceleration voltage, EX: extraction voltage, HP: potential difference between the two half plates, ZP: potential difference between the two z-plates, TR: trap current, EV: potential difference between filament and source block, IR: ion repeller voltage, MC: current of the solenoid magnet.)

Tuning Parameter	Value
AV (V)	4162.4
EX (% of AV)	80.84
HP (V)	105.7
ZP (V)	67.1
TR (μA)	400
EV (V)	88.86
IR (V)	-6.55
MC (A)	3.15000

and  $\delta^{15}\text{N}$  determined in a single gas species measurement are  $\leq 0.15\text{‰}$  for CO<sub>2</sub>- and  $\leq 0.20\text{‰}$  for N<sub>2</sub>-measurements respectively. The given precisions are the  $1\sigma$  standard deviations of the measurement results of 10 natural abundance, constant quantity samples, containing 50 μg carbon and 100 μg nitrogen respectively, obtained in one batch measurement. For 10 differing quantity samples (15 to 150 μg carbon and 20 to 200 μg nitrogen) the respective precisions are reported to be  $\leq 0.30\text{‰}$  for both gas species.

In practice, for all collagen samples the same amount was weighed to give similar C- and N-currents. The observed precisions were on average 0.10 ‰ (ranging from 0.04 to 0.13 ‰) for  $\delta^{13}\text{C}$  and 0.09 ‰ (ranging from 0.04 to 0.15 ‰) for  $\delta^{15}\text{N}$ , which is consistent with the specifications of the manufacturer.

**Table 3.4:** Typical tuning parameters for a CO<sub>2</sub> measurement.

Tuning Parameter	Value
AV (V)	3604.7
EX (% of AV)	80.65
HP (V)	70.5
ZP (V)	19.6
TR ( $\mu$ A)	200
EV (V)	89.83
IR (V)	-7.06
MC (A)	3.80285

However, the described single gas species method was applied only for a small number of archaeological collagen samples, the vast majority of the measurements was performed using the peak-jump method.

### Consecutive Measurement of CO<sub>2</sub> and N<sub>2</sub> in the Same Sample ("Peak-Jump Method")

The main aspects to be considered for this method are the timing of the reference gas pulses for each gas species as well as that of the respective background readings, also the procedure applied to switch the mass spectrometer from nitrogen to carbon dioxide isotope measurement (peak-jump) and the correct definition of the sample windows. Figure 3.6 shows the chromatogram recorded during a measurement of CO<sub>2</sub> and N<sub>2</sub> in one sample. The first half of it corresponds to the nitrogen measurement with a reference gas pulse and the nitrogen peak in its specific time interval. The background was read at the beginning of the measurement sequence. The second part consists of the carbon dioxide peak and the respective CO<sub>2</sub> reference gas pulse. A second background reading was performed at the end of the sequence after the signal had dropped to the background level.

Before each batch measurement, the mass spectrometer was tuned to CO<sub>2</sub> and N<sub>2</sub> and the respective optimized tune files were saved. The N<sub>2</sub> tune file was loaded at the beginning of the measurement sequence, the CO<sub>2</sub> file was loaded to perform the "peak jump". Since the currents of the solenoid magnet in the used tune files were different for the two gas species, the magnet was cycled<sup>3</sup> during the "peak jump". The time needed for this and an additional settle time was considered to allow the magnet to stabilize.

For the measurement of a first small group of archaeological collagen samples with the peak-jump method described above, 180  $\mu$ g of each sample were weighed into tin capsules. Nitrogen was measured at a trap current of 400  $\mu$ A and carbon dioxide at 200  $\mu$ A (see tables 3.3 and 3.4 for examples of tune files), which resulted in ion

<sup>3</sup>For this, the magnet current is brought to its maximum value and subsequently to zero. After that, the desired current is adjusted.

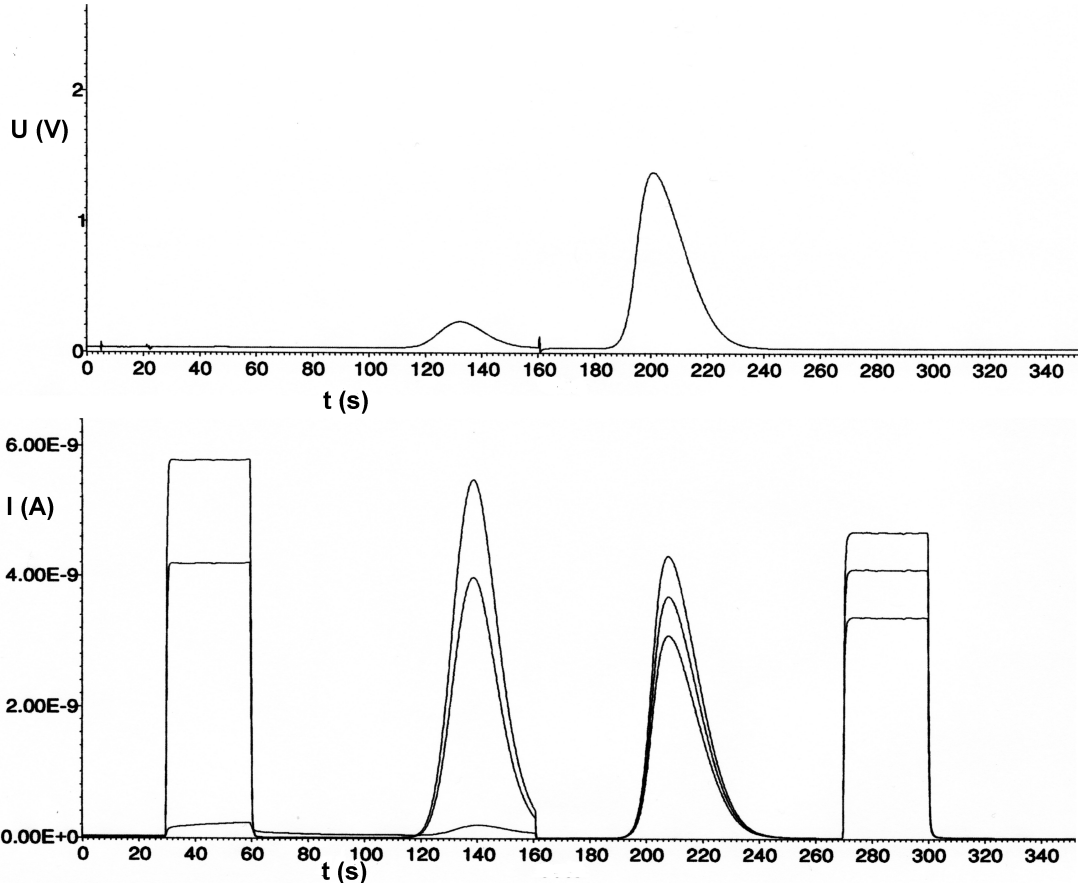


**Figure 3.6:** Recording of the TCD (upper diagram) and chromatogram detected by the Faraday cups during a simultaneous  $N_2$  and  $CO_2$  measurement.

currents around 3 and 10 nA for  $N_2$  and  $CO_2$  respectively without employment of the diluter. Standards used in the measurements were weighed to give approximately the same ion currents as the samples. The precisions for all measurements performed with this method ranged from 0.03 to 0.17 ‰ with a mean of 0.09 ‰ for  $\delta^{13}C$  and from 0.08 to 0.30 ‰ with a mean of 0.17 ‰ for  $\delta^{15}N$ . Compared to the single gas species method the precision for the determination of  $\delta^{15}N$  is here clearly lower, although still within an acceptable range. A higher measurement precision for  $\delta^{15}N$  values was achieved by increasing the sample amounts from  $\sim 180\mu g$  to  $\sim 950\mu g$ . In doing so, nitrogen could be measured at a trap current of  $200\mu A$ , whereby ion currents of 5 to 8 nA were obtained. However, the higher carbon content made the operation of the diluter necessary. At a low dilution level and by measuring at a trap current of  $400\mu A$ , suitable  $CO_2$  peak heights of 3 to 5 nA could be achieved. This method (using large sample amounts) resulted in good measurement precisions for both gas species ( $\delta^{13}C$ : 0.03 to 0.14 ‰ with a mean of 0.06 ‰;  $\delta^{15}N$ : 0.02 to 0.15 ‰ with a mean of 0.05 ‰) and therefore was chosen as the standard measurement procedure for the archaeological samples.

### 3.3.2 Calibrating Laboratory Standards

$\delta^{13}\text{C}$  and  $\delta^{15}\text{N}$  values are usually determined relative to isotope standards linked to the respective primary reference materials, which define the corresponding isotope scales (VPDB or AIR). For this, standards with known  $\delta$ -values have to be added to each sample batch. There are commercially available secondary reference materials with certified  $\delta^{13}\text{C}$  and/or  $\delta^{15}\text{N}$  values, distributed e.g., by the IAEA (International Atomic Energy Agency). However, such reference materials are generally in short supply and are not recommended for usage on a daily basis. They are usually used for the calibration of laboratory (or "in-house") standards, suited to the materials to be analyzed in a certain laboratory. When selecting a substance for the calibration as in-house standard, several criteria should be considered. Most important are homogeneity and stability of the isotopic composition. Further, the standard material should be similar to the material to be measured with respect to chemical and isotopic composition (see e.g., Werner & Brand, 2001).

For determinations of  $\delta^{13}\text{C}$  and  $\delta^{15}\text{N}$  values in collagen samples, the amino acid L-alanine was found a suitable candidate for a laboratory standard. It is a constituent of bone collagen and has carbon and nitrogen contents very similar to those of collagen ( $\sim 41\%$  wt.C and  $\sim 16\%$  wt.N respectively). In first test measurements, the  $\delta^{13}\text{C}$  and  $\delta^{15}\text{N}$  values of a batch of pure L-alanine (purchased from *Merck*) were determined to be approximately  $-19.5\%$  and  $-3.2\%$  respectively. Its  $\delta^{13}\text{C}$  value lies well within the range expected for palaeodiet samples, the  $\delta^{15}\text{N}$  value is at the lower margin of the  $\delta^{15}\text{N}$  value range occurring in living organisms. Therefore, this specific material was considered appropriate as in-house standard for collagen measurements.

To calibrate L-alanine, it was measured in several separate measurement runs, mainly in peak-jump mode, together with international reference materials from the United States Geological Survey (USGS) and the IAEA (USGS40, IAEA: CH-3, CH-6, CH-7, N-1 and N-2). A sample batch for one run consisted of 10 alanine replicates and at least two different isotope reference materials (3 replicates each). Furthermore an organic analytical standard (OAS) with certified carbon and nitrogen contents (Alanine OAS, *HEKAtech*, %wt.C:  $40.54 \pm 0.18$ ; %wt.N:  $15.58 \pm 0.19$ ) was added in triplicate so that the laboratory standard could also be calibrated as elemental standard. Every batch included 2 blank samples (empty, folded tin capsules) in order to enable blank correction of the measured peak areas. The possible sources for nitrogen blank signals are air entering the system when the tin cup is dropped from the autosampler into the oxidation reactor despite purging with helium (main source), a small amount of atmospheric nitrogen trapped in the tin capsule during sample weighing and an almost negligible amount associated with the tin itself. Carbon blank signal can be caused by organic residues adhering to the tin. The operation software applied the blank correction by subtracting the registered blank areas from all measured sample areas during the data evaluation of the whole batch (after all samples and blanks had been measured).

The results of a batch evaluation are the carbon and nitrogen contents determined by comparison with the elemental standard, and the  $\delta$ -values calculated with respect to one of the reference materials ("single-point anchoring") as described by

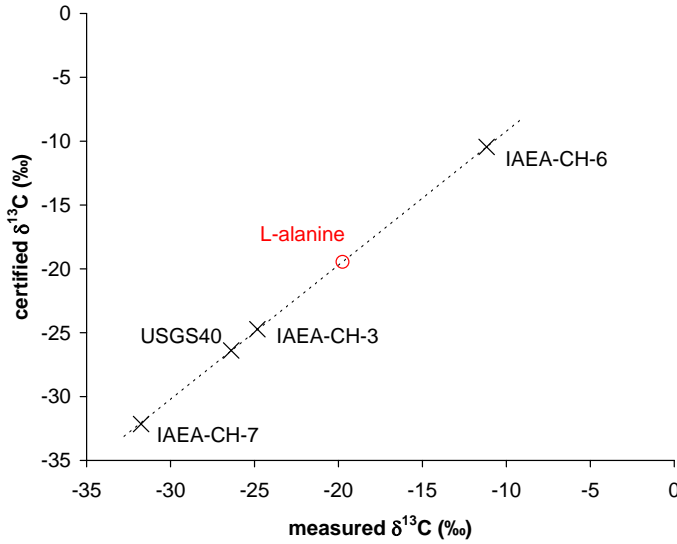


**Figure 3.7:** Multi-point normalization of a  $\delta^{13}\text{C}$  value.

Paul *et al.* (2007), since the software allows only one material to be specified as the reference. However, it is generally recommended to normalize measured  $\delta$ -values to the international isotope scales by a linear function defined by measured and known  $\delta$ -values of at least two isotope standards ("two-point" or "multi-point linear normalization"). Paul *et al.* (2007) found that this method produced lower normalization errors than the single-point method, when the  $\delta$ -values of the standards encompass those of the samples. Also, two-point normalization of the  $\delta^{13}\text{C}$  scale improved consistency of  $\delta^{13}\text{C}$  measurements between different laboratories according to Coplen *et al.* (2006a,b). Böhlke & Coplen (1995) observed a similar effect in an interlaboratory comparison of reference materials for  $\delta^{15}\text{N}$  measurements. Therefore, all  $\delta$ -values determined in the course of this work were normalized "off-line" using two-point or multi-point normalization as described by Paul *et al.* (2007). The certified  $\delta$ -values of the reference materials are plotted on the y-axis, their measured  $\delta$ -values on the x-axis and a straight line is fitted to the data points by applying the least squares method as depicted in Figure 3.7. The calculated regression function is then used to normalize the measured  $\delta$ -value of an unknown sample (in this case the material to be calibrated). To obtain the final  $\delta$ -value of the alanine laboratory standard, a weighted mean of the individual measurement results was calculated (see Section 3.4.2 for further details).

In order to perform two-point normalizations of the sample measurement results, a second laboratory standard with different  $\delta$ -values than those of the alanine standard was calibrated in the same way as described above. Ideally the  $\delta$ -values of both standards should bracket the  $\delta$ -values of the collagen samples to be measured. A suitable substance for this was gelatin produced from fish skin (*Sigma Aldrich*). The  $\delta^{15}\text{N}$  values of fish gelatin (13.88 ‰) and of alanine (-3.19 ‰) together sufficiently cover the possible range of most palaeodiet samples. The span between the  $\delta^{13}\text{C}$  values of fish gelatin (-15.61 ‰) and alanine (-19.45 ‰), represents only a section of

values of interest for palaeodietary reconstruction. This range can be extended by using cane sugar ( $C_4$  plant) as a standard, because its  $\delta^{13}C$  corresponds better to those values in collagen from marine or  $C_4$  consumers. In the case of a 100% marine diet, a  $\delta^{13}C$  value around -12 ‰ can be expected in the collagen of a consumer (Richards *et al.*, 2005), which is in the same range than  $\delta^{13}C$  values for cane sugar. However, due to the geographical positions, pronounced marine or  $C_4$  dietary signals were not expected for the samples from the sites investigated in this thesis. And since a laboratory standard should be similar in chemical composition to the investigated sample material, the fish gelatin and the L-alanine were selected as laboratory standards. The results of the laboratory standard calibration procedures are presented in Section 4.2.

#### 3.3.3 Collagen Batch-Measurements

Every archaeological collagen sample was measured three times, with each of these three subsamples in a different measurement run. Besides the samples, a measurement batch consisted of 10 replicates of the alanine laboratory standard, which was used as an isotope and elemental standard, and 3 replicates of at least one additional isotope standard, since two or more standards are needed for the normalization. In addition to alanine, fish gelatin and some of the international reference materials were included as standards in the sample measurements. The international standards were needed, when the expected range of measured  $\delta$ -values was not covered by the laboratory standards alone. For example, before the calibrated fish gelatin standard was available, the IAEA-N-2 standard was added to the measurement batches. L-alanine was always included ten-fold so that the instrument performance could be monitored and an estimate for the measurement uncertainty could be obtained. The 10 replicates were evenly distributed within a measurement batch to check for a possible instrument drift. One subsample of every additional standard was placed at the beginning, in the middle and at the end of the batch respectively. The first and the last position of every batch were filled with blank samples. Normalization of the measured sample  $\delta$ -values of every batch was achieved by two- or multi-point anchoring. The final  $\delta$ -value of a sample was obtained by calculating a weighted mean of the results of 3 separate batch measurements. In the following sections the applied mathematical procedures are described.

### 3.4 Uncertainty Estimation for EA-IRMS Measurement Results ( $\delta^{13}C$ and $\delta^{15}N$ )

In order to obtain the final  $\delta$ -value of a sample, a number of mathematical transformations has to be applied to the measurement results. These transformations are generally the normalization relative to several isotope standards (multi-point normalization) and the calculation of mean values in the case of multiple determinations. The input data for these calculations, however, have uncertainties, which propagate through the entire evaluation process. An important source of uncertainty originates



from the measurement procedure of the samples and the used isotope standards. But also the uncertainties of the certified  $\delta$ -values of the international reference materials influence the final values of the samples. Considering the achievable precisions of IRMS-measurements in the 0.1 ‰ range, it seemed important to know the sizes of the different contributions to the final uncertainty of a measured  $\delta$ -value.

Of interest was also the effect of possible correlations between  $\delta$ -values of standards and samples on the final uncertainties. Due to the calibration of different in-house standards against the same reference materials, correlations between the calibrated  $\delta$ -values of these laboratory standards arise. Such correlations influence the uncertainties of sample  $\delta$ -values normalized against the calibrated laboratory standard values. An increase of the uncertainties can be expected, but without careful investigation it is not predictable to what extent. Since rather small differences in  $\delta$ -values are generally interpreted as dietary changes e.g., the trophic level shift in  $\delta^{13}\text{C}$  between a predator and its prey is known to be around 1 ‰ (e.g., Bocherens & Drucker, 2003), it appeared necessary to check, whether the influence of the correlations leads to overall uncertainties of a magnitude that could distort the interpretations of C and N stable isotope data. Furthermore – when performing multi-point normalizations – the determined regression coefficients (slope and axis intercept) of the normalization equation are correlated with each other, which makes the determination of the uncertainties of the normalized  $\delta$ -values more complex.

For a quantification of the effects of the described correlations, a detailed uncertainty analysis for the determination of  $\delta^{13}\text{C}$  and  $\delta^{15}\text{N}$  values by EA-IRMS was performed (Rumpelmayr *et al.*, 2011). The propagation of uncertainty components, associated with the standards and the samples, in the entire process of  $\delta$ -value determination (from the calibration of laboratory standards to the sample  $\delta$ -values) was explored. Similarly, Skrzypek *et al.* (2010) investigated aspects of error propagation in the normalization of carbon stable isotope data. They performed systematic Monte Carlo simulations and laboratory experiments for a selection of the most commonly used isotope reference standards covering a wide range of  $\delta^{13}\text{C}$  values. In their laboratory experiments they investigated the influence of different carbon isotope standard sets used in normalization on the consistency of the normalized results. The uncertainty analysis presented here is based on both, the  $\delta^{13}\text{C}$  and  $\delta^{15}\text{N}$  values, obtained from bone collagen samples measured for palaeodietary reconstruction, and therefore examines  $\delta$ -value ranges frequently observed in human and animal collagen. In the next section an overview of the mathematical background is given, followed by its application to the problem stated above.

#### 3.4.1 General Overview of the Applied Mathematical Procedures

For the uncertainty assessment, a few mathematical procedures well known in the analysis of experimental data were used. These were the calculation of weighted means, fitting a straight line to a set of experimental data and applying the rules of uncertainty propagation to each step of the data analysis. For the treatment of correlated experimental results, covariances had to be considered to perform the propagation of uncertainties correctly. The methods applied are given in several text-

books on data analysis (e.g., Brandt, 1999; Branham, 1990; Smith, 1991b) and the basic procedures are briefly described in this section. Vectors and matrices help to formulate them in a very compact and concise manner and they can be easily implemented in computer algebra systems and even in standard spread sheet programs, as all matrices needed in the course of this work were small. Typical matrix sizes for which operations like inversion or multiplication had to be performed were  $3 \times 3$  or  $4 \times 4$ . Only in a few cases matrices up to the size  $10 \times 10$  had to be inverted.

#### Calculation of a weighted mean and its uncertainty

A set of independent data points  $y_1, y_2, \dots, y_n$  determined by measurement, can be written as data vector  $\mathbf{y}$  and with the help of the corresponding uncertainties  $\Delta y_1, \Delta y_2, \dots, \Delta y_n$  a  $n \times n$  variance matrix is defined with the squares of the uncertainties (the variances) as diagonal elements and zero elsewhere. But often, the quantities  $y_i$  are not independent from each other (i.e. they are correlated) e.g., if they are measured relative to the same standard and the uncertainty of the standard contributes to the uncertainties of all measured values. Their uncertainties and dependencies are then described by a variance-covariance matrix (often simply called covariance matrix)  $\mathbf{C}_y$ :

$$\mathbf{C}_y = \begin{pmatrix} \text{var}(y_1) & \text{cov}(y_1, y_2) & \cdots & \text{cov}(y_1, y_n) \\ \text{cov}(y_2, y_1) & & & \\ \vdots & & & \\ \text{cov}(y_n, y_1) & \dots\dots\dots & & \text{var}(y_n) \end{pmatrix} \quad (3.13)$$

In the case of independent data, only the diagonal elements (variances) have to be considered. However, covariances (off-diagonal elements) can occur between quantities deduced from the independent data. These covariances can then be estimated according to the generalized rules of error propagation discussed below. The covariance matrix is symmetrical ( $\text{cov}(y_i, y_j) = \text{cov}(y_j, y_i)$ ) and frequently correlation coefficients are used to describe the dependency of  $y_i$  and  $y_j$  :

$$\text{corr}(y_i, y_j) = \frac{\text{cov}(y_i, y_j)}{\sqrt{\text{var}(y_i)} \cdot \sqrt{\text{var}(y_j)}} = \frac{\text{cov}(y_i, y_j)}{\Delta y_i \cdot \Delta y_j} \quad (3.14)$$

If weights are to be applied to the measured data  $y$  e.g., to calculate a weighted mean value, a weight matrix  $\mathbf{W}$ , calculated as the inverted of the covariance matrix ( $\mathbf{W} = \mathbf{C}_y^{-1}$ ) is used. With this weight matrix the weighted mean is then calculated as described e.g., by Brandt (1999):

$$\bar{y} = -(\mathbf{a}^T \mathbf{W} \mathbf{a})^{-1} (\mathbf{a}^T \mathbf{W} \mathbf{y}) \quad (3.15)$$

The vector  $\mathbf{a}$  in this case is a single column vector

$$\mathbf{a} = \begin{pmatrix} -1 \\ \vdots \\ -1 \end{pmatrix} \quad (3.16)$$

### 3.4 Uncertainty Estimation for EA-IRMS Measurement Results ( $\delta^{13}\text{C}$ and $\delta^{15}\text{N}$ )

and  $\mathbf{a}^T$  is its transposed. In the case of independent  $y_i$  the covariance matrix is a diagonal matrix with the squares of the uncertainties  $\Delta y_i^2$  as diagonal elements and hence its inverted, the weight matrix  $\mathbf{W}$ , consists of the inverses of the squares of the uncertainties as diagonal elements and is zero elsewhere. As can be seen easily, Equation 3.15 then becomes the well known formula

$$\bar{y} = \left( \sum_{i=1}^n \Delta y_i^{-2} \right)^{-1} \cdot \sum_{i=1}^n (\Delta y_i^{-2} \cdot y_i) \quad (3.17)$$

To check the consistency of the data (within their uncertainties and covariances) the reduced  $\chi^2$  value can be calculated according to Equation 3.18, where  $\boldsymbol{\varepsilon}$  is the vector of the residuals (differences between the individual measurements  $y_i$  and the weighted mean) and  $\boldsymbol{\varepsilon}^T$  its transposed.  $\mathbf{W}$  is the weight matrix and  $f$  is the number of the degrees of freedom, which is  $n - 1$ , if a mean of  $n$  measurement values is calculated.

$$\chi_{red}^2 = \frac{\boldsymbol{\varepsilon}^T \mathbf{W} \boldsymbol{\varepsilon}}{f} \quad (3.18)$$

The square root of the reduced  $\chi^2$  can be interpreted as the ratio of the external (an uncertainty estimated from the scatter of the data) to the internal uncertainty (an uncertainty calculated from the individual uncertainties  $\Delta y_i$ ) and should be approximately one. There does not exist a general rule how to proceed, if  $\chi_{red}^2$  is significantly larger than unity, but individual solutions have to be found. How to treat data with inconsistent uncertainties will be discussed below. The internal uncertainty can be calculated using the weight matrix  $\mathbf{W}$  and the vector  $\mathbf{a}$  as given in Equation 3.16:

$$\Delta \bar{y} = \sqrt{(\mathbf{a}^T \mathbf{W} \mathbf{a})^{-1}} \quad (3.19)$$

#### Calculation of a linear fit through data points

The second procedure, which was applied in the determination of  $\delta$ -values, was fitting a straight line or linear function to a set of data points  $(x_i, y_i)$  (linear regression). In this case, the linear regression yields a calibration function through data points consisting of the measured ( $x$ ) and certified ( $y$ )  $\delta$ -values of the reference materials. For this, standard least-squares procedures were used as described e.g., by Brandt (1999), where it is assumed that the uncertainties of the  $y$ -values or the covariance matrix  $\mathbf{C}_y$  in case of correlated  $y$ -values are known or can be calculated, and that the  $x$ -values of the data points are known exactly (without uncertainties). The latter assumption is not valid in the case discussed here, since the measured  $\delta$ -values have uncertainties. Therefore the uncertainties of the  $x$ -values were transformed to  $y$ -value uncertainties (see Section 3.4.2). The fitting procedure results in a linear function described by the parameters  $a$  and  $b$ :

$$y = a + b \cdot x \quad (3.20)$$

The least-squares formalism provides "best estimates" for the parameters  $a$  and  $b$  given by the following equation:

$$\begin{pmatrix} a \\ b \end{pmatrix} = -(\mathbf{A}^T \mathbf{W} \mathbf{A})^{-1} (\mathbf{A}^T \mathbf{W} \mathbf{y}) \quad (3.21)$$

### 3 Methods

Here the vector  $\mathbf{y}$  contains the certified  $\delta$ -values of the reference materials ( $y$ -values), the weight matrix  $\mathbf{W}$  is the inverted of the corresponding covariance matrix  $\mathbf{C}_y$  and the matrix  $\mathbf{A}$  contains the measured  $\delta$ -values ( $x$ -values).

$$\mathbf{A} = - \begin{pmatrix} 1 & x_1 \\ \vdots & \vdots \\ 1 & x_n \end{pmatrix} \quad (3.22)$$

The linear function parameters  $a$  and  $b$  are derived from measured data and therefore also have uncertainties and in general they are correlated, even if the input data  $y_i$  are independent. Their covariance matrix  $\mathbf{C}(a, b)$  is given by Equation 3.23.

$$\mathbf{C}_{(a,b)} = (\mathbf{A}^T \mathbf{W} \mathbf{A})^{-1} \quad (3.23)$$

To check the consistency of the data also for the linear fit, the reduced  $\chi^2$  value can be calculated according to Equation 3.18. The vector of the residuals  $\varepsilon$  is calculated as the differences of the  $y$ -values of the individual data points and the expected values according to the fitted linear function. The number of the degrees of freedom  $f$  is in this case  $n - 2$  with  $n$  the number of data points.

#### Propagation of Uncertainties

If the data are not independent, the rules of error propagation can be generalized to the propagation of variances and covariances in the following way: Let  $f$  be a function depending on the variables  $y_1, y_2, \dots, y_n$ . Then the variance (or square of the uncertainty) of this function is given by:

$$\text{var}(f) = \Delta f^2 = \sum_{i=1}^n \sum_{j=1}^n \frac{\partial f}{\partial y_i} \frac{\partial f}{\partial y_j} \text{cov}(y_i, y_j) \quad (3.24)$$

In the case of independent  $y_i$  (i.e.,  $\text{cov}(y_i, y_j) = 0$ , for  $i \neq j$ ) Equation 3.24 becomes the usual "Gaussian error propagation law" as  $\text{cov}(y_i, y_i) = \text{var}(y_i)$  and all terms with  $i \neq j$  cancel.

$$\text{var}(f) = \Delta f^2 = \sum_{i=1}^n \left( \frac{\partial f}{\partial y_i} \right)^2 \cdot \text{var}(y_i) = \sum_{i=1}^n \left( \frac{\partial f}{\partial y_i} \cdot \Delta y_i \right)^2 \quad (3.25)$$

When a second function  $g$  depending on the same variables  $y_1, y_2, \dots, y_n$  is introduced, the covariance between these two functions  $\text{cov}(f, g)$  can be calculated according to:

$$\text{cov}(f, g) = \sum_{i=1}^n \sum_{j=1}^n \frac{\partial f}{\partial y_i} \frac{\partial g}{\partial y_j} \text{cov}(y_i, y_j) \quad (3.26)$$

The covariance  $\text{cov}(f, g)$  will not be zero for independent  $y_i$ , as both  $f$  and  $g$  depend on the variables  $y_i$  and non-zero contributions to the sum in Equation 3.26 are present for  $i = j$ .

### 3.4 Uncertainty Estimation for EA-IRMS Measurement Results ( $\delta^{13}\text{C}$ and $\delta^{15}\text{N}$ )

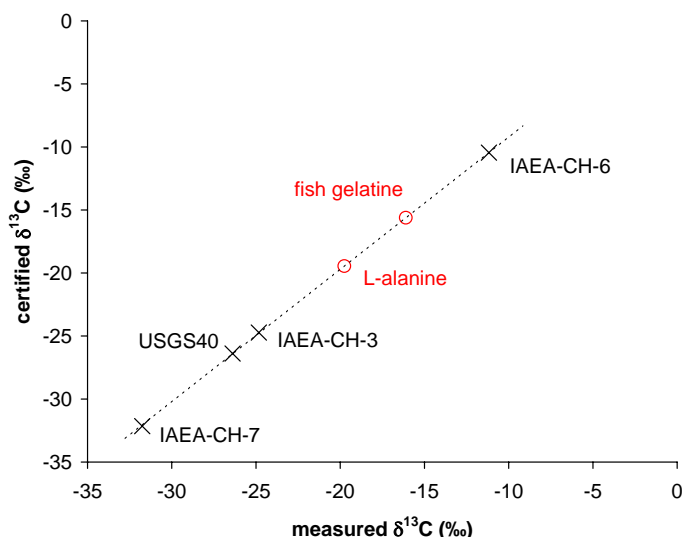


**Figure 3.8:** Normalization of laboratory standard  $\delta^{13}\text{C}$  values during the calibration procedure.

A major goal of this investigation was to trace the contributions of the initial (independent) sources of uncertainties throughout the process of  $\delta$ -value determination. The uncertainties, which had to be considered are the uncertainties of the reference material  $\delta$ -values provided by the distributor and the measurement uncertainties introduced by the precision of the individual measurements. The contributions of these sources of uncertainties were calculated individually for any intermediate and final result according to the uncertainty propagation rules. Thus, for any numerical value derived from the performed measurements, the square of the uncertainty can be represented as a quadratic sum of independent uncertainty contributions (see Section 3.4.2).

#### 3.4.2 Uncertainty Estimation for $\delta$ -values of Laboratory Standards

In order to produce laboratory standards, two organic substances (L-alanine and fish gelatin) were calibrated against various international isotope reference materials by multi-point normalization as already described in Section 3.3.2. The  $\delta$ -values and uncertainties of the used reference materials as given by the distributor are listed in Table 3.5.

Table 3.6 shows how many measurements were performed for each laboratory standard and how often a specific reference material was included in a measurement batch.

The normalization of the measured  $\delta^{13}\text{C}$  and  $\delta^{15}\text{N}$  values of the laboratory standards is depicted in Figures 3.8 and 3.9, respectively, for the case that all four reference materials were present in the measurement run.

If three or more reference materials were used, the calibration parameters  $a$  and  $b$  were derived by employing least-squares fitting procedures. It should be noted, that

**Table 3.5:** Consensus  $\delta$ -values and uncertainties of the international reference materials used for the calibration of the laboratory standards (see IAEA, 2010).

Reference Material	$\delta^{13}\text{C}$ (‰)	Uncertainty	$\delta^{15}\text{N}$ (‰)	Uncertainty
IAEA-CH-3	-24.724	0.041		
IAEA-CH-6	-10.449	0.033		
IAEA-CH-7	-32.151	0.05		
USGS40	-26.389	0.042	-4.5	0.1
IAEA-N-1			0.4	0.2
IAEA-N-2			20.3	0.2
IAEA-NO-3			4.7	0.2

**Table 3.6:** Number of measurements carried out during the calibration procedure of the laboratory standards together with the number of times a specific reference material was present (in triplicate) in a measurement batch.

Standard	$\delta^{13}\text{C}$ measurements	USGS40	IAEA-CH-6	IAEA-CH-3	IAEA-CH-7
L-alanine	8	8	8	3	1
fish gelatin	7	5	7	7	4
Standard	$\delta^{15}\text{N}$ measurements	USGS40	IAEA-N-1	IAEA-N-2	IAEA-NO-3
L-alanine	8	8	8	8	0
fish gelatin	5	3	3	5	3

the data points through which the calibration function is fitted, have uncertainties in their  $x$ -values (the measured  $\delta$ -values) as well as in their  $y$ -values (the certified  $\delta$ -values). Estimates of the measurement uncertainties were derived from the standard deviation of the 10 laboratory standard replicates present in the batch. The measurement uncertainties were transformed to the  $y$ -axis and added in quadrature to the given uncertainties of the reference materials to enable the application of standard least-squares procedures (which rely on the assumption that the abscissa data are known exactly and which use the ordinate data uncertainties to derive a weight matrix). Such a procedure has been widely adopted in nuclear reaction data measurements and evaluations. More general approaches have been extensively discussed in the metrological literature (see e.g., Krystek & Anton, 2007). The preliminary slope, which was used to convert the measurement uncertainties to the  $y$ -axis was obtained by linear regression without considering data weights. With a set of three or four measured  $\delta$ -values ( $x_i$ ) and a corresponding set of certified  $\delta$ -values ( $y_i$ ) together with the combined uncertainties  $\Delta y_i$ , the parameters  $a$  and  $b$  of the linear calibration function and their variance-covariance matrix were derived according to the weighted standard least squares fitting procedure given in Section 3.4.1. In this case, the covariance matrix needed for the fit contained only the variances of the measured  $\delta$ -values  $y_i$  as diagonal elements i.e., the squares of the combined uncertainties  $(\Delta y_i)^2$ , since the international standards are considered as independent. However, the calibration function parameters i.e., the slope and the axis intercept in the linear equation, cal-

### 3.4 Uncertainty Estimation for EA-IRMS Measurement Results ( $\delta^{13}\text{C}$ and $\delta^{15}\text{N}$ )

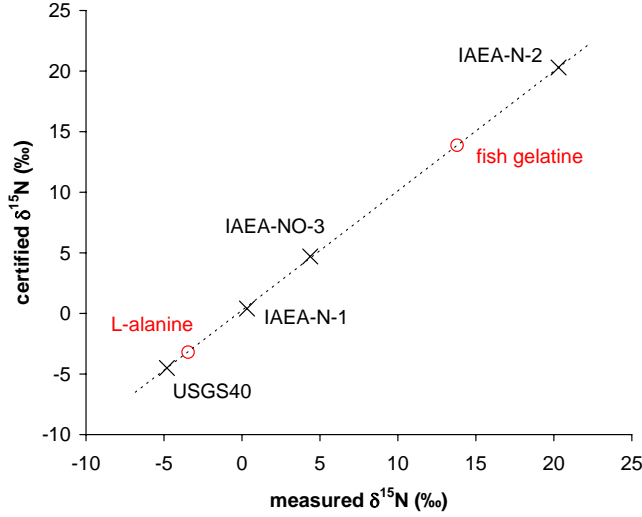


**Figure 3.9:** Normalization of laboratory standard  $\delta^{15}\text{N}$  values during the calibration procedure.

culated according to Equation 3.21 are not independent and their covariance matrix  $\mathbf{C}(a, b)$  is given by Equation 3.23 according to the rules of uncertainty propagation. This matrix contains the uncertainties  $\Delta a$  and  $\Delta b$  of the parameters  $a$  and  $b$  as well as their covariance  $\text{cov}(a, b)$ .

In measurement runs where only two international isotope standards were measured together with the replicates of the laboratory standards, the calculation of the calibration function parameters is straightforward. It does not require any least-squares fitting procedures and the covariance matrix  $\mathbf{C}(a, b)$  can be calculated according to the generalized rules of uncertainty propagation as described in Section 3.4.1.

For each measurement run, the calibration function was then applied to calculate the normalized  $\delta$ -value of the laboratory standard ( $S_L$ ). The overall uncertainty of the normalized  $\delta$ -value ( $\Delta S_L$ ) was estimated by generalized uncertainty propagation as shown in Equation 3.27, where  $\Delta x_L$  is the uncertainty associated with the laboratory standard measurement,  $\Delta a$  the uncertainty of the axis intercept and  $\Delta b$  the uncertainty of the slope of the calibration function. Apart from  $\text{cov}(a, b)$ , no other covariances arise, because  $a$  and  $b$  have been obtained from the  $\delta$ -values of the international reference materials and thus are independent from the measured  $\delta$ -value of the laboratory standard ( $x_L$ ).

$$\Delta S_L^2 = \left( \frac{\partial S_L}{\partial x} \Delta x_L \right)^2 + \left( \frac{\partial S_L}{\partial a} \Delta a \right)^2 + \left( \frac{\partial S_L}{\partial b} \Delta b \right)^2 + 2 \frac{\partial S_L}{\partial a} \frac{\partial S_L}{\partial b} \text{cov}(a, b) \quad (3.27)$$

The square of the overall uncertainty ( $\Delta S_L^2$ ) was also expressed as quadratic sum of independent uncertainty components. The primary (independent) sources of the uncertainties are the measurement uncertainty of the laboratory standard  $\Delta x_L$ , the measurement uncertainties of the  $n$  isotope reference standards (which have been transformed to the y-axis)  $\Delta S_{im}$  and the given  $\delta$ -value uncertainties of the refer-

### 3 Methods

ence materials  $\Delta S_{ic}$ . Alternatively to Equation 3.27 the overall uncertainty of the normalized  $\delta$ -value ( $\Delta S_L$ ) can also be calculated by applying the "Gaussian error propagation law":

$$\Delta S_L^2 = \left( \frac{\partial S_L}{\partial x} \Delta x_L \right)^2 + \sum_{i=1}^n \left( \frac{\partial S_L}{\partial S_i} \sqrt{\Delta S_{im}^2 + \Delta S_{ic}^2} \right)^2 \quad (3.28)$$

with  $S_i$  denoting the certified  $\delta$ -value of an individual reference material. As the uncertainty components stemming from the measurement uncertainties ( $\Delta x_L$  and  $\Delta S_{im}$ ) do not contribute to covariances amongst the individual laboratory standard measurements, they can be combined to a "statistical" (sometimes called "random") component  $\Delta S_{Ls}$ . Thus Equation 3.28 was re-arranged and the total uncertainty for the result of any of the laboratory standard measurements could be written as:

$$\begin{aligned} \Delta S_L^2 &= \left( \frac{\partial S_L}{\partial x} \Delta x_L \right)^2 + \sum_{i=1}^n \left( \frac{\partial S_L}{\partial S_i} \Delta S_{im} \right)^2 + \sum_{i=1}^n \left( \frac{\partial S_L}{\partial S_i} \Delta S_{ic} \right)^2 \\ &= \Delta S_{Ls}^2 + \sum_{i=1}^n \left( \frac{\partial S_L}{\partial S_i} \Delta S_{ic} \right)^2 \end{aligned} \quad (3.29)$$

From these independent uncertainty components, the variance-covariance matrix for each set of individual measurements of the two laboratory standards (alanine and fish gelatin) was calculated according to Equation 3.26. For the final  $\delta$ -values of the laboratory standards, a weighted mean of the results of all individual measurements was calculated according to Equation 3.15, with the vector  $\mathbf{y}$  containing the  $\delta$ -values of the laboratory standard from the single measurements. The reduced  $\chi^2$  was calculated according to Equation 3.18. As described in Section 3.4.1, its numerical value should be approximately one, indicating that the internal and the external uncertainty are about the same size. But for both  $\delta$ -values of the alanine laboratory standard and for the  $\delta^{13}\text{C}$  of the fish gelatin it was significantly larger than one. A common procedure to deal with this problem, especially if the input data are uncorrelated, is to multiply the entire variance-covariance matrix by a scaling factor  $s = \chi_{red}^2$  to force agreement between internal and external uncertainties. It must be noted that this procedure is not based on any theoretical principle, but is nothing more than increasing those uncertainties, which seem to be underestimated and that a careful inspection of the data is inevitable. (See e.g. the discussion given in Smith (1991a), Section 12.1 and the comment of Brandt (1999), Section 9.1). As "suspicious" data or outliers could not be identified, only the measurement uncertainties were enhanced by applying the scaling factor  $s$ . This can be justified by the analysis of the  $\delta$ -values, which were determined in different runs performed over a longer time period (several months). The analysis indicated larger variations on a long-term scale compared to the variation of 10 identical samples in a single measurement run, which was initially used as the estimate of the measurement uncertainty. Since the uncertainties of the IAEA standards are well known, they were not multiplied by the scaling factor. The overall uncertainty of the weighted mean of the laboratory standards was calculated using the rules of uncertainty propagation (Equation 3.24)



and afterwards split into contributions of the different independent uncertainty components (measurement and reference material uncertainties) as described above. As a result of the calibration procedure, the  $\delta$ -values of the laboratory standards are correlated with each other and with those of the international reference materials, because the same reference materials were used for the calibration of both laboratory standards. From the uncertainty components caused by the reference materials, covariances can be calculated according to Equation 3.26, which are needed for the calibration of palaeodiet samples described in the next section.

#### 3.4.3 Uncertainty Estimation for $\delta$ -values of Palaeodiet Samples

The normalization of the measured  $\delta$ -values of the investigated collagen samples followed basically the same procedure as described for the laboratory standards. As shown above, the laboratory standards are correlated with each other and with the international standards used for their calibration. Therefore the off-diagonal elements of the weight matrix for calculating the parameters of the linear normalization function for the unknown samples are different from zero. As an estimate of the measurement uncertainty for the sample runs, the standard deviation of the  $\delta$ -values of all L-alanine laboratory standards measured throughout the period of about one year, was used. This long-term variation (0.11‰ for  $\delta^{13}\text{C}$  and 0.09‰ for  $\delta^{15}\text{N}$  values) was taken as the minimum measurement uncertainty for every sample run. The standard deviation determined for the 10 laboratory standard replicates in a measurement batch was used when it was larger than the long-term variation. The overall uncertainty for a single  $\delta$ -value was estimated according to the generalized rules of error propagation and split into the different components as described above. The final  $\delta$ -value of a sample was calculated as the weighted mean of the three measurement runs according to Equation 3.15. Again, its overall uncertainty was split into the different mutually uncorrelated components. The results of this procedure are shown in Section 4.2.

### 3.5 Uncertainty Estimation for Elemental Contents

In addition to the  $\delta^{13}\text{C}$  and  $\delta^{15}\text{N}$  values, the carbon and nitrogen contents (in %wt.) were determined in the EA-IRMS measurements. The elemental contents of the samples were calculated using the mass spectrometer peak areas according to Equation 3.11. From the elemental contents, the atomic C/N ratio was calculated, since it is a widely accepted parameter for collagen quality. The uncertainties of the measured C- and N-contents and the C/N ratios were estimated on the basis of a typical measurement run as indicated below.

Ten replicates of the laboratory standard L-alanine ("M-ala") with sample weights around 950  $\mu\text{g}$  were measured together with an elemental standard ("Ala OAS"). In these measurements, carbon and nitrogen data were obtained in one sample (peak-jump mode). Table 3.7 lists the measurement results of the 10 L-alanine replicates and their respective atomic ratios.

### 3 Methods

The standard deviations ( $SD$ ) of the %C and %N data and the atomic C/N ratios were calculated according to Equation 3.30, where the  $x_i$  are the respective measured values and  $\bar{x}$  is their arithmetic mean value.

$$SD = \sqrt{\frac{1}{1-n} \sum_{i=1}^n (x_i - \bar{x})^2} \quad (3.30)$$

The calculated standard deviation was taken as a proxy for the statistical uncertainty of a single determination result respectively.

**Table 3.7:** Measured carbon and nitrogen contents and atomic C/N ratios of 10 L-alanine replicates together with the values needed in the uncertainty assessment for elemental data.

		%wt.C	%wt.N	atomic C/N
		40.6	15.6	3.0
		40.4	15.5	3.0
		41.0	15.6	3.1
		40.6	15.7	3.0
		40.7	15.7	3.0
		40.7	15.6	3.0
		40.5	15.4	3.1
		40.5	15.5	3.0
		40.5	15.3	3.1
		40.8	15.7	3.0
<i>a</i>	SD	0.2	0.1	0.02
<i>b</i>	$\bar{x}$	40.6	15.6	3.0
<i>c</i>	$SD_{rel}$ (%)	0.4	0.9	0.7
<i>d</i>	$SD_{rel}/\sqrt{10}$ (%)	0.1	0.3	0.2
<i>e</i>	$SD_{rel}/\sqrt{3}$ (%)	0.2	0.5	0.4
<i>f</i>	$\Delta_{rel}$ Ala OAS (%)	0.4	1.2	1.3
<i>g</i>	$\Delta_{rel(10)}$ M-ala (%)	0.4	1.2	1.3
<i>h</i>	$\Delta_{rel(3)}$ M-ala (%)	0.5	1.3	1.4

Line *a* in Table 3.7 shows the calculated standard deviations, in line *b* the mean %C and %N values and the mean atomic C/N ratios of the 10 replicates are given. From these mean values and the standard deviations, the relative standard deviations for each of the 3 parameters was calculated (see line *c*). According to the Gaussian error propagation law, the statistical uncertainty of an arithmetic mean can be estimated as  $SD/\sqrt{n}$ . Therefore the relative statistical uncertainty of the mean value calculated from the 10 measurement results was calculated as shown in line *d*. Since all archaeological samples were measured in triplicate, the reported carbon and nitrogen contents and consequently the C/N ratios are mean values of 3 determination results. However, a standard deviation value of only 3 measurement results is not very conclusive. Therefore, the statistical uncertainties determined for the 10 laboratory standard replicates ( $SD_{rel}$ ) were taken as the basis for the calculation of the statistical uncertainties for a mean value of 3 determination results as listed in line *d*. Other uncertainty contributions considered in this estimation were the precisions

of the elemental standard values. The certified elemental contents of Alanine OAS given by the distributor are  $(40.54 \pm 0.18) \% \text{wt.C}$  and  $(15.58 \pm 0.19) \% \text{wt.N}$ . Their respective relative uncertainties are denoted as  $\Delta_{rel}$  Ala OAS in line *f* of Table 3.7. Quadratic addition of both values gives the relative C/N uncertainty of Ala OAS. A combined uncertainty (statistical component and contribution from the elemental standard) for a final result (mean value of 10 measurement results) of M-ala was then determined by quadratic addition of  $SD_{rel}/\sqrt{10}$  and  $\Delta_{rel}$  Ala OAS for %C, %N and C/N respectively (line *g*). In the same way the combined uncertainty for the case that the mean values were determined from only 3 measurement results was calculated (see line *h*). The results of this estimation indicate that the elemental data uncertainties of M-ala are largely dominated by those of the elemental standard Ala OAS, whereas the contribution from the measurement precision influences the final uncertainty only to a minor extent.

From this it is inferred that the elemental data uncertainties of an unknown sample, which is measured with respect to M-ala as in-house elemental standard, are mainly derived from the corresponding uncertainties of M-ala, whereas the measurement uncertainty can be neglected. Hence the relative %C, %N and C/N uncertainties of an unknown sample (if measured 3 times) are assumed to be in the same range than the respective uncertainties of M-ala in line *h* of Table 3.7. For the purpose of collagen quality assessment in palaeodietary studies, C/N ratios are usually expressed to one decimal place. %C and %N values are given as integral numbers, since the accepted ranges of these quality parameters are comparatively wide (see Section 1.4.3). The uncertainties estimated in Table 3.7 are in a range, which is much smaller than the required precisions for this purpose. Therefore a sophisticated uncertainty analysis for elemental data is not considered necessary for this application.

## 3.6 Inter-Laboratory Comparison

In order to test for consistency of the determined  $\delta^{13}\text{C}$  and  $\delta^{15}\text{N}$  values, subsamples of 3 human collagen samples from Thunau were measured at the "SILVER" facility (Stable Isotope Laboratory University of Vienna Environmental Research, Faculty of Life Sciences) by EA-IRMS (*CE Instruments 1110* elemental analyzer, *Finnigan MAT Delta<sup>PLUS</sup>* isotope ratio mass spectrometer). For this reason, 5 subsamples of every collagen sample and 3 replicates of several isotope standards (M-ala laboratory standard, USGS40, IAEA: CH-3, CH-6, CH-7, N-1, N-2, NO-3) were submitted to SILVER. All standards and samples were measured in one batch measurement. The raw  $\delta$ -values of the samples were normalized with respect to all included isotope standards using multi-point normalization. The long term measurement precisions (determined by the standard deviations of the results of repeated working standard measurements) for the used EA-IRMS System at SILVER are 0.10 ‰ for  $\delta^{13}\text{C}$  and 0.15 ‰ for  $\delta^{15}\text{N}$  (personal communication Wolfgang Wanek). Table 3.8 lists the final results, which were obtained by the calculation of an arithmetic mean of the 5 measured values per sample.

The  $\delta$ -values that had previously been determined at the Faculty of Physics –

### 3 Methods

Isotope Research by the peak-jump method with a sample size of  $\sim 180\mu\text{g}$  (described in Section 3.3.1) are weighted mean values of 3 separate batch measurement results. Average measurement precisions for this method are  $0.09\text{‰}$  for  $\delta^{13}\text{C}$  and  $0.17\text{‰}$  for  $\delta^{15}\text{N}$  determined using 10 replicates of a laboratory standard per batch as given in Section 3.3.1. The mean  $\delta$ -values in Table 3.8, obtained by the two laboratories for a specific sample material, are in excellent agreement.

**Table 3.8:** Results of the inter-laboratory comparison with the stable isotope facility of the Department for Chemical Ecology and Ecosystem Research "SILVER".

Laboratory	Sample ID	$\delta^{13}\text{C}$ (‰)	$\delta^{15}\text{N}$ (‰)
Isotope Research	19	-17.55	10.34
SILVER	19	-17.58	10.47
Isotope Research	22	-17.98	8.47
SILVER	22	-18.00	8.40
Isotope Research	25	-17.73	10.45
SILVER	25	-17.80	10.55

## 4 Results and Discussion

### 4.1 Collagen Preparation Methods

The results of the comparison of collagen extraction methods, carried out as described in Section 3.1.1, are listed in Table 4.1. All investigated extraction methods yielded collagen amounts above 1 %wt. of the processed cattle bone material<sup>1</sup>. The highest yield was achieved using method 1, however, the respective sample showed the lowest carbon and nitrogen contents compared to the samples produced by the other 6 methods. This can probably be attributed to the presence of inorganic salts, which were not completely removed during the washing of the residue in the centrifugation tubes. However, this is an isolated result. For example, some of the human bone samples from Thunau were treated by method 1 at the VERA laboratory as indicated in Section 3.1.2. The carbon and nitrogen contents of the collagen samples obtained in this way (sample IDs 19 to 25 in Table 4.9) did not exhibit any systematic deviation from those of the other samples prepared with Method 2 (see Table 4.9 in Section 4.3.2).

**Table 4.1:** Results of the comparison of collagen extraction procedures using aliquots of a cattle bone. A description of the single methods is given in Table 3.1, Section 3.1.1. All values are mean values determined from the results of three separate measurements, the given uncertainties were calculated using Gaussian error propagation as described in Section 3.4.

Sample ID	Method	$\delta^{13}\text{C}$ (‰)	$1\sigma$	$\delta^{15}\text{N}$ (‰)	$1\sigma$	%wt.C	%wt.N	atomic C/N	Yield (%wt.)
1/1	1	-21.12	0.08	7.59	0.20	32.3	11.8	3.2	8
1/2	2	-21.09	0.08	7.38	0.14	42.3	15.3	3.2	5
1/3	3	-21.22	0.08	7.42	0.13	43.3	16.2	3.1	5
1/4	4	-21.10	0.08	7.67	0.16	40.7	15.0	3.2	5
1/5	5	-21.17	0.08	7.25	0.14	44.3	16.4	3.2	3
1/6	6	-21.14	0.08	7.34	0.14	41.2	15.3	3.2	4
1/7	7	-21.16	0.08	7.03	0.14	39.5	14.7	3.2	4

In all other methods, fritted filter funnels were used, which allowed the fast and efficient washing of the residue. Apart from method 1, there seems to be little difference between the collagen yields obtained with the different methods. There were no notable differences between the C/N ratios of the collagen samples produced using the

<sup>1</sup>All collagen yields in this text are expressed in %wt. of the initial bone material used for the extraction.

7 different methods.

A plot of the  $\delta$ -values measured in the collagen samples, which were prepared using extraction methods 1 to 7, is given in Figure 4.1. The determined  $\delta^{13}\text{C}$  values vary within a small range (the difference between the two extreme values is  $0.13\text{‰}$ , which is smaller than the  $2\sigma$  uncertainty of the  $\delta^{13}\text{C}$  values). This is taken as an evidence that none of the methods causes a systematic deviation of the product's  $\delta^{13}\text{C}$  with respect to the other methods. Thus, all examined methods are assumed to produce collagen  $\delta^{13}\text{C}$  values comparable to each other.

Looking at the  $\delta^{15}\text{N}$  results, which are plotted in Figure 4.1, gives the impression that most values are very similar with the exceptions of the ones obtained by methods 4 and 7. Therefore, it was tested by means of a  $\chi^2$ -Test, if the observed data-variation can still be explained by the variation originating from the measurement procedure (instrument variation, uncertainties of standards), or whether there was additional variation introduced by the different extraction methods. The  $\chi^2$  was calculated

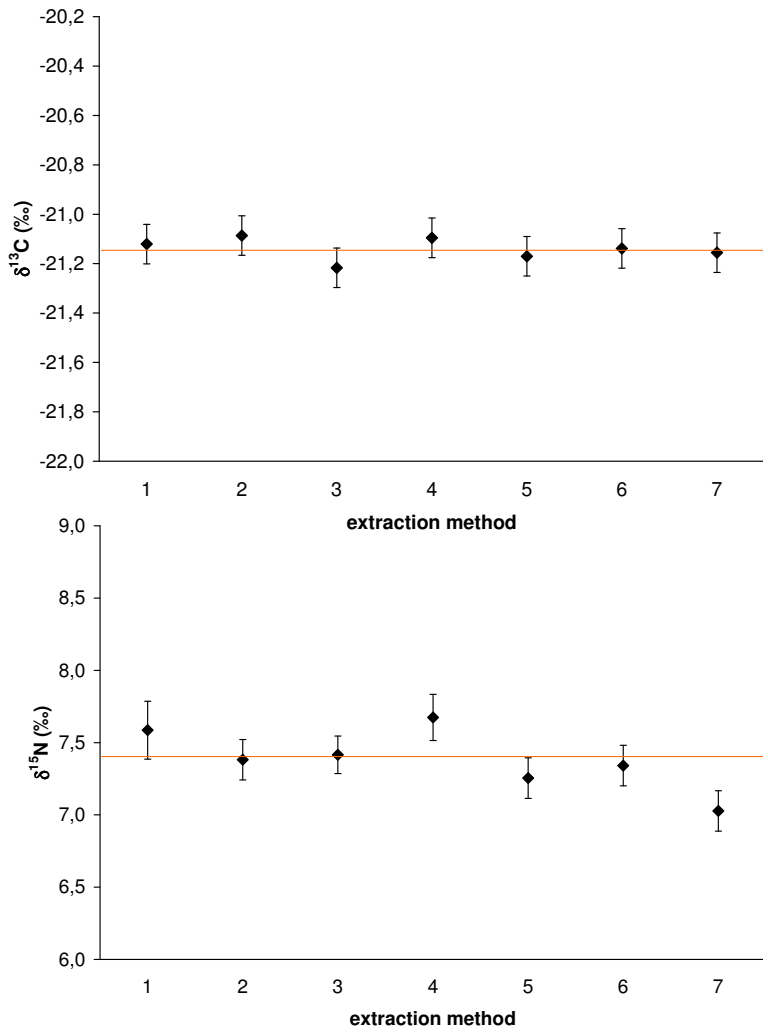


**Figure 4.1:**  $\delta$ -values of the collagen samples prepared using collagen extraction methods 1 to 7. (Error bars:  $1\sigma$  uncertainties, red line: weighted mean of the results of all samples)

according to:

$$\chi^2 = \sum_{i=1}^n \frac{(y_i - \bar{y})^2}{\sigma_i^2} \quad (4.1)$$

with  $\bar{y}$ , the arithmetic mean of the seven  $y_i$  (i.e., the  $\delta^{15}\text{N}$  values in Table 4.1) and  $\sigma_i^2$  the variance of a single  $y_i$ . For a significance level  $\alpha = 0.05$  the calculated test statistic ( $\chi_{calc}^2 = 11.50$ ) was smaller than the critical value ( $\chi_{crit}^2 = 12.59$ ) taken from a  $\chi^2$  distribution table (e.g., Bronstein *et al.*, 2000) for the respective degrees of freedom ( $f = n - 1 = 6$ ). Hence, the null hypothesis, stating that the examined  $\delta^{15}\text{N}$  values actually are different determination results originating from the same  $\delta^{15}\text{N}$  value, can be retained.

Another point to mention is that the results of the method comparison do not indicate any collagen yield reducing effect or alteration of carbon and nitrogen isotopic compositions by NaOH treatment. When the determined isotope ratios and elemental data of samples prepared with methods 3 and 5, which do not include NaOH steps, are compared with those of the other methods in Table 4.1, no evidence for a difference between the values can be found.

**Table 4.2:** Results of the comparison of drying procedures during collagen extraction. The samples were prepared using the manual collagen extraction method 2 as described in Table 3.1. Only the drying step was different for a sample pair. All values are mean values determined from the results of three separate measurements, the given uncertainties were calculated using Gaussian error propagation as described in Section 3.4.

Sample ID	Drying method	$\delta^{13}\text{C}$ (‰)	1 $\sigma$	$\delta^{15}\text{N}$ (‰)	1 $\sigma$	%wt. C	%wt. N	atomic C/N	Yield (%wt.)
3	evaporated	-19.75	0.07	10.21	0.14	44.7	16.2	3.2	12
3/1	lyophilized	-19.82	0.07	10.23	0.13	42.5	15.1	3.3	8
5	evaporated	-19.60	0.07	10.34	0.14	42.0	15.5	3.2	6
5/1	lyophilized	-19.75	0.07	10.47	0.14	43.9	15.7	3.3	6
14	evaporated	-19.94	0.07	7.68	0.12	42.0	15.2	3.2	8
14/1	lyophilized	-20.00	0.07	7.66	0.12	40.2	14.2	3.3	6
15	evaporated	-20.89	0.08	7.07	0.12	31.1	11.5	3.1	2
15/1	lyophilized	-20.71	0.08	7.31	0.12	38.1	13.6	3.3	2
37	evaporated	-18.57	0.07	8.29	0.12	46.4	16.5	3.3	16
37/1	lyophilized	-18.55	0.07	8.34	0.12	43.6	15.4	3.3	13
38	evaporated	-19.00	0.07	10.12	0.13	47.5	16.9	3.3	17
38/1	lyophilized	-18.98	0.07	10.09	0.13	44.9	15.9	3.3	15
39	evaporated	-18.04	0.07	10.50	0.14	43.2	15.5	3.3	3
39/1	lyophilized	-17.88	0.07	10.69	0.14	42.2	15.2	3.2	3

### Comparison of Drying Procedures

Table 4.2 lists  $\delta^{13}\text{C}$ ,  $\delta^{15}\text{N}$  and the collagen quality parameters determined for sample pairs (each pair originating from one bone specimen), where one collagen sample was

dried by evaporation and one by lyophilization, all other steps being equal. The  $\delta$ -values from the table are plotted in Figure 4.2. They are in good agreement (within their  $2\sigma$  uncertainties) for every sample pair. Thus, it is concluded that  $\delta^{13}\text{C}$  and  $\delta^{15}\text{N}$  values of collagen samples prepared using an evaporation step and samples dried by lyophilization do not systematically deviate from each other.

### Comparison of Semi-automated and Manual Collagen Extraction

The data obtained from a comparison of the semi-automated collagen extraction and the manual method 2 can be found in Table 4.3. For each sample triple the  $\delta$ -values were plotted in Figure 4.3. Apart from sample 84, whose  $\delta^{13}\text{C}$  value seems to deviate slightly from that of the aliquots extracted manually, the values match well within their uncertainties and do not show any systematic deviation from each other. Also the excellent reproducibility of  $\delta$ -values, atomic C/N ratios and collagen yields for repeated extractions using the manual method can be seen from the results in Table 4.3.

**Table 4.3:** Results of the comparison of semi-automated and manual collagen extraction. All values are mean values determined from the results of three separate measurements, the given uncertainties were calculated using Gaussian error propagation as described in Section 3.4.

Sample ID	Method	$\delta^{13}\text{C}$ (‰)	$1\sigma$	$\delta^{15}\text{N}$ (‰)	$1\sigma$	%wt. C	%wt. N	atomic C/N	Yield (%wt.)
63	automated	-20.19	0.08	10.44	0.14	41.3	15.0	3.2	6
63/1	manual	-20.08	0.08	10.55	0.13	41.6	15.1	3.2	5
63/2	manual	-20.20	0.08	10.68	0.13	42.7	15.3	3.3	5
65	automated	-19.98	0.08	10.04	0.13	39.3	14.3	3.2	11
65/1	manual	-19.93	0.08	10.05	0.13	44.0	15.9	3.2	9
65/2	manual	-19.94	0.08	10.21	0.13	41.7	15.0	3.2	9
78	automated	-20.08	0.08	9.60	0.13	43.0	15.6	3.2	15
78/1	manual	-20.12	0.08	9.58	0.13	44.7	16.0	3.3	15
78/2	manual	-20.05	0.08	9.76	0.13	44.4	15.9	3.3	15
84	automated	-19.45	0.09	10.29	0.14	36.6	13.5	3.2	3
84/1	manual	-19.80	0.08	10.03	0.13	39.0	14.2	3.2	2
84/2	manual	-19.82	0.08	9.97	0.13	39.9	14.6	3.2	2

### Conclusions of the Method Comparison

According to the results of the comparison of seven collagen extraction procedures based on published methods (with and without NaOH treatment and some methods containing ultrafiltration steps), the  $\delta^{13}\text{C}$  values in the produced samples did not significantly differ from each other. The obtained  $\delta^{15}\text{N}$  values were slightly more variable, but still, this variation could be explained by uncertainties inherent to the measurement method. The collagen quality parameters (carbon and nitrogen



contents, atomic C/N and collagen yield) were within the commonly accepted ranges for all produced collagen samples. These results confirm the suitability of all tested methods for the extraction of bone collagen for palaeodietary reconstruction.

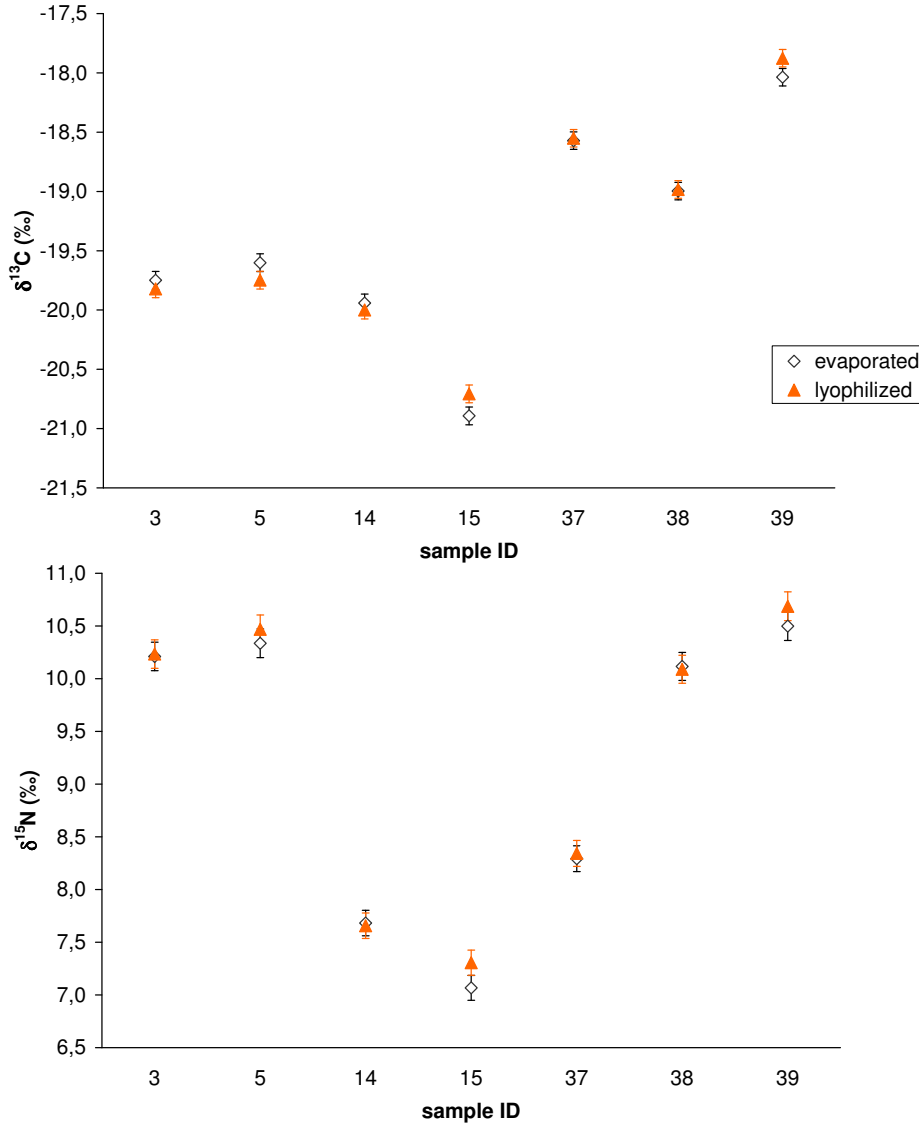


**Figure 4.2:** Comparison of drying procedures for collagen extraction. (Error bars:  $1\sigma$  uncertainties)

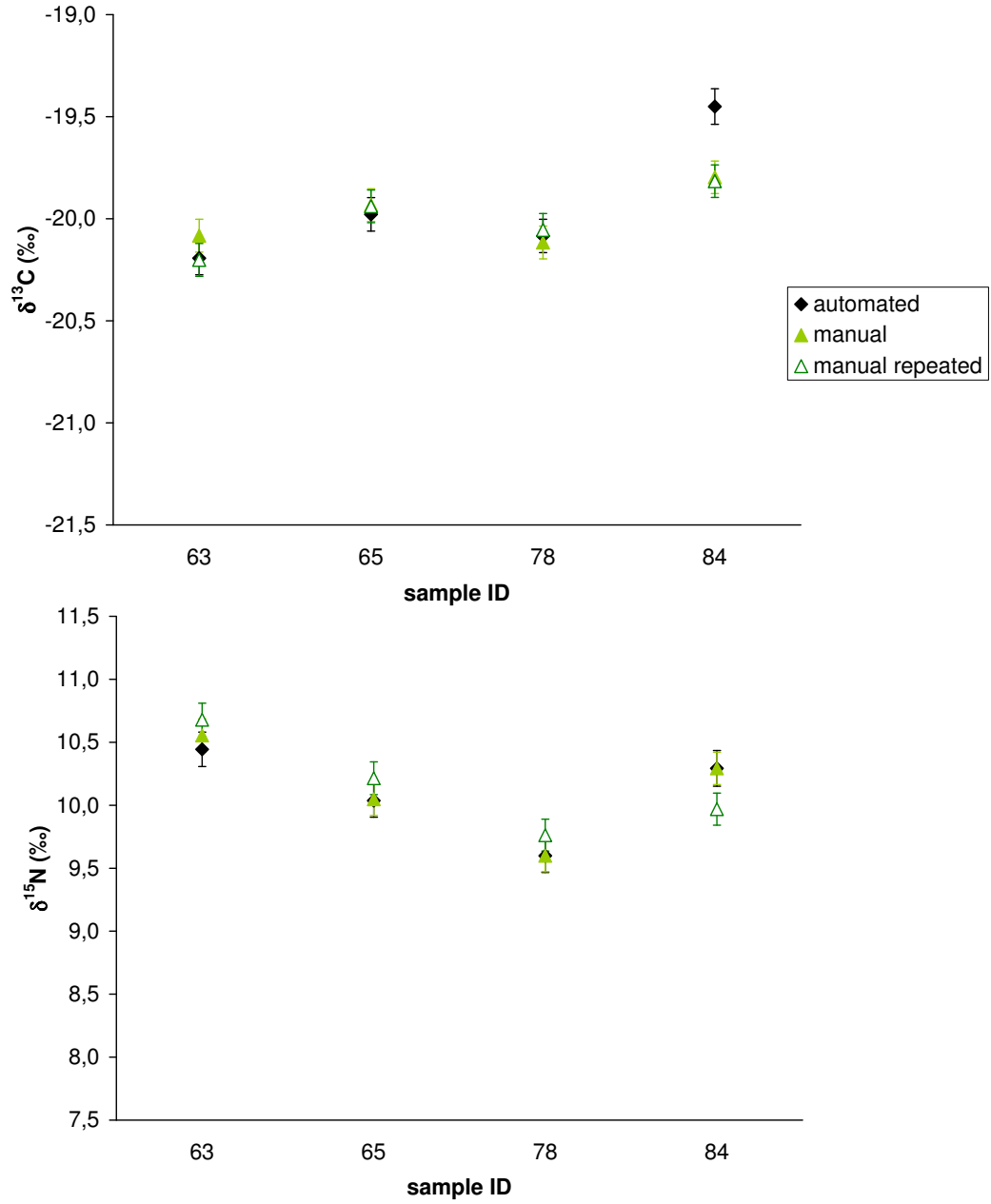


**Figure 4.3:** Results of the comparison of the semi-automated and manual collagen extraction procedures. (Error bars:  $1\sigma$  uncertainties)

## 4.2 Uncertainty analysis

### 4.2.1 Laboratory Standards

Table 4.4 lists the results of the calibration procedures for the alanine and fish gelatin laboratory standards. The given uncertainty components, determined according to Equation 3.29, are independent (i.e., uncorrelated) and thus add up quadratically to the overall uncertainty. The component denoted as "statistical" includes the measurement uncertainties of the laboratory standard replicates and the international reference materials used in the calibration procedure and does not contribute to the covariance between the two laboratory standards. The other columns of the table contain further uncertainty components named after the individual reference materials. They denote the contributions from the uncertainties of the certified  $\delta$ -values provided by the distributor. The  $\delta^{15}\text{N}$  values of both laboratory standards show larger uncertainties than the respective  $\delta^{13}\text{C}$  values. This is caused by the larger  $\delta^{15}\text{N}$  uncertainties of the available reference materials (see Table 3.5) compared to those of the  $\delta^{13}\text{C}$  reference materials.

**Table 4.4:**  $\delta^{13}\text{C}$  and  $\delta^{15}\text{N}$  values of the calibrated laboratory standards with their  $1\sigma$  uncertainties and the different independent uncertainty components, which add up quadratically to the  $1\sigma$  uncertainty. For the uncertainty components, four positions after the decimal point are shown so that the smallest contribution, which lies in the range of  $10^{-4}$ , can be displayed.

Standard	$\delta^{13}\text{C}$ (‰)	$1\sigma$	Uncertainty components				
			Statistical	USGS40	IAEA-CH-6	IAEA-CH-3	IAEA-CH-7
L-alanine	−19.45	0.04	0.0331	0.0169	0.0127	0.0058	0.0005
fish gelatin	−15.61	0.05	0.0415	0.0045	0.0197	0.0088	0.0005

Standard	$\delta^{15}\text{N}$ (‰)	$1\sigma$	Uncertainty components				
			Statistical	USGS40	IAEA-N-1	IAEA-N-2	IAEA-NO-3
L-alanine	−3.19	0.10	0.0406	0.0797	0.0374	0.0032	
fish gelatin	13.88	0.14	0.0253	0.0065	0.0193	0.1307	0.0371

The magnitudes of the individual uncertainty contributions are largely influenced by the position of the laboratory standard's  $\delta$ -value on the regression line relative to that of the reference materials that were used for the calibration. The smaller its distance to the  $\delta$ -value of a specific reference material is, the larger is the contribution of the respective reference material. Another influencing factor, besides the uncertainties of the international standard's  $\delta$ -values, is the number of times a certain reference material was used in the calibration process. The more often an international standard is present in the measurements, the larger is its contribution to the total uncertainty of the calibrated laboratory standard's value (see Table 4.4). It can be seen from this table that the statistical component accounts for the major part of the overall  $\delta^{13}\text{C}$  uncertainties. Whereas in the case of the  $\delta^{15}\text{N}$  uncer-

tainty of the L-alanine standard it is only the second largest contribution after the USGS40-component. The  $\delta^{15}\text{N}$  uncertainty of fish gelatin is mainly caused by the corresponding uncertainty of IAEA-N-2, since its  $\delta^{15}\text{N}$  value is rather close to that of the fish gelatin (see Figure 3.9). The correlations between the individual isotope standards determined from the "non-statistical" uncertainty components given in Table 4.4 according to Equations 3.26 and 3.14 are displayed in Table 4.5 ( $\delta^{13}\text{C}$ ) and Table 4.6 ( $\delta^{15}\text{N}$ ). The numerical value of a correlation strongly depends on the same parameters, which also determine the magnitude of the uncertainty components (the position of the laboratory standard's  $\delta$ -value on the regression line, the number of times a reference material is used during the calibration process and the uncertainty of a reference material's  $\delta$ -value). In this regard, note the large correlation (94%) of fish gelatin with IAEA-N-2 in Table 4.6.

**Table 4.5:** Correlation coefficients between the  $\delta^{13}\text{C}$  values of the laboratory standards and the international reference materials in percent. Only the upper triangle of the symmetric matrix is displayed.

	L-alanine	fish gelatin	USGS40	IAEA-CH-6	IAEA-CH-3	IAEA-CH-7
L-alanine	100	20	43	32	15	1
fish gelatin		100	10	42	19	1
USGS40			100	0	0	0
IAEA-CH-6				100	0	0
IAEA-CH-3					100	0
IAEA-CH-7						100

**Table 4.6:** Correlation coefficients between the  $\delta^{15}\text{N}$  values of the laboratory standards and the international reference materials in percent.

	L-alanine	fish gelatin	USGS40	IAEA-N-1	IAEA-N-2	IAEA-NO-3
L-alanine	100	12	82	39	3	0
fish gelatin		100	5	14	94	27
USGS40			100	0	0	0
IAEA-N-1				100	0	0
IAEA-N-2					100	0
IAEA-NO-3						100

### 4.2.2 Palaeodiet Samples

Table 4.7 shows a few typical examples of final  $\delta$ -values of palaeodiet samples determined as weighted means of three measurement results. The component called "stat." includes the uncertainty associated with the measurements of the sample and the standards used in these determinations. "M-ala" and "fish gelatin" are the contributions of the laboratory standard's measurement uncertainties and of the international reference materials originating from the respective laboratory standard

**Table 4.7:** Final  $\delta^{13}\text{C}$  and  $\delta^{15}\text{N}$  values of typical samples with their  $1\sigma$  uncertainties and the respective independent uncertainty components, which add up quadratically to the overall  $1\sigma$  uncertainty. For the uncertainty components four positions after the decimal point are shown so that the smallest contribution, which lies in the range of  $10^{-4}$ , can be displayed.

Sample- ID	$\delta^{13}\text{C}$ (‰)	$1\sigma$	Stat.	USGS40	CH-6	CH-3	CH-7	M-ala	fish gelatin
31	-22.29	0.08	0.0690	0.0267	0.0075	0.0030	0.0003	0.0174	
156	-22.12	0.09	0.0724	0.0210	0.0075	0.0084	0.0007	0.0397	0.0070
116	-21.32	0.09	0.0731	0.0204	0.0091	0.0069	0.0006	0.0401	0.0109
151	-20.89	0.08	0.0706	0.0187	0.0099	0.0077	0.0006	0.0350	0.0073
109	-20.75	0.08	0.0719	0.0192	0.0102	0.0067	0.0006	0.0374	0.0096
28	-19.87	0.07	0.0682	0.0208	0.0121	0.0029	0.0002	0.0166	
138	-19.29	0.08	0.0690	0.0156	0.0129	0.0067	0.0005	0.0290	0.0077
55	-18.16	0.07	0.0679	0.0156	0.0153	0.0039	0.0003	0.0135	0.0071
133	-17.76	0.08	0.0682	0.0127	0.0159	0.0058	0.0004	0.0231	0.0081
50	-17.58	0.07	0.0684	0.0152	0.0164	0.0028	0.0002	0.0158	
51	-16.27	0.07	0.0688	0.0120	0.0189	0.0027	0.0002	0.0153	
Sample- ID	$\delta^{15}\text{N}$ (‰)	$1\sigma$	Stat.	USGS40	N-1	N-2	NO-3	M-ala	fish gelatin
28	4.01	0.11	0.0567	0.0514	0.0356	0.0616		0.0120	
31	4.80	0.11	0.0568	0.0483	0.0355	0.0680		0.0113	
116	5.82	0.11	0.0557	0.0410	0.0279	0.0705	0.0196	0.0192	0.0133
109	6.23	0.11	0.0557	0.0393	0.0274	0.0735	0.0204	0.0182	0.0139
156	7.25	0.11	0.0585	0.0349	0.0264	0.0812	0.0227	0.0158	0.0155
151	8.05	0.12	0.0588	0.0315	0.0255	0.0871	0.0244	0.0139	0.0166
133	9.49	0.12	0.0595	0.0253	0.0240	0.0979	0.0275	0.0104	0.0188
51	9.56	0.13	0.0580	0.0293	0.0349	0.1065		0.0074	
55	10.38	0.13	0.0573	0.0221	0.0312	0.1075	0.0172	0.0049	0.0117
138	11.36	0.14	0.0606	0.0173	0.0220	0.1118	0.0316	0.0060	0.0215
50	11.44	0.14	0.0587	0.0218	0.0347	0.1217		0.0058	

calibration. Here these two components have to be treated as non-statistical contributions as they contribute to the uncertainties of all palaeodiet samples calibrated against them. The other uncertainty components (named after the international reference materials) comprise the contributions of the respective international standard's uncertainty originating from the sample measurement and from the laboratory standard calibration process.

From the uncertainty components given in Table 4.7, which represent the associated "error matrix", covariances between individual sample results can be derived according to Equation 3.26. This might be of interest, if further statistical procedures are applied, as some statistical procedures require that correlations within the studied data set are small.

Similar to the results of the laboratory standard calibration, the overall  $\delta^{13}\text{C}$  uncertainties of the samples were mainly caused by the "statistical" component and the biggest contribution to the  $\delta^{15}\text{N}$  uncertainties came from the  $\delta^{15}\text{N}$  uncertainty

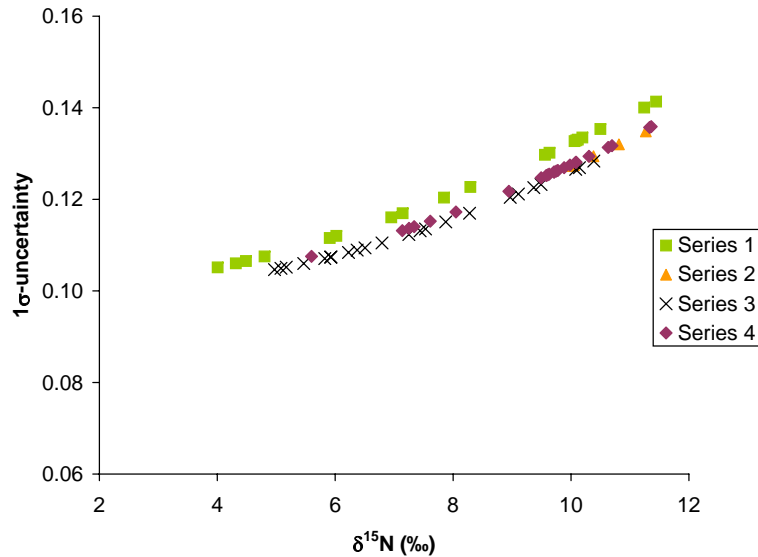


**Figure 4.4:** Dependency of the final uncertainty of a sample on its numerical  $\delta^{15}\text{N}$  value, found in the data of this study. The samples combined in one batch were measured three times on different days using the same combination of isotope standards. The final  $\delta^{15}\text{N}$  value of a sample, plotted in this diagram, is a weighted mean of the three determinations. The small – almost negligible – offset between the different series along the y-axis is an effect of variations in the standard sets used for normalization from one series to another.

of an international reference material's certified value. The reference material that contributed to the highest degree to the  $\delta^{15}\text{N}$  uncertainties of the samples was the IAEA-N-2 standard. Although the  $\delta^{15}\text{N}$  value of the NO-3 standard matches best with the  $\delta^{15}\text{N}$  values of the samples, no significant contribution was generated by this standard, as it was never directly employed in the sample measurements and in the calibration of L-alanine. Further it was seldom used in the calibration of the fish gelatin. In contrast, the N-2 standard was present in many sample measurements and used as an anchor point in the calibration of both laboratory standards. Consequently this standard has the biggest influence on the sample uncertainties, with the magnitude of the contribution depending on the numerical  $\delta^{15}\text{N}$  value of the sample. The closer a sample's  $\delta^{15}\text{N}$  value matches the value of the N-2 standard, the larger is the magnitude of the N-2 contribution, which is also reflected in the final uncertainties. This is depicted in Figure 4.4, where the final uncertainties of the samples from four "measurement series" are plotted against their  $\delta^{15}\text{N}$  values. A series comprises 3 determinations of a sample batch, for which the same combination of isotope standards was used. From Figure 4.4 it is evident, that the lower  $\delta^{15}\text{N}$  values as e.g., found in herbivore collagen, were determined with smaller uncertainties than the higher ones (closer to that of the N-2 standard) in the range of omnivore/carnivore collagen. This finding is a consequence of the chosen measurement protocol and is mainly caused by the selection of the reference materials used for the normalization of the laboratory standards and the  $\delta$ -values of the samples to the international isotope scales.

### 4.2.3 Conclusions

An in-depth error propagation study was performed to investigate the uncertainties as they arise in the determination of  $\delta^{13}\text{C}$  and  $\delta^{15}\text{N}$  values, when multi-point normalization of the  $\delta$ -values is used. This study contains a quantification of the influence of correlated uncertainties, which are a consequence of the calibration and normalization procedures, on the final uncertainties of sample  $\delta$ -values. The uncertainties of  $\delta$ -values, determined in collagen samples for a palaeodiet study, were assessed using a method, that allowed the tracing of different uncertainty components arising from the precision of the measurement and from the uncertainties of the used isotope standard  $\delta$ -values, throughout the entire evaluation process. The contributions of the individual uncertainty components were investigated, from the calibration of the laboratory standards to the calculation of the weighted means of triplicate  $\delta$ -value determinations for real samples. At each step of this process, numerical values for the correlations between the standards, which had been introduced due to normalization to the same reference materials, and also between the different measurement runs for a sample batch were calculated and considered during the normalization and the calculation of weighted means of the  $\delta$ -values. The combination of isotope reference materials chosen for the calibration of laboratory standards influences the final  $\delta$ -value uncertainty of the samples normalized with respect to these laboratory standards. Furthermore, the uncertainty of a  $\delta$ -value is affected by the position of the  $\delta$ -value on the regression line with respect to the anchor points. The uncertainties of the  $\delta^{13}\text{C}$  values are mainly caused by the respective statistical components resulting from the measurement process, since the certified  $\delta$ -values of the used international  $\delta^{13}\text{C}$  reference materials are very precise. However, the  $\delta$ -values of the available  $\delta^{15}\text{N}$  reference materials show significantly larger uncertainties and thus more strongly affect the uncertainties of the determined  $\delta^{15}\text{N}$  values. Consequently the uncertainties of sample  $\delta^{15}\text{N}$  values can be underestimated, when only the statistical component is considered. However, the final uncertainties obtained in this analysis are small in magnitude compared to the variation in  $\delta$ -values relevant for diet interpretation. The investigated correlations had an enlarging effect on the uncertainties of the normalized  $\delta$ -values, but this effect was small. Hence, the overall uncertainties of the sample  $\delta$ -values can in most cases be neglected for further statistical examination like the comparison of group means, as it is frequently employed in the area of palaeodietary studies. For certain applications it is though useful to have accurate estimates of uncertainties e.g., when the reproducibility of sample  $\delta$ -values within a laboratory or between different laboratories is investigated, since the underestimation of uncertainties might imply a false disagreement of the measured values.

### 4.3 Palaeodiet Reconstruction for the Skeletal Samples from Thunau/Gars am Kamp

Each measured sample from Thunau was evaluated for its collagen integrity using the yield of the extraction procedure, the carbon and nitrogen contents and the atomic C/N ratio, which together are widely accepted parameters for collagen quality assessment in palaeodiet studies as described in Section 1.4.3 (Ambrose, 1990; DeNiro & Epstein, 1981; van Klinken, 1999). All bone samples from Thunau yielded collagen exceeding 1 %wt. of the processed bone material. Carbon and nitrogen contents are within the ranges found in modern collagen and C/N ratios between 3.1 and 3.3 were obtained (see Tables 4.8 and 4.9). Thus, all collagen samples from Thunau fulfilled the necessary quality criteria.

#### 4.3.1 Stable Isotope Data of the Animal Remains

The results of the EA-IRMS measurements of the animal collagen samples are listed in Table 4.8. All  $\delta$ -values are reported as weighted mean values of three separate measurement results and the given  $1\sigma$  uncertainties were calculated as specified in Section 3.4. Carbon and nitrogen contents and the atomic C/N ratios are arithmetic mean values of three measurement results and the relative uncertainties for these three quantities were estimated to be approximately 1 % (see Table 3.7). In Figure 4.5, the obtained  $\delta^{13}\text{C}$  values of the animal and human collagen samples are plotted against the  $\delta^{15}\text{N}$  values. The diagram shows that the animal  $\delta^{13}\text{C}$  values span a range over 4 ‰ from -22.3 ‰ to -18.3 ‰. Since the carbon stable isotope signatures of pre-industrial  $\text{C}_3$  plants most likely ranged between -34 ‰ and -18 ‰ (see Section 1.4.1) and the plant to collagen spacing for herbivore  $\delta^{13}\text{C}$  is generally assumed to be approximately +5 ‰, the determined  $\delta^{13}\text{C}$  values of the animal samples fall within the expected range for consumers of  $\text{C}_3$  plants. Also the  $\delta^{13}\text{C}$  values of the omnivorous animals like pigs were found within this range, which is concordant to the prevailing evidence in literature demonstrating that  $\delta^{13}\text{C}$  increases only slightly with increasing trophic level (e.g., Bocherens & Drucker, 2003).

All animals show  $\delta^{15}\text{N}$  values between 4.0 ‰ and 10.1 ‰ and herbivorous and omnivorous animals cannot clearly be distinguished by their  $\delta^{15}\text{N}$  values. The highest  $\delta^{15}\text{N}$  value found in this sample set belongs to a bird, most likely a domestic fowl. The three bear samples exhibit the lowest  $\delta^{15}\text{N}$  values of all investigated animal samples (all three around 4 ‰), which points to a purely herbivorous diet. Since both  $\delta$ -values of all three specimen cluster tightly together, the individual animals probably had very similar diets.



**Table 4.8:** Results of the stable isotope analysis of the animal bone collagen samples from Thunau. In column 3 the exact find spots of the samples within the archaeological site are given for information (FMA=Frühmittelalter, Early Medieval). Apart from one sample (sample ID 33), which originates from the valley area, all animal bones were recovered at the Schanzberg area (personal communication Hajnalka Herold, Institute for Prehistoric and Medieval Archaeology, University of Vienna).

Sample-ID	Find-Nr.	Excavation area	Species	Bone	Yield (%wt.)	%wt. C	%wt. N	atomic C/N	$\delta^{13}\text{C}$ (‰)	1 $\sigma$	$\delta^{15}\text{N}$ (‰)	1 $\sigma$
28	46471	Siedlung	<i>Ursus arctos</i>	Metapodium	13	46.1	16.6	3.2	-19.87	0.07	4.01	0.11
29	38036	Gräberfeld	<i>Ursus arctos</i>	Metapodium	2	36.9	13.9	3.1	-19.80	0.07	4.31	0.11
30	38135	StF.13	<i>Ursus arctos</i>	Metapodium	3	41.4	15.4	3.1	-19.71	0.07	4.49	0.11
31	49077	Siedlung	<i>Cervus elaphus</i>	Phalanx	15	45.7	16.5	3.2	-22.29	0.08	4.80	0.11
32	49078	Siedlung	<i>Sus scrofa dom.</i>	Phalanx	2	35.9	13.6	3.1	-20.34	0.07	5.91	0.11
33	57	Schmiedsprunggasse	<i>Ovis orientalis aries/</i> <i>Capra aegagrus hircus</i>	Radius	8	45.1	16.4	3.2	-19.85	0.07	7.85	0.12
34	36693	Gräberfeld	<i>Ovis orientalis aries</i>	Radius	7	42.2	15.3	3.2	-19.95	0.07	6.02	0.11
35	38437	Gräberfeld	<i>Bos taurus</i>	Mandibula	1	38.5	13.9	3.2	-19.18	0.07	7.14	0.12
36	35445	Siedlung	<i>Bos taurus</i>	Os coxae	2	36.2	13.5	3.1	-20.50	0.07	6.95	0.12
109	41819	Grubenhaus FMA	<i>Bos taurus</i>	Radius	3	38.0	13.8	3.2	-20.75	0.08	6.23	0.11
110	53465	Grube 1, Kontrollprofil	<i>Bos taurus</i>	Metacarpus	6	38.7	14.2	3.2	-18.31	0.08	7.53	0.11
111	43921	Palisade	<i>Bos taurus</i>	Radius	4	38.2	13.9	3.2	-20.30	0.08	6.51	0.11
112	52266	Grube 1	<i>Bos taurus</i>	Costa	5	39.6	14.3	3.2	-20.67	0.08	6.79	0.11
113	53076	Verfärbung 1/A	<i>Bos taurus</i>	Mandibula	17	44.5	16.2	3.2	-19.16	0.08	7.44	0.11
115	45211	Palisade (Nr. 2)	<i>Bos taurus</i>	Metatarsus	7	40.9	15.0	3.2	-20.80	0.08	7.25	0.11
116	52808	Grube 1, Riegel 319/318	<i>Ovis orientalis aries/</i> <i>Capra aegagrus hircus</i>	Metacarpus	4	38.6	13.6	3.3	-21.32	0.09	5.82	0.11
117	52808	Grube 1, Riegel 319/318	<i>Ovis orientalis aries/</i> <i>Capra aegagrus hircus</i>	Tibia	4	39.9	14.4	3.2	-20.60	0.08	7.88	0.12
118	41108	Grubenhaus FMA	<i>Ovis orientalis aries/</i> <i>Capra aegagrus hircus</i>	Radius	9	42.3	15.3	3.2	-20.51	0.08	6.37	0.11
119	43584	Grubenhaus FMA	<i>Capra aegagrus hircus</i>	Maxilla	16	43.9	15.9	3.2	-20.40	0.08	8.28	0.12
120	41834	Grubenhaus FMA	<i>Sus scrofa dom.</i>	Radius	5	42.1	15.2	3.2	-21.03	0.09	8.97	0.12
121	53250	Verfärbung 1	<i>Sus scrofa dom.</i>	Mandibula	5	39.7	14.3	3.2	-20.33	0.08	5.93	0.11
122	50301	Graben 1	<i>Sus scrofa</i>	Os coxae	5	40.2	14.7	3.2	-21.19	0.08	5.17	0.11
123	53392	Verfärbung 1/B	<i>Sus scrofa</i>	Metapodium	7	43.0	15.7	3.2	-18.60	0.08	5.47	0.11
124	52808	Grube 1, Riegel 319/318	<i>Equus ferus caballus</i>	Os tarsale	6	39.5	14.3	3.2	-21.56	0.09	4.97	0.10
125	51916	Grube 1	<i>Capreolus capreolus</i>	Metatarsus	16	44.0	15.9	3.2	-20.50	0.08	5.08	0.10
126	51914	Grube 1	<i>Cervus elaphus</i>	Phalanx	20	41.5	15.2	3.2	-21.40	0.09	5.92	0.11
127	41108	Grubenhaus FMA	<i>Gallus gallus dom.</i>	Os coracoideum, Femur	15	42.6	15.2	3.3	-19.59	0.08	10.14	0.13

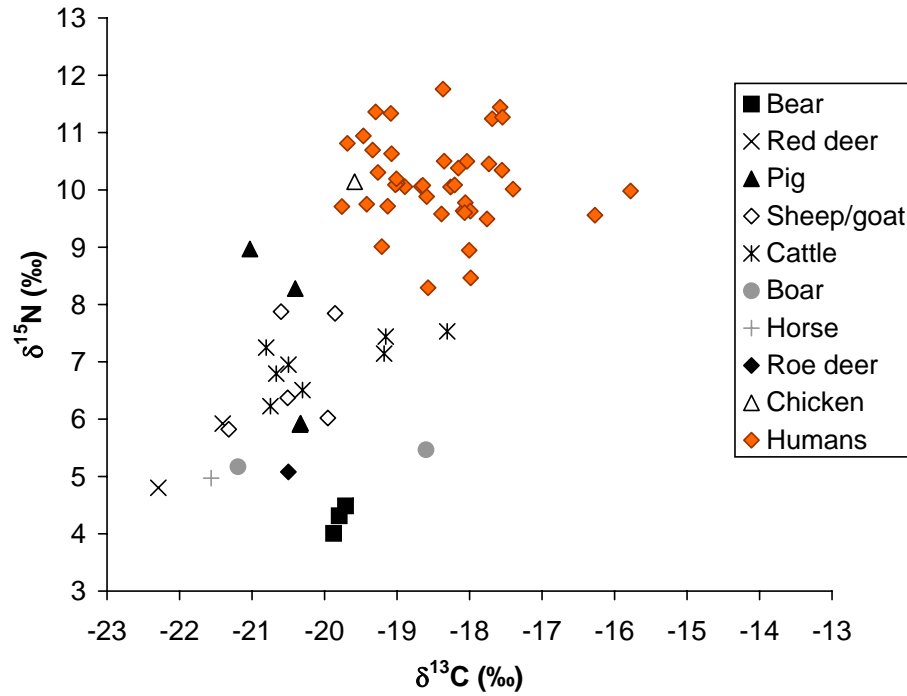


**Figure 4.5:** Scatter plot of the  $\delta^{13}\text{C}$  and  $\delta^{15}\text{N}$  values of the collagen samples from Thunau.

The observed variation of the animal  $\delta$ -values is not only due to differences between the species, but there is also significant variability within the species. For example, a large variability can be found in the cattle data. Their  $\delta^{13}\text{C}$  values seem to cluster in two separate groups. A possible explanation for this could be different origins of the animals and/or varying feeding practices. Archaeozoologists presume that part of the cattle in Thunau could have been imported from the foothills of the Alps in Upper Austria and Salzburg (Riedel & Pucher, 2008).

### 4.3.2 Stable Isotope Data of the Human Remains

Table 4.9 lists the  $\delta$ -values obtained for the human collagen samples, which also scatter over a wide range. The lowest  $\delta^{13}\text{C}$  value found in this group of samples is  $-19.8\text{‰}$ , the highest is  $-15.8\text{‰}$ . However, if two outliers (sample-IDs 51 and 150) are removed from the sample set, the  $\delta^{13}\text{C}$  range is substantially reduced ( $-19.8\text{‰}$  to  $-17.4\text{‰}$ ). The human  $\delta^{15}\text{N}$  values range from  $8.3\text{‰}$  to  $11.8\text{‰}$  and the highest value belongs to the sample of a two- to three-year-old child (sample-ID 24) and can be explained by the elevation of  $\delta^{15}\text{N}$  values due to breast feeding. When a child is nursed, its trophic level will be higher than that of the nursing mother (Fogel *et al.*, 1997). After the weaning, the bone collagen produced during breast feeding will be replaced by newly built collagen, causing the "breast-feeding signal" to vanish<sup>2</sup>. For example, the  $\delta^{15}\text{N}$  value of a sample from a 9-10 year-old child (sample-ID 21) did

<sup>2</sup>The collagen turnover rate in infants is much higher than in adults (see the discussion in Section 1.4.3).

not indicate a higher trophic level for this child than for the adults from the sample set.

Based on the  $\delta$ -values of the animals, under the assumption that the investigated animal species were the main protein sources, the expected  $\delta$ -value range for the humans can be estimated. For this, the area spanned by the animal values (the rectangle drawn by a continuous line in Figure 4.6) was shifted by +3.0 ‰ on the y-axis ( $\delta^{15}\text{N}$ ) and +1.0 ‰ on the x-axis ( $\delta^{13}\text{C}$ ), which corresponds approximately to an elevation by one trophic level respectively (Schoeninger & Moore, 1992). Except for two individuals (sample-IDs 51 and 150), the determined  $\delta$ -values of the humans fall within this expected range, which is indicated by a dashed line in the diagram.

However, the mean  $\delta^{13}\text{C}$  value of the human samples without the two outliers (-18.5 ‰) is shifted by +1.8 ‰ with respect to the mean of the animals (-20.3 ‰), which is larger than the expected shift for one trophic level. Hence, a  $\text{C}_4$  component in the diet (probably millet or animals fed on millet, see also below) could have been responsible for this shift in the human values. It is, however, difficult to quantify smaller amounts of  $\text{C}_4$  plants in omnivorous diets, since it is generally believed that the  $\delta^{13}\text{C}$  value in bone collagen mainly reflects the protein component of the diet. Thus, plants will be underrepresented considering their low protein content (see e.g., Ambrose & Norr, 1993; Jim *et al.*, 2006; Tieszen & Fagre, 1993). Nevertheless, the  $\delta^{13}\text{C}$  values of the humans suggest a diet comprising a large amount of  $\text{C}_3$  resources (i.e., plant and animal foods originating from a  $\text{C}_3$  ecosystem). The consumed  $\text{C}_3$  plants could have been wheat, barley, rye or leguminous plants like peas, beans and lentils, since these were wide spread crops in Early Medieval times (Popovtschak *et al.*, 2003).

The  $\delta^{15}\text{N}$  values of the humans overlap with the range of the animals indicating a mixed diet of plant and animal protein, which could be meat, milk, dairy products, eggs etc., for the humans.

Furthermore, the carbon and nitrogen stable isotope ratios do not suggest the consumption of freshwater foods in large amounts. Often freshwater fish exhibit collagen  $\delta^{13}\text{C}$  values in the range of terrestrial  $\text{C}_3$  plants and many species frequently consumed by humans are high trophic level fish with correspondingly high  $\delta^{15}\text{N}$  values (see e.g., Dürrwächter *et al.*, 2006; Dufour *et al.*, 1999; Lillie & Jacobs, 2006; Müldner & Richards, 2005; Schoeninger & DeNiro, 1984). Therefore the massive consumption of such fish would lead to a  $\text{C}_3$  signal in the collagen  $\delta^{13}\text{C}$  value of the consumer and a high  $\delta^{15}\text{N}$ , which would not be explainable by the consumption of terrestrial protein. However, this is not the case in the present data set. The observed nitrogen stable isotope signatures of the humans are consistent with a terrestrial diet containing slightly varying amounts of animal protein.

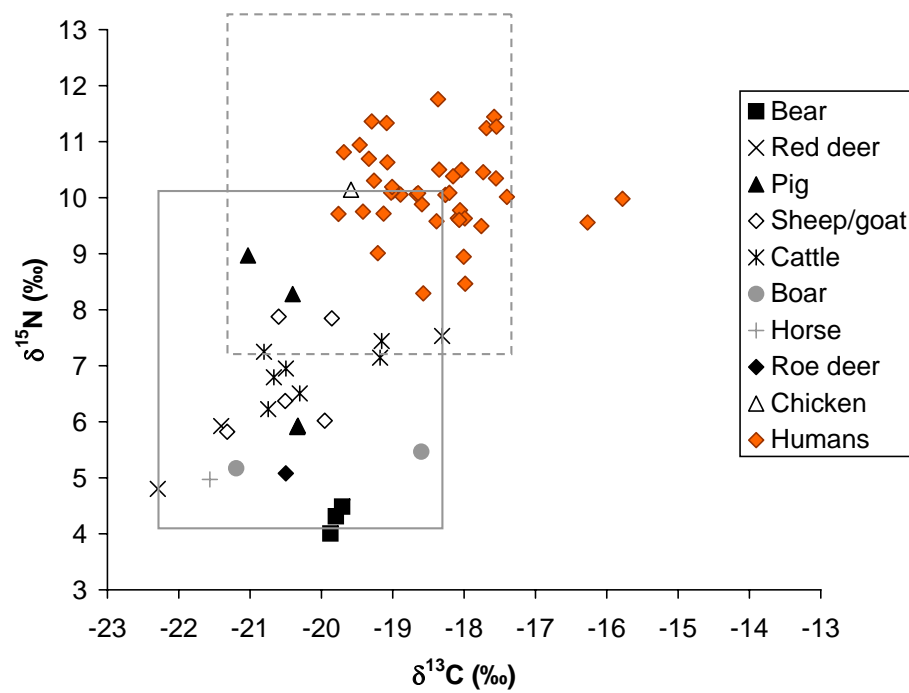


**Figure 4.6:** Scatter plot of the  $\delta^{13}\text{C}$  and  $\delta^{15}\text{N}$  values of the human and animal collagen samples from Thunau. The gray box drawn by a continuous line encloses the animal  $\delta$ -values, the dashed line symbolizes the expected  $\delta$ -values for the humans based on the animal values.

**Table 4.9:** Results of the stable isotope analysis of the human bone collagen samples from Thunau. (m=male, f=female, n.a.=not applicable)

sample-ID	Grave-Nr.	Inventory-Nr.	Excavation area	Bone	Sex	Age	Yield (%wt.)	%wt. C	%wt. N	atomic C/N	$\delta^{13}\text{C}$ (‰)	1 $\sigma$	$\delta^{15}\text{N}$ (‰)	1 $\sigma$
19	22	24.974	Herrenhof	Costa	m	20-25	5	43.0	16.1	3.1	-17.55	0.07	10.34	0.15
20	1985/6	25.260	Saugrube	Costa	m	40-50	7	43.8	16.1	3.2	-18.35	0.07	10.50	0.15
21	1985/7	25.261	Saugrube	Costa	n.a.	9-10	1	40.3	15.1	3.1	-18.89	0.07	10.06	0.14
22	1999/1	25.363	Schanze/ Nordtor	Cranium	m	30-40	16	45.3	16.8	3.1	-17.98	0.07	8.47	0.14
23	1968/1	25.215	Schanze	Costa	f	25-35	10	45.0	16.2	3.2	-19.21	0.07	9.01	0.14
24	1982/1	25.247	untere Holzweise	Costa	n.a.	2-3	10	45.6	16.3	3.3	-18.37	0.07	11.76	0.15
25	1985/4	25.399	Goldberggasse	Costa	m	50-70	9	45.8	16.9	3.2	-17.73	0.07	10.45	0.15
37	48	25.004	Herrenhof	Costa	f	18-20	12	46.4	16.5	3.3	-18.57	0.07	8.29	0.12
38	208	25.190	Herrenhof	Metatarsus	f	20-25	15	47.5	16.9	3.3	-19.00	0.07	10.12	0.13
39	1983/6	25.388	Goldberggasse	Costa	m	30-50	3	43.2	15.5	3.3	-18.04	0.07	10.50	0.14
40	129	25.099	Herrenhof	Costa	m	40-50	15	40.6	14.5	3.3	-17.69	0.07	11.24	0.14
41	56	25.012	Herrenhof	Costa	m	20-25	4	39.9	14.6	3.2	-17.40	0.07	10.01	0.13
42	81	25.036	Herrenhof	Costa	m	30-40	13	43.4	15.5	3.3	-19.46	0.07	10.94	0.13
45	126	25.096	Herrenhof	Costa	f	35-45	13	37.8	13.6	3.2	-19.02	0.07	10.09	0.13
46	100	25.063	Herrenhof	Costa	f	25-35	15	40.0	14.4	3.2	-19.01	0.07	10.19	0.13
47	1983/3	25.385	Goldberggasse	Costa	m	35-50	5	40.0	14.3	3.3	-18.67	0.07	10.06	0.13
49	1987/6	25.408	Goldberggasse	Costa	f	30-40	6	41.1	14.9	3.2	-18.09	0.07	9.63	0.13
50	1983/8	25.390	Goldberggasse	Costa	f	30-50	17	44.6	16.2	3.2	-17.58	0.07	11.44	0.14
51	2004/18	25.427	Schimmelsprungg.	Costa	m	20-30	11	37.6	13.7	3.2	-16.27	0.07	9.56	0.13
51/2	2004/18	25.427	Schimmelsprungg.	Costa	m	20-30	16	47.0	16.4	3.2	-16.28	0.07	9.62	0.12
51/1	2004/18	25.427	Schimmelsprungg.	Dens	m	20-30	5	43.4	16.2	3.2	-14.42	0.07	11.02	0.13
54	12	24.963	Herrenhof	Costa	m	35-50	2	38.5	13.8	3.3	-18.26	0.07	10.05	0.13
55	1985/2-1	25.396	Goldberggasse	Costa	f	30-50	5	42.7	15.0	3.3	-18.16	0.07	10.38	0.13

sample-ID	Grave-Nr.	Inventory-Nr.	Excavation area	Bone	Sex	Age	Yield (%wt.)	%wt. C	%wt. N	atomic C/N	$\delta^{13}\text{C}$ (‰)	1 $\sigma$	$\delta^{15}\text{N}$ (‰)	1 $\sigma$
56	1986/5	25.407	Goldberggasse	Costa	f	40-60	3	40.5	14.6	3.2	-19.69	0.07	10.81	0.13
57	2004/34	25.443	Schimmelsprung.	Costa	m	50-60	10	42.9	15.3	3.3	-17.55	0.07	11.27	0.13
133	90/3/1	25.381	Asenbaumacker	Costa	m	25-35	17	44.9	16.1	3.2	-17.76	0.08	9.49	0.12
134	1983/2	25.384	Goldberggasse	Costa	m	18-20	9	42.0	15.1	3.2	-19.08	0.08	10.63	0.13
135	2004/4	25.413	Schimmelsprung.	Phalanx	m	30-50	16	44.0	16.0	3.2	-19.42	0.08	9.75	0.13
136	2004/6	25.415	Schimmelsprung.	Costa	m	50-70	20	43.8	15.9	3.2	-18.06	0.08	9.78	0.13
137	2006/3	25.455	Goldberggasse	Costa	m	35-45	18	43.9	15.8	3.2	-18.21	0.08	10.09	0.13
138	2	25.193	obere Holzweise	Costa	m	40-60	7	42.5	14.5	3.2	-19.29	0.08	11.36	0.14
139	146	25.123	obere Holzweise	Costa	m	25-35	7	39.9	14.3	3.3	-19.09	0.08	11.33	0.14
140	24	24.977	obere Holzweise	Costa	m	30-40	13	42.2	15.3	3.2	-17.99	0.08	9.63	0.13
141	207	25.189	obere Holzweise	Costa	m	40-60	17	44.0	15.9	3.2	-19.76	0.08	9.71	0.13
142	20	24.972	obere Holzweise	Costa	f	30-40	20	43.7	15.8	3.2	-19.26	0.08	10.30	0.13
143	88/1	25.047	obere Holzweise	Costa	f	25-30	20	42.5	14.4	3.2	-18.59	0.08	9.88	0.13
144	138/1	25.114	obere Holzweise	Costa	f	40-60	6	41.4	15.0	3.2	-19.13	0.08	9.72	0.13
145	198	25.177	obere Holzweise	Costa	f	18-23	7	41.3	14.9	3.2	-18.39	0.08	9.58	0.13
146	1983/4	25.386	Goldberggasse	Costa	f	40-60	15	44.6	16.1	3.2	-18.07	0.08	9.60	0.13
147	1986/3	25.404	Goldberggasse	Costa	f	50-70	21	42.8	15.4	3.2	-18.65	0.08	10.08	0.13
148	2004/11/1	25.420	Schimmelsprung.	Costa	f	35-45	12	42.5	15.3	3.2	-18.00	0.08	8.95	0.12
149	2004/23/1	25.432	Schimmelsprung.	Costa	f	30-50	16	44.8	16.2	3.2	-19.34	0.08	10.69	0.13
150	2004/27	25.438	Schimmelsprung.	Costa	f	18-20	11	42.3	15.3	3.2	-15.78	0.07	9.98	0.13
150/2	2004/27	25.438	Schimmelsprung.	Costa	f	18-20	9	44.9	16.0	3.3	-15.74	0.08	9.97	0.12
150/1	2004/27	25.438	Schimmelsprung.	Dens	f	18-20	14	46.0	16.5	3.3	-17.81	0.07	10.50	0.13

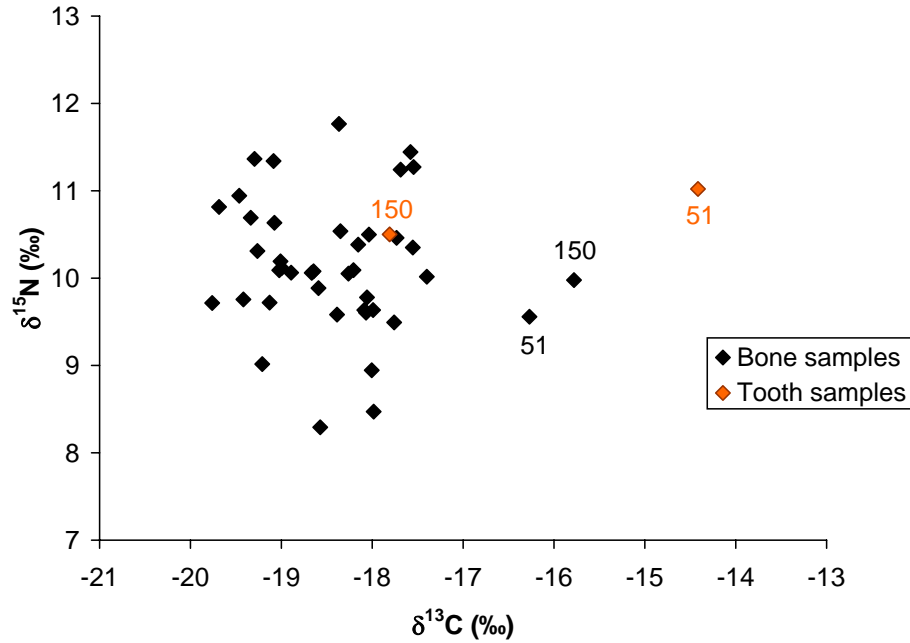


**Figure 4.7:**  $\delta^{13}\text{C}$  and  $\delta^{15}\text{N}$  values of the human bone and tooth collagen samples from Thunau.

The two individuals, whose  $\delta^{13}\text{C}$  values clearly deviate from those of the other investigated humans, are a young woman (sample-ID 150) and a 20 to 30 year-old man (sample-ID 51), both from the valley area. To ascertain that the deviating  $\delta^{13}\text{C}$  values are reproduceable, collagen was extracted from two further aliquots of the previously sampled bones and measured by EA-IRMS. Table 4.9 lists the results of these determinations with the sample-IDs 51/2 and 150/2. The  $\delta^{13}\text{C}$  and  $\delta^{15}\text{N}$  values of both samples match very well with the values determined for the first samples within the respective uncertainties.

In addition to the repeated determinations in bone collagen, permanent teeth of both individuals were investigated. Therefore, collagen was extracted from the roots of the man's left upper canine (tooth number [23] according to the Fédération Dentaire Internationale) and the young woman's left first molar of the mandible (FDI-number [36]). The time frame for tooth root formation is between the age of two to nine and four to twelve for the molar and the canine respectively (Smith, 1991a). Consequently, the analysis of collagen from these tooth roots reveals diet information from the childhood of the two individuals. The measured C- and N-isotopic compositions of these samples (IDs 51/1 and 150/1 in Table 4.9) point to a diet change somewhere between the childhood and the time of death for both individuals. Figure 4.7 shows that the values in the dentin of the woman fall within the range obtained from the other investigated individuals, but later on in her life the  $\delta^{13}\text{C}$  value (in bone collagen) is substantially increased. Also for the male individual, a shift of the  $\delta^{13}\text{C}$  value can be observed from infancy to adulthood. However, in contrast to the woman, there is a clearly higher value during childhood compared to the years before his death. A possible reason for the higher  $\delta^{13}\text{C}$  values of the two "outliers" compared



**Figure 4.8:** Maxilla of a male individual with severe abrasion of the front incisors (picture: Natural History Museum Vienna).

to the bulk of the investigated humans is a significant amount of  $C_4$  foods in their diet. The only  $C_4$  plant to be considered for direct consumption by humans (bearing in mind the geographical position and the time frame) is millet, which was identified within the plant remains recovered in Early Medieval Thunau (Popovtschak *et al.*, 2003). A marine component to the diet of the examined population is less likely due to the inland situation of Thunau, but (based on the observed  $\delta^{13}C$  values) it cannot completely be ruled out for the male outlier in case he was an immigrant from a coastal region. Regarding the  $\delta^{15}N$  values, the two individuals do not deviate from the other sampled humans.  $\delta^{15}N$  values in this range can be explained by the consumption of terrestrial animal protein. One would expect higher  $\delta^{15}N$  values, if a significant amount of marine fish formed part of the diet (e.g., Schoeninger & DeNiro (1984) found  $\delta^{15}N$  values from 11.4 ‰ to 16.0 ‰ in an elaborate isotopic survey of marine fish).

Also worth mentioning is the unusual abrasion of the male individual's (sample-ID 51) upper incisors on their vestibular side (see Figure 4.8). This abrasion presumably is artificial in its origin, since it is hard to imagine that natural processes lead to such a result. At present, it is not clear, if and how this anomaly is connected to the deviating  $\delta^{13}C$  value. It is, however, possible that this mutilation necessitated a special nutrition.

### 4.3.3 Statistical Examination

The  $\delta^{13}C$  and  $\delta^{15}N$  values were analyzed with statistical methods to check whether the data revealed evidence for gender-related or social differences between subgroups of the sampled human population. All statistical analyses were performed with the software package *PASW Statistics 17 (SPSS Inc.)*. The sample set was split according to the categories sex (males and females) and location of the burial (Schanzberg and valley), which could reflect two different social strata. Figure 4.9 displays the  $\delta^{13}C$  and  $\delta^{15}N$  values of the males and the females, together with the arithmetic means of both groups and their  $1\sigma$  standard deviations. The mean  $\delta$ -values of the male group, appear to be higher than the corresponding means of the females, where the difference in  $\delta^{13}C$  and  $\delta^{15}N$  amounts to 0.32 ‰ and 0.35 ‰ respectively. Regarding the  $\delta$ -values of the groups from the Schanzberg and the valley in Figure 4.10, gives the impression that the mean  $\delta^{13}C$  value of the valley group is higher than



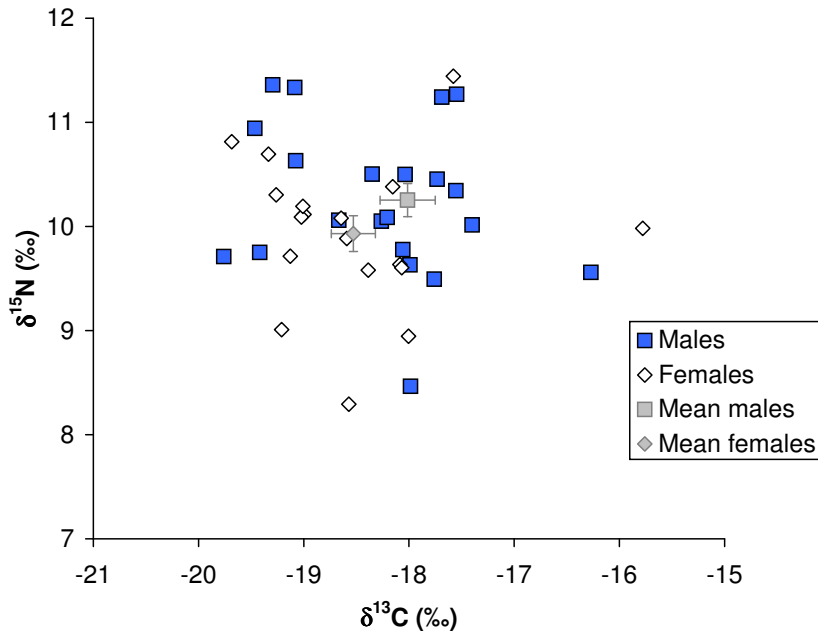


**Figure 4.9:** Diagram of the  $\delta^{13}\text{C}$  and  $\delta^{15}\text{N}$  values of the males and females from Thunau including the mean values of both groups (the results of the children are not displayed). The error bars indicate the  $1\sigma$  uncertainties of the mean.

that of the Schanzberg group. However, it has to be considered that both outliers fall within the valley category and therefore distort the group mean towards more elevated values. Therefore, excluding these two extreme values clearly diminishes the difference between the group means.

To test for significant differences between the population groups, univariate and multivariate analysis of variance (ANOVA and MANOVA respectively) were found to be suitable statistical methods. The basics of ANOVA are covered in many textbooks (e.g., Field, 2005; Janssen & Laatz, 2007). Briefly, with ANOVA differences between multiple groups, which are classified by one or several independent variables (here: sex and burial location) can be investigated. The influence of these independent variables, also called "factors", on a dependent variable (here:  $\delta^{13}\text{C}$  or  $\delta^{15}\text{N}$ ) are tested for significance via an F-test. MANOVA can be regarded as an extension of ANOVA, which allows the simultaneous examination of group differences concerning multiple dependent variables. Detailed introductions to MANOVA are for example given by Bray & Maxwell (1985) or Tabachnick & Fidell (2007).

Generally, in statistical hypothesis testing, the decision, whether an effect discovered in the data is significant or not is taken on the basis of the test statistic calculated by the test algorithm e.g., the "F-statistic" or "F-ratio" in the case of an F-Test. The F-statistic, in principle the ratio of systematic variance to unsystematic variance in the data, follows the well-known F-distribution and therefore a theoretical F-statistic for the appropriate degrees of freedom according to the test situation and a pre-defined level of significance can be calculated. This number, often called

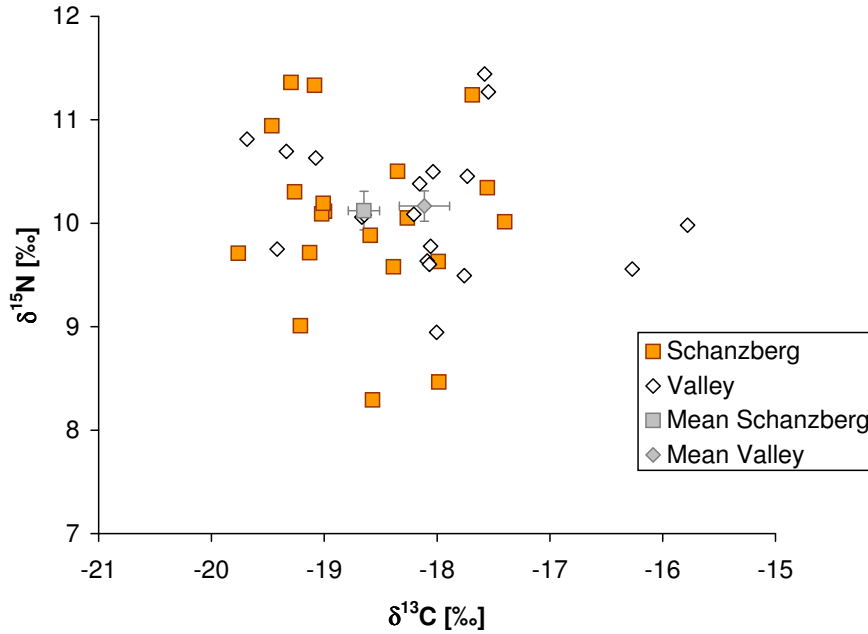


**Figure 4.10:** Diagram of the  $\delta^{13}\text{C}$  and  $\delta^{15}\text{N}$  values of the individuals from the Schanzberg and the valley (without the children) including the mean values of both groups (error bars:  $1\sigma$  uncertainty of the mean).

"critical F-value", can be taken from published F-distribution tables and serves as a threshold for the test decision. The test is considered significant on the previously selected level (mostly 5 %), when the numerical value of the test statistic calculated from the sample data is larger than the critical F-value. Alternatively, the test decision can be taken with the help of the "statistical significance" or "*p*-value", which is frequently calculated by modern software packages for statistics. The *p*-value represents the probability that an observed difference between groups of a random sample occurred by chance. Test results are generally accepted as significant, when a *p*-value below 0.05 is obtained.

Since ANOVA and MANOVA are both known to be sensitive to outliers (e.g., Tabachnick & Fidell, 2007, p.251), the two individuals with the deviating  $\delta^{13}\text{C}$  values were removed from the sample set prior to the statistical examination in order to avoid distortion of the test results. Hence, the total number of cases included in the statistical analysis is 37, of which 20 individuals are male and 17 are female, 20 individuals are assigned to the hill settlement and 17 to the valley.

As ANOVA is a parametric test, whose formalism is based on the normal distribution, several assumptions are made when this method is applied to sample data. These assumptions should be valid for the specific data set in order to produce reliable ANOVA results. Therefore, ANOVA requires data for which the dependent variable is normally distributed within each test group and the variances between the groups are similar in magnitude (homogeneity of variances). In the data from Thunau, these two requirements were tested using the Kolmogorov-Smirnov- and the

Levene-Test respectively. MANOVA additionally requires the homogeneity of the variance-covariance matrices for the investigated data set, which was checked by applying Box's M-Test. Descriptions of these three test procedures can also be found in the textbooks cited above. Furthermore, the multivariate normal distribution of the dependent variables in each group is presumed when using MANOVA. However, there is no commonly accepted method to test for this assumption, only the univariate normal distribution is verifiable to date in a simple way. Although the above mentioned assumptions are mathematical requirements for the two statistical techniques, both ANOVA and MANOVA are fortunately relatively robust to violations of these assumptions (e.g., Bray & Maxwell, 1985, pp.33-34).

When testing for the described prerequisites, a significant Kolmogorov-Smirnov test result was obtained for the  $\delta^{13}\text{C}$  values in the valley ( $D(17) = 0.235, p = 0.013$ )<sup>3</sup>. This points to a deviation from the normal distribution of the data in this group. Via the Levene-test an inhomogeneity of variances was detected concerning the  $\delta^{13}\text{C}$  data ( $F(3; 33) = 3.130, p = 0.039$ )<sup>4</sup>. However, since the F-test is known to be relatively robust against violations of homogeneity of variances and the normal distribution criterion (Donaldson, 1968), the outcome of the ANOVA is still considered reliable. MANOVA is fairly robust to deviations from multivariate normal distribution (e.g., Bray & Maxwell, 1985, p.33). This is also true for violations of the homogeneity of variance criterion, as long as the group sizes are not highly divergent (e.g., Tabachnick & Fidell, 2007, pp.315-316). In the underlying data, Box's M-test did not reveal any inhomogeneity of the variance-covariance matrices. Hence, the results of the MANOVA were also regarded as reliable.

Both statistical tests were applied to the data set of Thunau. However, based on a Pearson correlation coefficient,  $\delta^{13}\text{C}$  and  $\delta^{15}\text{N}$  values in these data are not significantly correlated with each other ( $r = 0.043, p = 0.796$ ). Considering the lower test power of MANOVA in case of uncorrelated dependent variables compared to ANOVA, the focus was put on the outcome of ANOVA.

The results of a two-factorial ANOVA indicated no statistically significant differences with respect to the  $\delta^{13}\text{C}$  values between the two sex categories ( $F(1; 33) = 2.093, p = 0.157$ )<sup>5</sup> and the two location categories ( $F(1; 33) = 1.989, p = 0.168$ ). Neither the mean  $\delta^{15}\text{N}$  values of the males and females ( $F(1; 33) = 1.846, p = 0.183$ ), nor of the Schanzberg and valley groups ( $F(1; 33) = 0.700, p = 0.409$ ) were significantly

---

<sup>3</sup>D is the test statistic of the Kolmogorov-Smirnov test, it is a measure for the distance between the empirical distribution function of the sample data and the cumulative distribution function of the reference distribution (here, the normal distribution). The number in brackets after the test statistic symbol is the number of cases included in the analysis (the 17 individuals from the valley settlement).

<sup>4</sup>Here, the numbers in brackets after the test statistic are the number of degrees of freedom for the respective test situation, calculated as K-1 and N-K respectively, with K the number of groups regarded in the overall test approach and N the number of all included cases. For this test situation K=4 (males, females, hill, valley) and N=37.

<sup>5</sup>The given degrees of freedom are calculated as k-1, with k the number of groups defined by the regarded factor (here: the factor sex divides the data into the two groups "males" and "females") and as N-K, with N the total number of cases included in the overall model of the two-factorial ANOVA i.e., 37 individuals and K the total number of groups in the overall model i.e., 4 groups.

different. MANOVA confirmed the obtained results, it did not detect any significant differences between the investigated groups.

In the course of the two-factorial ANOVA and the MANOVA, the data were also examined for possible interactions between the factors (sex and location). None of the conducted analyses found evidence for significant interactions. This means that within a location category, the sex of the group members did not influence their  $\delta$ -values and that there was no correlation between the burial locations (hypothetically representing different social levels) and the  $\delta$ -value within a sex category.

### 4.3.4 Conclusions

To sum up the outcome of this study, the stable isotope analysis of faunal and human remains from Early Medieval Thunau/Gars revealed evidence for a diverse diet based on  $C_3$  resources (including both, plants and animal protein) with possible inputs from  $C_4$  foods, especially in the cases of two individuals substantially deviating from the bulk of the  $\delta^{13}C$  values. A hypothetical influence of gender or social status as inferred from the burial location of an individual on its bone collagen  $\delta^{13}C$  or  $\delta^{15}N$  values could not be confirmed in this data set by univariate and multivariate analysis of variance. However, this does not necessarily mean that there were no differences concerning diet between the population subgroups from the Schanzberg and the valley or between the males and the females. It has to be kept in mind that  $\delta^{13}C$  and  $\delta^{15}N$  values are measures for the amount of  $C_3$  and  $C_4$  resources in the diet and for the trophic level respectively. Also, it must be recalled here that the isotopic composition of bone collagen mainly reflects that of dietary protein. Effects concerning other aspects of the diet than the mentioned ones remain undetected by these two parameters. Additional insights could therefore be gained by conducting complementary analyses like the determination of  $\delta^{13}C$  in bone apatite, which rather reflects the isotopic composition of all dietary macronutrients (carbohydrates, lipids and proteins)(see Section 1.4.3).

## 4.4 Palaeodiet Reconstruction for the Sample-Set from Gemeinlebarn F

The suitability of the bone samples from Gemeinlebarn F (with regard to collagen preservation) for palaeodiet reconstruction was checked as already described in Section 4.3 using collagen yields, carbon and nitrogen contents and atomic C/N ratios of the collagen samples. The lowest collagen yield of a sample was 2 %wt., carbon contents were within 31 %wt. and 45 %wt., nitrogen contents between 12 %wt. and 16 %wt. and atomic C/N ratios ranged from 3.1 to 3.3 (see Tables 4.10 and 4.11). Therefore all samples were considered sufficiently well preserved for the diet study.

### 4.4.1 Results of the Stable Isotope Analysis for the Animal Samples

Table 4.10 shows the results of the carbon and nitrogen stable isotope analysis of the animal collagen samples from Pottenbrunn and Franzhausen, which were taken as a substitute for the missing animal remains from the Gemeinlebarn necropolis. In Figure 4.11 the measured  $\delta^{13}\text{C}$  values of the human and animal samples are plotted against the corresponding  $\delta^{15}\text{N}$  values.

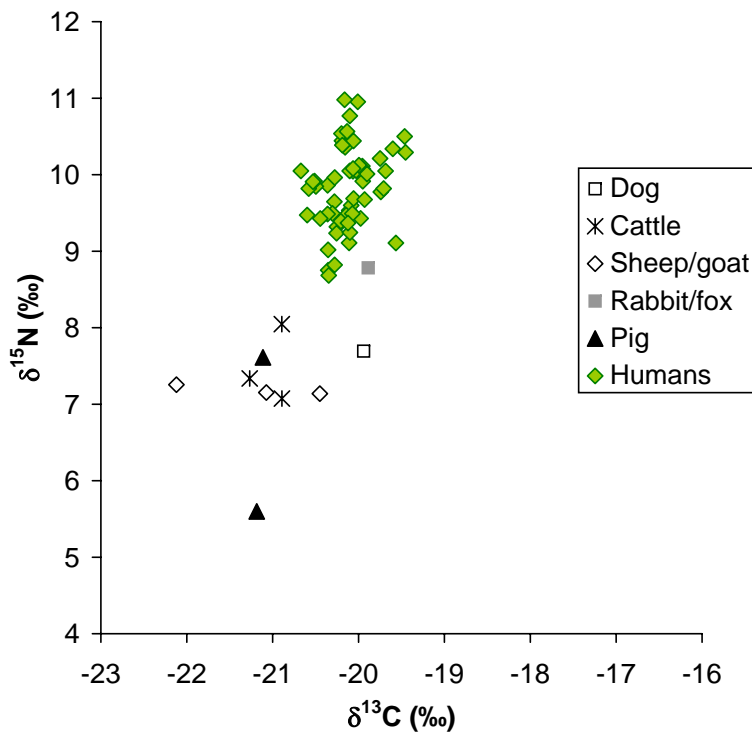


**Figure 4.11:** Scatter plot of the final  $\delta^{13}\text{C}$  and  $\delta^{15}\text{N}$  values of the human collagen samples from Gemeinlebarn F and the animal collagen samples from Pottenbrunn and Franzhausen.

**Table 4.10:** Results of the  $\delta^{13}\text{C}$  and  $\delta^{15}\text{N}$  determination of the faunal collagen samples from Pottenbrunn and Franzhausen.

Sample-ID	Find-Nr.	Location	Species	Bone	Yield (%wt.)	%wt.C	%wt.N	atomic C/N	$\delta^{13}\text{C}$ (‰)	$1\sigma$	$\delta^{15}\text{N}$ (‰)	$1\sigma$
14	1738/G/7/7	Pottenbrunn	<i>Canis lupus familiaris</i>	Mandibula	8	42.0	15.2	3.2	-19.94	0.07	7.69	0.12
15	1738/G/7/7	Pottenbrunn	<i>Bos taurus</i>	Mandibula	2	31.1	11.5	3.1	-20.89	0.08	7.07	0.12
16	1738/G/7/7	Pottenbrunn	<i>Ovis orientalis aries/</i> <i>Capra aegagrus hircus</i>	Tibia	3	37.5	13.8	3.2	-21.07	0.08	7.15	0.12
17	1738/G/3/6	Pottenbrunn	<i>Lepus europaeus/</i> <i>Vulpes vulpes</i>	Metapodium	5	41.7	15.3	3.2	-19.89	0.07	8.78	0.13
151	1738/G/2/8	Franzhausen	<i>Bos taurus</i>	Costa	12	42.3	15.3	3.2	-20.89	0.08	8.05	0.12
152	901/4	Franzhausen	<i>Bos taurus</i>	Scapula	9	42.2	15.3	3.2	-21.27	0.08	7.34	0.11
153	117/16	Franzhausen	<i>Sus scrofa domestica</i>	Costa	5	39.7	14.3	3.2	-21.18	0.08	5.60	0.11
154	941/3	Franzhausen	<i>Sus scrofa domestica</i>	Os ilium	9	43.3	15.6	3.2	-21.11	0.08	7.61	0.12
155	271/2	Franzhausen	<i>Ovis orientalis aries/</i> <i>Capra aegagrus hircus</i>	Radius	4	40.0	14.7	3.2	-20.45	0.08	7.14	0.11
156	300/4	Franzhausen	<i>Ovis orientalis aries/</i> <i>Capra aegagrus hircus</i>	Humerus	5	39.5	14.3	3.2	-22.12	0.09	7.25	0.11

All  $\delta$ -values were determined as already described for the samples from Thunau. The data represent the weighted mean values calculated from the results of three separate measurements. The  $1\sigma$  uncertainties of these mean values were determined as specified in Section 3.4. For uncertainty estimates of the elemental data (carbon and nitrogen contents and the atomic C/N ratio) see Table 3.7.

The investigated animal collagen samples were taken from herbivorous species like sheep or goat and cattle and from omnivorous species like pigs and a domesticated dog. Samples of exclusively carnivorous animals were not available. One of the samples (ID 17) had initially been classified as a rabbit bone in the archaeo-zoological examination. However, its determined  $\delta^{15}\text{N}$  value (8.8‰) is not consistent with a herbivorous diet, but rather points to a higher trophic level comparable to the sampled human population. A re-investigation (personal communication Erich Pucher, 1<sup>st</sup> Zoological Department, Natural History Museum of Vienna) came to the result, that the bone in question – a small metapodial bone – could also originate from a fox, who is an opportunistic feeder usually with a high input of animal protein in its diet (e.g., Goldyn *et al.*, 2003).

The animal  $\delta^{13}\text{C}$  values spread over a rather narrow range from -22.1 to -19.9‰ and indicate that these animals subsisted on resources from a  $\text{C}_3$  environment. Apart from the presumed fox sample and a low value of a pig (sample ID 153), the  $\delta^{15}\text{N}$  values vary within 1.0‰.

Interestingly, the dog sample exhibits a  $\delta^{15}\text{N}$  value clearly lower than all human samples, rather in the range of the value obtained for a pig. Its  $\delta^{13}\text{C}$  value however is indistinguishable from those of the humans. It is therefore possible, that the dog's diet consisted partly of kitchen leftovers but with a higher plant content than any of the investigated humans.

#### 4.4.2 Results of the Stable Isotope Analysis for the Human Samples

The  $\delta$ -values determined for the samples of the human population from Gemeinlebarn are given in Table 4.11, and Figure 4.11 shows a plot of these values together with the results of the animal samples. This plot nicely clarifies the tight clustering of the human  $\delta^{13}\text{C}$  values around a mean value<sup>6</sup> of  $(-20.11 \pm 0.03\text{‰})$ . The whole range is encompassed by -20.7‰ and -19.5‰. These values indicate that the investigated population subsisted on terrestrial  $\text{C}_3$  resources. The mean human  $\delta^{13}\text{C}$  value is shifted by approximately +1‰ with respect to the mean value of the animals<sup>7</sup>,  $(-21.12 \pm 0.17\text{‰})$ , which roughly corresponds to an increase of one trophic level. However, the  $\delta^{13}\text{C}$  value is not a very sensitive indicator for the trophic level, therefore the nitrogen isotopic composition is regarded for this purpose.

<sup>6</sup>All means are reported  $\pm 1$  standard deviation of the mean.

<sup>7</sup>For the calculation of the animal mean value, the results of the canid samples (fox and dog) were excluded, since it is assumed that they did not contribute to the human diet in significant amounts.

**Table 4.11:** Results of the  $\delta^{13}\text{C}$  and  $\delta^{15}\text{N}$  determination of the human collagen samples from Gemeinlebarn F. (m=male, f=female, r=rich, p=poor, n.d.=not determined, PL=Phalanx)

Sample- ID	Grave- Nr.	Bone	Sex	Age	Social status	Yield (%wt.)	%wt.C	%wt.N	atomic C/N	$\delta^{13}\text{C}$ (‰)	1 $\sigma$	$\delta^{15}\text{N}$ (‰)	1 $\sigma$
3	7	Costa	m?	40-50	r	12	44.7	16.2	3.2	-19.75	0.07	10.21	0.14
4	78	Costa	m	30-40	p	7	42.7	15.7	3.2	-20.02	0.07	10.05	0.13
5	17	Costa	n.d.	n.d.	r	6	42.0	15.5	3.2	-19.60	0.07	10.34	0.14
10	23	Costa	f	25-35	p	16	44.3	15.7	3.3	-20.36	0.07	9.86	0.13
11	3	Costa	f	15-18	p	10	42.9	15.5	3.2	-20.25	0.07	9.32	0.13
12	61	Costa	f	40-50	r	6	42.5	15.4	3.2	-20.28	0.07	9.65	0.13
13	121	Costa	f	50-80	r	11	43.6	15.6	3.3	-20.60	0.08	9.47	0.13
59	96	Costa	m	40-50	p	8	42.6	15.4	3.2	-20.16	0.08	10.36	0.14
60	122	Costa	m	30-40	p	18	43.1	15.7	3.2	-19.69	0.08	10.05	0.13
61	136	Costa	m	27-33	p	7	41.9	15.1	3.2	-20.01	0.08	10.95	0.14
62	143	Costa	m	24-30	p	6	40.0	14.5	3.2	-20.11	0.08	9.53	0.13
63	149	Costa	m	30-40	p	6	41.3	15.0	3.2	-20.19	0.08	10.44	0.14
64	156	Costa	m	30-40	p	12	42.0	15.2	3.2	-19.98	0.08	9.43	0.13
65	161	Costa	m	24-30	p	11	39.3	14.3	3.2	-19.98	0.08	10.04	0.13
66	183	Costa	m	30-40	p	12	44.0	16.0	3.2	-20.14	0.08	9.46	0.13
67	186	Costa	m	24-30	p	10	43.0	15.6	3.2	-20.07	0.08	10.05	0.13
68	216	Costa	m	27-33	p	10	41.9	15.2	3.2	-19.96	0.08	10.11	0.13
69	221	Costa	m	35-45	p	6	40.6	14.7	3.2	-20.28	0.08	9.96	0.13
70	243	Costa	m	24-30	p	20	44.1	15.9	3.2	-20.18	0.08	10.40	0.13
71	244	Costa	m	35-45	p	10	42.5	15.2	3.2	-20.30	0.08	9.49	0.13
72	43	Costa	f	22-24	p	7	41.1	15.0	3.2	-20.20	0.08	10.54	0.14
73	53	Costa	f	30-40	p	8	42.8	15.6	3.2	-20.50	0.08	9.85	0.13
74	56	Costa	f	22-25	p	10	43.4	15.7	3.2	-19.94	0.08	10.00	0.13
75	58	Costa	f	27-33	p	11	42.5	15.4	3.2	-20.11	0.08	9.11	0.13
76	99	Costa	f	22-25	p	9	43.2	15.6	3.2	-20.58	0.08	9.82	0.13
77	135	Costa	f	30-40	p	11	43.1	15.6	3.2	-20.51	0.08	9.92	0.13
78	152	Costa	f	30-40	p	15	43.0	15.6	3.2	-20.08	0.08	9.60	0.13
79	154	Costa	f	30-40	p	7	41.7	15.0	3.2	-20.53	0.08	9.91	0.13
80	168	Costa	f	22-30	p	11	44.3	16.0	3.2	-20.35	0.08	8.75	0.12



#### 4.4 Palaeodiet Reconstruction for the Sample-Set from Gemeinlebarn F

Sample-ID	Grave-Nr.	Bone	Sex	Age	Social status	yield (%wt.)	%wt. C	%wt. N	atomic C/N	$\delta^{13}\text{C}$ (‰)	$1\sigma$	$\delta^{15}\text{N}$ (‰)	$1\sigma$
81	180	Costa	f	30-40	p	13	44.3	16.1	3.2	-20.26	0.08	9.23	0.13
82	230	Long bone	f	22-40	p	15	43.3	15.7	3.2	-20.03	0.08	10.06	0.13
84	12	Long bone	f	35-60	r	3	36.6	13.5	3.2	-19.45	0.09	10.29	0.14
85	25	Costa, PL	f	50-60	r	10	44.6	15.9	3.3	-19.74	0.09	9.77	0.14
86	92	PL	f	30-40	r	15	44.3	16.0	3.2	-20.35	0.09	9.02	0.14
87	132	Costa	f	40-60	r	9	42.2	15.3	3.2	-20.35	0.09	8.68	0.13
88	163	Costa	f	40-60	r	11	44.0	15.8	3.2	-19.95	0.09	10.07	0.14
89	185	Costa	f	45-55	r	8	40.1	14.6	3.2	-19.95	0.09	9.92	0.14
90	253	Costa	f	40-60	r	12	43.6	15.8	3.2	-19.99	0.09	10.12	0.14
91	64	Costa	f	45-55	p	9	44.0	15.9	3.2	-20.67	0.09	10.05	0.14
92	71	Costa	f	30-40	p	12	44.0	15.9	3.2	-20.06	0.09	9.69	0.14
93	187	Costa	f	22-30	p	11	44.4	16.0	3.2	-20.06	0.09	10.44	0.14
94	207	Costa, PL	f	30-40	p	11	44.0	15.8	3.3	-20.28	0.09	8.82	0.13
95	11	Costa	m	30-40	r	11	43.4	15.7	3.2	-20.16	0.09	10.98	0.15
96	46	Costa	m	35-45	r	11	43.1	15.6	3.2	-19.71	0.09	9.82	0.14
97	65	Costa	m	22-25	r	16	44.3	16.0	3.2	-20.14	0.09	9.47	0.14
98	84	Costa	m	27-33	r	11	42.4	15.3	3.2	-20.10	0.09	9.24	0.14
99	138	Costa	m	40-50	r	10	43.1	15.5	3.2	-20.36	0.09	9.49	0.14
100	150	Costa	m	40-50	r	13	42.5	15.4	3.2	-19.46	0.09	10.50	0.14
101	78	Costa	m	30-40	p	8	43.3	15.7	3.2	-20.10	0.09	10.05	0.14
102	123	Costa	m	40-60	p	8	44.6	16.0	3.2	-19.90	0.09	10.01	0.14
103	159	Costa	m	24-30	p	6	44.0	15.7	3.3	-20.45	0.09	9.43	0.14
104	164	Costa	m	27-33	p	5	42.4	15.4	3.2	-20.10	0.09	10.77	0.14
105	210	Costa	m	27-33	p	9	39.0	14.2	3.2	-19.93	0.09	9.68	0.14
106	215	Costa	m	27-33	p	12	43.8	15.7	3.2	-20.13	0.09	10.56	0.14
107	255	Costa	m	30-40	p	13	41.2	14.8	3.2	-20.21	0.09	9.39	0.14
128	57	Costa	f	22-30	p	8	42.8	15.6	3.2	-19.57	0.08	9.11	0.12
129	15	Costa	f	25-35	p	6	40.0	14.4	3.2	-20.19	0.08	10.39	0.13
130	93	Costa	f	30-40	p	12	42.7	15.6	3.2	-20.07	0.08	9.49	0.12
131	101	Costa	f	27-33	p	11	43.2	15.4	3.3	-20.06	0.08	10.08	0.13
132	197	Costa	f	20-40	p	9	42.9	15.6	3.2	-20.12	0.08	9.37	0.12

With respect to the  $\delta^{15}\text{N}$  values, more variation than in the  $\delta^{13}\text{C}$  values can be observed, which is possibly caused by the consumption of slightly varying amounts of animal protein or of animal foods of differing trophic levels. The obtained  $\delta^{15}\text{N}$  values range from 8.7‰ to 11.0‰ with a mean value of  $(9.84 \pm 0.07 \text{‰})$ , which is elevated by approximately +2.7‰ over the animal mean value,  $(7.15 \pm 0.25 \text{‰})$ , calculated without the fox and dog samples. This shift is slightly lower than expected for a whole trophic level, therefore it is assumed that the humans consumed an omnivorous diet containing protein originating from both, animals and plants. Since all human  $\delta^{15}\text{N}$  values are clearly elevated over the animal values it is presumed that every individual consumed significant amounts of animal protein.

Similar to the investigated samples from Thunau, the carbon and nitrogen stable isotope ratios of the Gemeinlebarn samples do not suggest the consumption of freshwater foods in significant amounts (see the discussion in Section 4.3.2). Also here, the observed nitrogen stable isotope signatures of the humans are consistent with a terrestrial diet containing slightly varying amounts of animal protein.

### 4.4.3 Statistical Examination

A major goal of this investigation was to check, whether differences attributed to gender or social rank within the population sample of Bronze Age Gemeinlebarn are reflected in diet aspects that can be reconstructed using carbon and nitrogen stable isotope analysis. Categorization into social ranks was adopted from the previously performed Cluster Analysis (Stadler, 1991, see also Section 2.1.2 for further details).

In Figures 4.12 and 4.13 the  $\delta^{13}\text{C}$  and  $\delta^{15}\text{N}$  values of the individuals assigned to a specific population subgroup (males or females, rich or poor individuals) are plotted. The diagram reveals a tendency of the male individuals for higher  $\delta^{15}\text{N}$  values ( $\bar{x}_m = 9.99 \pm 0.09 \text{‰}$ ,  $N=28$  and  $\bar{x}_f = 9.69 \pm 0.09 \text{‰}$ ,  $N=31$ ). However, the mean  $\delta^{13}\text{C}$  values of the male group and the female group are rather similar ( $\bar{x}_m = -20.06 \pm 0.04 \text{‰}$  and  $\bar{x}_f = -20.18 \pm 0.05 \text{‰}$ ).

The mean  $\delta^{15}\text{N}$  values of the rich ( $9.79 \pm 0.14 \text{‰}$ ,  $N=16$ ) and the poor ( $9.85 \pm 0.08 \text{‰}$ ,  $N=43$ ) groups are almost identical. For the wealthy and the poor categories, the mean  $\delta^{13}\text{C}$  values are  $-20.02 \pm 0.08 \text{‰}$  and  $-20.15 \pm 0.03 \text{‰}$  respectively.

A suitable statistical method to test for significant differences between group means is MANOVA, since this method is capable of analyzing the effect of several independent variables (sex, wealth) on several dependent variables ( $\delta^{13}\text{C}$  and  $\delta^{15}\text{N}$ ). Especially when the dependent variables are intercorrelated, it is frequently recommended to use MANOVA for statistical hypothesis testing (see e.g., the discussion and literature given by Field, 2005, p.573). A Pearson correlation coefficient revealed a small but statistically significant correlation ( $r = 0.277$ ,  $p = 0.032$ ) between the  $\delta^{13}\text{C}$  and  $\delta^{15}\text{N}$  values of this data set, which is why MANOVA was selected as the method of choice. MANOVA is an "overall" or "omnibus" test, i.e. it tests the null hypothesis that the means of all groups (as they were differentiated by an independent variable) are equal for all dependent variables. In case of a significant MANOVA result and more than two groups are regarded, follow-up analyses are needed to identify between which groups the difference(s) was (were) actually found. For this reason, the

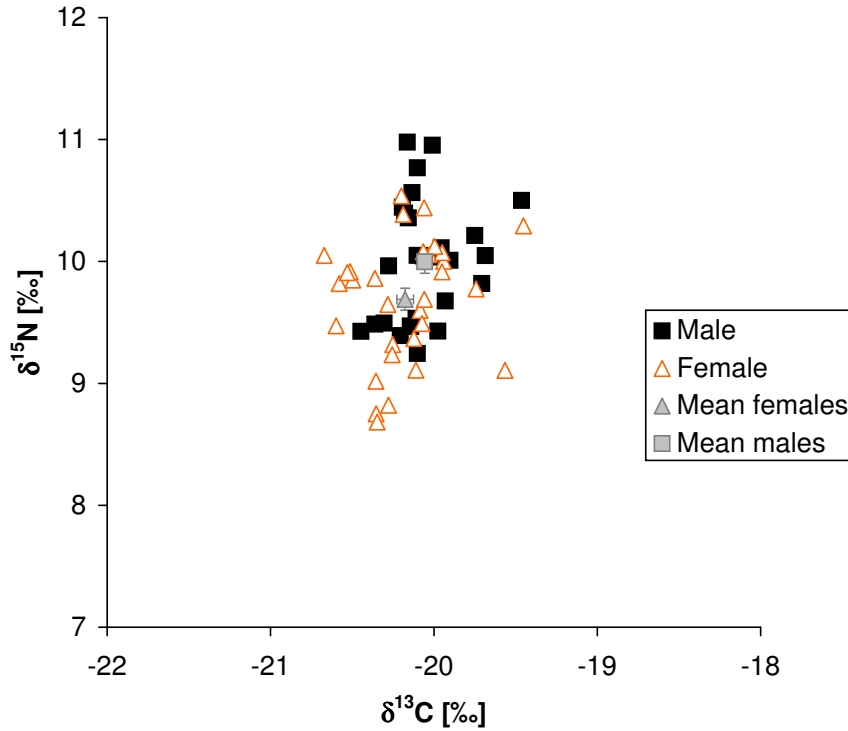


**Figure 4.12:**  $\delta^{13}\text{C}$  and  $\delta^{15}\text{N}$  values of the males and females from Gemeinlebarn, together with the group mean values. The individual with indeterminate sex was excluded. (error bars:  $1\sigma$ )

software package *PASW Statistics* automatically provides ANOVA-tests as follow-up analyses for the MANOVA. Both methods (MANOVA and ANOVA) were also used for the statistical investigation of the sample data from Thunau. Hence the procedure applied to the Gemeinlebarn data set is similar to that performed with the Thunau data described in Section 4.3.3.

The mathematical requirements for ANOVA and MANOVA, the normal distribution of the dependent variables, homogeneity of variances between the groups and homogeneity of the variance-covariance matrices, were tested using the Kolmogorov-Smirnov-Test, the Levene-Test and Box's M-Test respectively. In doing so, an inhomogeneity of variances was detected with respect to the  $\delta^{13}\text{C}$  values ( $F(3; 55) = 3.798$ ,  $p = 0.015$ ). This is caused by the notably greater variance of the  $\delta^{13}\text{C}$  values in the rich category, compared to values in the poor group. However, considering the robustness of both procedures, the reliability of the results was presumed (see also the remarks and citations in Section 4.3.3).

The results of the MANOVA do not indicate any significant differences between the  $\delta$ -values belonging to the two wealth categories, nor between the male and female groups. There were no significant interactions between the two independent variables (wealth and sex). In contrast to this, ANOVA (which treats  $\delta^{13}\text{C}$  and  $\delta^{15}\text{N}$  separately) found a significant difference in  $\delta^{15}\text{N}$  values between the males and the females ( $F(1; 55) = 4.061$ ,  $p = 0.049$ ). Nevertheless the difference between the mean  $\delta^{15}\text{N}$  values of these two groups is small ( $0.30\text{‰}$ ).

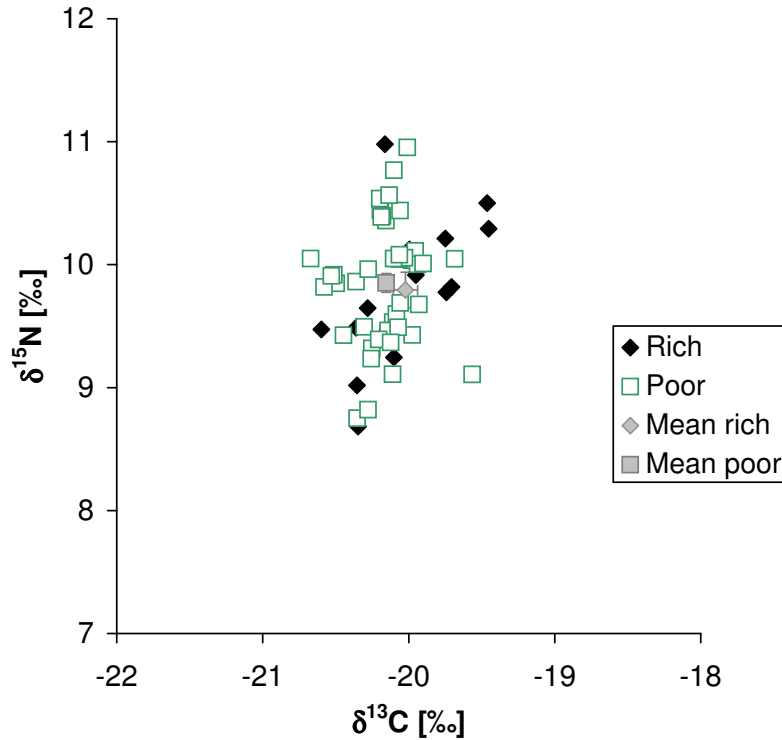


**Figure 4.13:** Diagram of the  $\delta^{13}\text{C}$  and  $\delta^{15}\text{N}$  values of the individuals from Gemeinlebarn categorized as wealthy and poor. The individual with indeterminate sex was excluded. (error bars:  $1\sigma$ )

These results imply that the social rank as inferred from several parameters (number and nature of grave goods, grave dimensions or degree of deterioration due to grave robbery) is not reflected in the bone collagen  $\delta^{13}\text{C}$  and  $\delta^{15}\text{N}$  values, neither within the total sample, nor in the male or the female categories. If the statistically significant correlation between social rank and body height within the male individuals found by Teschler-Nicola (1989) is connected to dietary habits, then it is most likely not caused by a higher or lower protein intake in one of the groups (under the assumption that both groups consumed animal protein of the same trophic level).

Judging from the results of the ANOVA, the males could have consumed a little more animal protein than the females. Note that the individuals with the highest  $\delta^{15}\text{N}$  values are males and those with the lowest values are females (see Figure 4.12).

#### 4.4.4 Conclusions

The  $\delta^{13}\text{C}$  in bone collagen samples of human and faunal remains from the necropolis F in Gemeinlebarn suggest the subsistence on resources originating from a terrestrial  $\text{C}_3$  ecosystem. Judging from the  $\delta^{15}\text{N}$  values, the humans consumed both, animal and plant protein. The observed ranges of  $\delta$ -values are rather narrow, hence it is presumed that diet (as far as it can be reconstructed by  $\delta^{13}\text{C}$  and  $\delta^{15}\text{N}$  values) was relatively uniform within the population.

The hypothesis that social stratification (deduced from several parameters like grave goods, grave dimensions and degree of deprivation) could have influenced dietary habits in a way that it would be reflected in the carbon and/or nitrogen isotopic signatures of the individuals could not be confirmed by this investigation. Using MANOVA and ANOVA for statistical hypothesis testing, no significant differences between the mean  $\delta$ -values of population subgroups categorized as rich and poor could be found.

Furthermore, the mean  $\delta$ -values of the males and the females in this sample were compared with each other. MANOVA could not detect any significant effect of the sex on the  $\delta$ -values, whereas ANOVA was significant for the  $\delta^{15}\text{N}$  values. It is therefore possible that the males consumed slightly higher amounts of animal protein, although it has to be noted that the observed difference is small.

These results allow several interpretations. First, social status and the sex of an individual might not have affected the availability of food items that influence carbon and nitrogen stable isotope signatures e.g., animal protein. Or the differences in nutritional habits were too subtle to be significantly reflected in the  $\delta^{13}\text{C}$  and  $\delta^{15}\text{N}$  values. Even though carbon and nitrogen stable isotope ratios in bone collagen record important aspects of diet, there are still other diet factors that elude detection by stable isotope analysis. Therefore it cannot be ruled out, that differences in nutritional status of the human individuals like varying supply with vitamins or mineral nutrients, caused the socio-biological differentiation in Gemeinlebarn observed by Teschler-Nicola (1989).



## 5 Final Remarks

### Uncertainty Analysis of $\delta^{13}\text{C}$ and $\delta^{15}\text{N}$ values

Since no extensive work on the calculation of uncertainties for  $\delta^{13}\text{C}$  and  $\delta^{15}\text{N}$  values and the implications for dietary interpretations could be found in published literature, a detailed uncertainty analysis was performed for the measured data from both archaeological sites investigated in the present work. In doing so, an evaluation of the variation of  $\delta$ -values due to the chosen measurement procedure (including normalization to international isotope scales) could be obtained. This analysis showed that variation in  $\delta^{13}\text{C}$  is mainly due to the statistical nature of the measurement results, whereas  $\delta^{15}\text{N}$  uncertainties are largely influenced by the uncertainties associated with the isotope standards used in the normalization. This difference is the result of the considerably larger uncertainties of the nitrogen stable isotope reference materials compared to those for carbon. Thus, overall  $\delta^{15}\text{N}$  uncertainties were significantly larger than the statistical component alone. Therefore – especially in the case of  $\delta^{15}\text{N}$  values – a more accurate estimate of  $\delta$ -value variability due to methodological factors can be gained by considering the contributions related to the used isotope standards. In summary, it can be stated that the overall  $\delta^{13}\text{C}$  and  $\delta^{15}\text{N}$  uncertainties obtained in this analysis are small in magnitude compared to the variation in  $\delta$ -values relevant for palaeodietary interpretations and hence, can in most cases be neglected.

### Social Stratification and Stable Isotope Analysis

According to the results of several published palaeodiet studies, there is evidence that social stratification within ancient populations might in some cases be reflected in dietary patterns, which are detectable using carbon and nitrogen stable isotope analysis (see the discussion in Section 1.1). For both archaeological sites, investigated in the course of this work, previous archaeological and/or anthropological examinations indicated social differentiation within the respective population. In the case of the Bronze Age population from Gemeinlebarn, a socio-biological differentiation appearing as a difference in body height between social groups could be observed and the particular situation of the Early Medieval town of Thunau, which consisted of two separated inhabited areas (a hill top settlement and the production orientated site in the river valley), led to the assumption that both areas were occupied by members of distinct social strata (see Sections 2.1 and 2.2). It was therefore expected that differences in nutritional behavior between the respective social groups existed and that these variations could be revealed by carbon and nitrogen stable isotope analysis. However, no considerable differences between mean  $\delta$ -values of population subgroups representing distinct social categories could be confirmed. There was only one sta-

tistically significant ANOVA result, which points to a difference in  $\delta^{15}\text{N}$  between the males and the females in Gemeinlebarn. A potential interpretation of this result is an unequal extent of animal protein consumption of the males and the females.

Nevertheless, the results of this study provide insights into the dietary habits of two ancient human populations from central Europe. For example, individuals substantially deviating in their carbon isotopic composition from the bulk of the values could be detected within the samples from Thunau. Further interpretations can be made when the stable isotope values of both data sets (from Gemeinlebarn and Thunau) are compared with each other.

### **Comparison of the Results from Gemeinlebarn and Thunau: Differences between a Bronze Age and an Early Medieval Population in Lower Austria**

The results of the carbon and nitrogen stable isotope analysis of the collagen samples from Gemeinlebarn and Thunau/Gars am Kamp exhibit a few differences, which become obvious in Figure 5.1. First, the  $\delta$ -values of the human samples from Thunau show a considerably greater variability than those from Gemeinlebarn especially with respect to the  $\delta^{13}\text{C}$  values. This implies a more heterogeneous diet for the population from Thunau compared to the investigated humans from Gemeinlebarn. The obtained isotopic compositions actually represent the population sample from Gemeinlebarn as an extremely homogeneous group. This can on the one hand be understood in terms of the relatively short occupancy period of Gemeinlebarn's necropolis F of about 80-100 years (Teschler-Nicola, 1989). On the other hand the data raise the question, if these differences in diet variability can be regarded in the light of distinct subsistence strategies in the two different time periods. In Bronze Age Gemeinlebarn the population probably relied on locally produced agricultural foodstuffs, whereas the inhabitants of Early Medieval Thunau had access to more diverse diet sources that could partly originate from other geographic regions (see the discussion in Section 4.5). Hence, the evidence could be interpreted as a result of changes in the utilization and access to food sources between the two societies. The determined isotope data for the Bronze Age population from Gemeinlebarn match with the picture of a typical rural society, where all individuals relied on similar dietary (agricultural) items, whereas the results for Thunau seem to be reflective of a more complex societal structure as it would be expected in an early, urbanized agglomeration. In this way, changes in nutritional strategies in the course of different time periods – possibly linked with cultural developments – can be detected for a specific area.

A similar variability pattern to that of the humans can be observed in the scatter of the animal values, which vary over a substantially wider range in the case of Thunau. It has, however, to be kept in mind that the animal sample set for Gemeinlebarn is smaller and includes not as many species than the Thunau samples. Due to this small number of available samples, a more profound statistical examination would not be conclusive and was therefore not performed.

It is also noticeable that the whole human sample set of Thunau plots on aver-



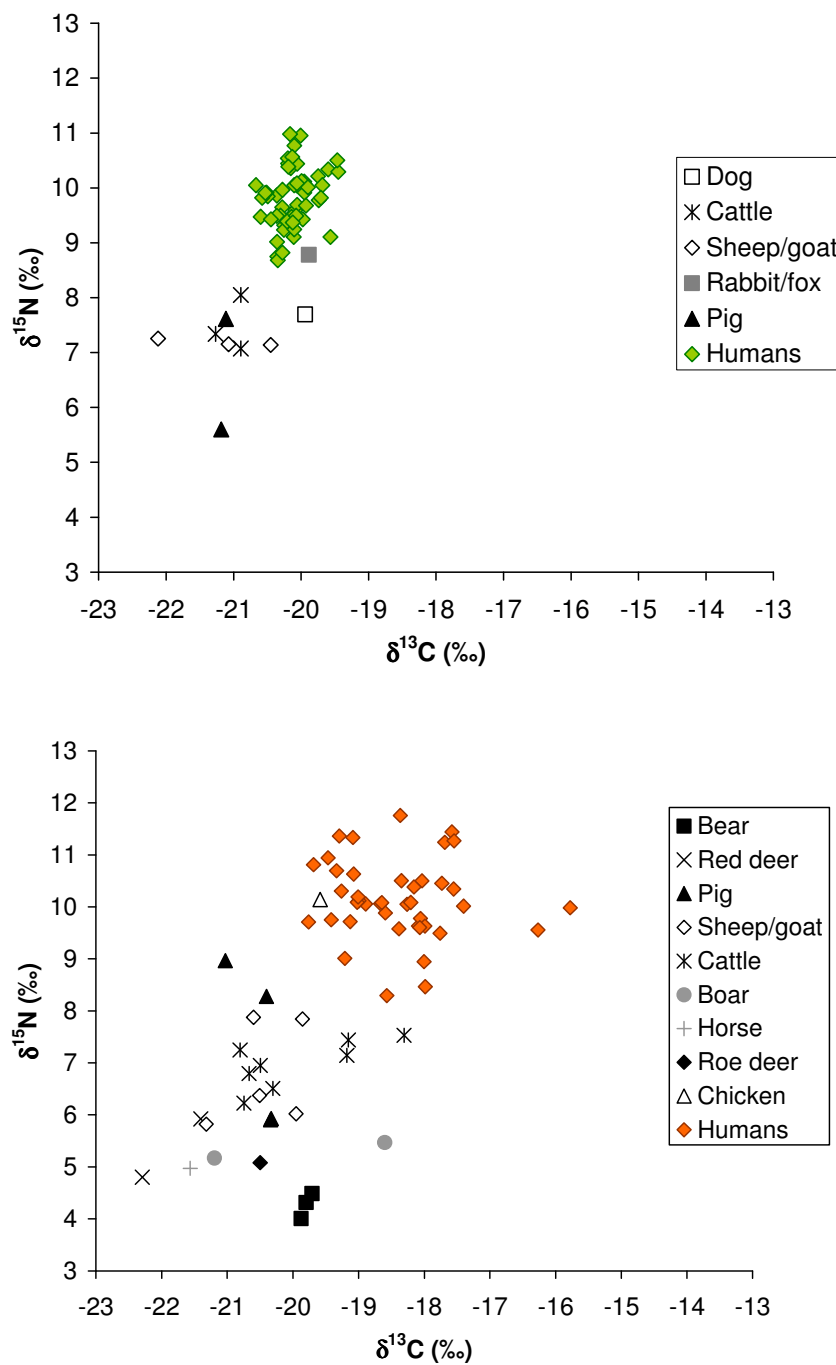


**Figure 5.1:** Scatter plots of the final  $\delta^{13}\text{C}$  and  $\delta^{15}\text{N}$  values of Gemeinlebarn (above) and Thunau/Gars (below) with identical scales to facilitate comparison.

age at higher  $\delta^{13}\text{C}$  values. The difference of 1.6 ‰ between the mean  $\delta^{13}\text{C}$  values<sup>1</sup> (Gemeinlebern:  $(-20.1 \pm 0.3) \text{‰}$  and Thunau:  $(-18.5 \pm 0.7) \text{‰}$ ) is statistically highly significant ( $t = 14.218$ ,  $p < 0.000$ )<sup>2</sup>. This difference is unlikely to be caused by a climatic influence on the  $\delta$ -values. van Klinken *et al.* (1994) found a correlation between bone collagen  $\delta^{13}\text{C}$  values and temperature of approximately +0.2 ‰ per °C increase in temperature. Hence it can be expected that climate variations in the investigated region – even if they are in the range of several degrees Celsius – would influence  $\delta^{13}\text{C}$  values only in the position after the decimal point. Thus, the observed difference of 1.6 ‰ in  $\delta^{13}\text{C}$  values more likely points to the exploitation of a food source with comparatively high  $\delta^{13}\text{C}$  values in the Thunau sample, which seems to be absent in the diet of Gemeinlebern's population. It is therefore likely that at least part of Thunau's humans included  $\text{C}_4$  plants in their diet. The humans could either have eaten such plants directly or indirectly by the consumption of animals, who fed on these plants.

---

<sup>1</sup>Calculated excluding the two outliers in the sample set of Thunau, thus N=99.

<sup>2</sup>Calculated by an independent samples T-test (also called Student's T-test), which is used to test for statistically significant differences between two independent group means (see e.g., Field, 2005; Janssen & Laatz, 2007). Basically, the t-statistic is the ratio of systematic to unsystematic variation in the data, similar to the concept of the F-statistic as described in Section 4.3.3. Note, that the statistical significance "p" is only computed to three digits after the comma by the used software package *PASW*. The prerequisite for the T-test is the normal distribution in both data groups, which was checked by a Kolmogorov-Smirnov test.

# Bibliography

- AMBROSE, S.H. 1990. Preparation and characterization of bone and tooth collagen for isotopic analysis. *Journal of Archaeological Science*, **17**, 431–451.
- AMBROSE, S.H. 1991. Effects of diet, climate and physiology on nitrogen abundance in terrestrial foodwebs. *Journal of Archaeological Science*, **18**, 293–317.
- AMBROSE, S.H., & KRIGBAUM, J. 2003. Bone chemistry and bioarchaeology. *Journal of Anthropological Archaeology*, **22**, 193–199.
- AMBROSE, S.H., & NORR, L. 1993. Experimental evidence for the relationship of the carbon isotope ratios of whole diet and dietary protein to those of bone collagen and carbonates. *Pages 1–37 of: LAMBERT, J.B., & GRUPE, G. (eds), Prehistoric human bone: archaeology at the molecular level.* Springer, Berlin.
- BABEL, W. 1996. Gelatine – ein vielseitiges Biopolymer. *Chemie in unserer Zeit*, **30**, 86–95.
- BACKHAUS, K., ERICHSON, B., PLINKE, W., & WEIBER, R. 2006. *Multivariate Analysenmethoden*. 11 edn. Springer, Berlin, Heidelberg.
- BÖHLKE, J.K., & COPLEN, T.B. 1995. Interlaboratory comparison of reference materials for nitrogen-isotope-ratio measurements. *Pages 51–66 of: Reference and intercomparison materials for stable isotopes of light elements.* IAEA TECDOC 825. International Atomic Energy Agency.
- BOCHERENS, H., & DRUCKER, D. 2003. Trophic Level Isotopic Enrichment of Carbon and Nitrogen in Bone Collagen: Case Studies from Recent and Ancient Terrestrial Ecosystems. *International Journal of Osteoarchaeology*, **13**, 46–53.
- BOGAARD, A., HEATON, T.H.E., POULTON, P., & MERBACH, I. 2007. The impact of manuring on nitrogen isotope ratios in cereals: archaeological implications for reconstruction of diet and crop management practices. *Journal of Archaeological Science*, **34**, 335–343.
- BOL, R., ERIKSEN, J., SMITH, P., GARNETT, M.H., COLEMAN, K., & CHRISTENSEN, B.T. 2005. The natural abundance of  $^{13}\text{C}$ ,  $^{15}\text{N}$ ,  $^{34}\text{S}$  and  $^{14}\text{C}$  in archived (1923–200) plant and soil samples from the Askov long-term experiment on animal manure and fertilizer. *Rapid Communications in Mass Spectrometry*, **19**, 3216–3226.

- BORGGREVEN, J.M.P.M., HOPPENBROUWERS, P.M.M., & GORISSEN, R. 1979. Radiochemical determination of the metabolic activity of collagen in mature dentin. *Journal of Dental Research*, **58**, 2120–2124.
- BOSKEY, A.L. 1999. Mineralization, structure, and function of bone. *Pages 153–164 of: SEIBEL, M.J., ROBINS, S.P., & BILEZIKIAN, J.P. (eds), Dynamics of bone and cartilage metabolism.* Academic Press, San Diego London.
- BRAND, W.A. 2004. Mass spectrometer hardware for analyzing stable isotope ratios. *Pages 836–858 of: DE GROOT, P.A. (ed), Handbook of stable isotope analytical techniques, Volume-I.* Elsevier, Amsterdam.
- BRANDT, S. 1999. *Data Analysis: Statistical and computational methods for scientists and engineers.* 3 edn. Springer Verlag, New York, Berlin, Heidelberg.
- BRANHAM, R.L.JR. 1990. *Scientific data analysis, an introduction to overdetermined systems.* Springer Verlag, New York, Berlin, Heidelberg.
- BRAY, J.H., & MAXWELL, S.E. 1985. *Multivariate Analyses of Variance.* Sage University Paper Series on Quantitative Research Methods, vol. 54. Sage Publications, Newbury Park.
- BRENNA, J.T., CORSO, T.N., TOBIAS, H.J., & CAIMI, R.J. 1997. High-precision continuous-flow isotope ratio mass spectrometry. *Mass Spectrometry Reviews*, **16**, 227–258.
- BRINCKMANN, J. 2005. Collagens at a glance. *Pages 1–6 of: BRINCKMANN, J., NOTBOHM, H., & MÜLLER, P.K. (eds), Collagen. Primer in structure, processing and assembly.* Springer, Berlin Heidelberg.
- BRONK RAMSEY, C., HIGHAM, T., BOWLES, A., & HEDGES, R. 2004. Improvements to the pretreatment of bone at Oxford. *Radiocarbon*, **46**, 155–163.
- BRONSTEIN, I.N., SEMENDJAJEW, K.A., MUSIOL, G., & MÜHLIG, H. 2000. *Taschenbuch der Mathematik.* 5 edn. Verlag Harri Deutsch, Thun, Frankfurt am Main.
- BROWN, T.A., NELSON, D.E., VOGEL, J.S., & SOUTON, J.R. 1988. Improved collagen extraction by modified Longin method. *Radiocarbon*, **30**, 171–177.
- BUDZIKIEWICZ, H. 1998. *Massenspektrometrie.* 4 edn. Wiley-VCH, Weinheim.
- BUIKSTRA, J.E., & MILNER, G.R. 1991. Isotopic and archaeological interpretations of diet in the central Mississippi valley. *Journal of Archaeological Science*, **18**, 319–329.
- CERLING, T.E., HARRIS, J.M., & LEAKY, M.G. 1999. Browsing and grazing in elephants: the isotope record of modern and fossil proboscideans. *Oecologia*, **120**, 364–374.

- CHISHOLM, B.S., NELSON, D.E., HOBSON, K.A., SCHWARCZ, H.P., & KNYF, M. 1983. Carbon isotope measurement techniques for bone collagen: Notes for the archaeologist. *Journal of Archaeological Science*, **10**, 355–360.
- COLLINS, M.J., NIELSEN-MARSH, C.M., HILLER, J., SMITH, C.I., ROBERTS, J.P., PRIGODICH, R.V., WESS, T.J., CSAPÒ, J., MILLARD, A.R., & TURNER-WALKER, G. 2002. The survival of organic matter in bone: a review. *Archaeometry*, **44**, 383–394.
- COOK, G.T., DUNBAR, E., BLACK, S.M., & XU, S. 2006. A preliminary assessment of age at death determination using the nuclear weapons testing  $^{14}\text{C}$  activity of dentine and enamel. *Radiocarbon*, **48**, 305–313.
- COPLEN, T.B., BÖHLKE, J.K., DE BIÈVRE, P., DING, T., HOLDEN, N.E., HOPPLE, J.A., KROUSE, H.R., LAMBERTY, A., PEISER, H.S., RÉVÉSZ, K., RIEDER, S.E., ROSMAN, K.J.R., ROTH, E., TAYLOR, P.D.P., VOCKE, R.D.JR., & XIAO, Y.K. 2002. Isotope-abundance variations of selected elements. *Pure and Applied Chemistry*, **74**, 1987–2017.
- COPLEN, T.B., BRAND, W.A., GEHRE, M., GRÖNING, M., MEIJER, H.A. J., TOMAN, B., & VERKOUTEREN, R.M. 2006a. After two decades a second anchor for the VPDB  $\delta^{13}\text{C}$  scale. *Rapid Communications in Mass Spectrometry*, **20**, 3165–3166.
- COPLEN, T.B., BRAND, W.A., GEHRE, M., GRÖNING, M., MEIJER, H.A. J., TOMAN, B., & VERKOUTEREN, R.M. 2006b. New guidelines for  $\delta^{13}\text{C}$  Measurements. *Analytical Chemistry*, **78**, 2439–2441.
- CRAIG, H. 1954. Carbon-13 in plants and the relationship between carbon-13 and carbon-14 variations in nature. *The Journal of Geology*, **62**, 115–149.
- CRAIG, H. 1957. Isotopic standards for carbon and oxygen and correction factors for mass-spectrometric analysis of carbon dioxide. *Geochimica et Cosmochimica Acta*, **12**, 133–149.
- DELWICHE, C.C., & STEYN, P.L. 1970. Nitrogen isotope fractionation in soils and microbial reactions. *Environmental Science & Technology*, **4**, 929–935.
- DENIRO, M.J. 1985. Postmortem preservation and alteration of in vivo bone collagen isotope ratios in relation to palaeodietary reconstruction. *Nature*, **317**, 806–809.
- DENIRO, M.J. 1987. Stable Isotopy and Archaeology. *American Scientist*, **75**, 182–192.
- DENIRO, M.J., & EPSTEIN, S. 1978. Influence of diet on the distribution of carbon isotopes in animals. *Geochimica et Cosmochimica Acta*, **42**, 495–506.

- DENIRO, M.J., & EPSTEIN, S. 1981. Influence of diet on the distribution of nitrogen isotopes in animals. *Geochimica et Cosmochimica Acta*, **45**, 341–351.
- DJAGNY, K.B., WANG, Z., & XU, S. 2001. Gelatin: A valuable protein for food and pharmaceutical industries: Review. *Critical Reviews in Food Science and Nutrition*, **41**, 481–492.
- DONALDSON, T.S. 1968. Robustness of the F-Test to errors of both kinds and the correlation between the numerator and denominator of the F-Ratio. *Journal of the American Statistical Association*, **63**, 660–676.
- DÜRRWÄCHTER, C., CRAIG, O.E., COLLINS, M.J., BURGER, J., & ALT, K.W. 2006. Beyond the grave: variability in Neolithic diets in Southern Germany? *Journal of Archaeological Science*, **33**, 39–48.
- DUFOUR, E., BOCHERENS, H., & MARIOTTI, A. 1999. Palaeodietary implications of isotopic variability in Eurasian lacustrine fish. *Journal of Archaeological Science*, **26**, 617–627.
- DUPRAS, T.L., & TOCHERI, M.W. 2007. Reconstruction infant weaning histories at roman period Kellis, Egypt using stable isotope analysis of dentition. *American Journal of Physical Anthropology*, **134**, 63–74.
- ELLIOTT, W.H., & ELLIOTT, D.C. 2001. *Biochemistry and Molecular Biology*. Oxford University Press, Oxford.
- ENGEL, J., & BÄCHINGER, H.P. 2005. Structure, stability and folding of the collagen triple helix. *Pages 7–33 of: BRINCKMANN, J., NOTBOHM, H., & MÜLLER, H.P. (eds), Collagen. Primer in structure, processing and assembly*. Springer, Berlin Heidelberg.
- ERIKSSON, G., LINDERHOLM, A., FORNANDER, E., KANSTRUP, M., SCHOULTZ, P., OLOFSSON, A., & LIDÉN, K. 2008. Same island, different diet: Cultural evolution of food practice on Öland, Sweden, from the Mesolithic to the Roman period. *Journal of Anthropological Archaeology*, **27**, 520–543.
- FARQUHAR, G.D., O’LEARY, M.H., & BERRY, J.A. 1982. On the relationship between carbon isotope discrimination and the intercellular carbon dioxide concentration in leaves. *Australian Journal of Plant Physiology*, **9**, 121–37.
- FARQUHAR, G.D., EHLENGER, J.R., & HUBICK, K.T. 1989. Carbon isotope discrimination and photosynthesis. *Annual Review of Plant Physiology and Plant Molecular Biology*, **40**, 503–537.
- FARQUHAR, J., BAO, H., & THIEMENS, M. 2000. Atmospheric influence of earth’s earliest sulfur cycle. *Science*, **289**, 756–759.
- FIELD, A. 2005. *Discovering Statistics Using SPSS*. 2 edn. ISM Introducing Statistical Methods. Sage Publications, London, Thousand Oaks, New Delhi.

- FISCHER, A., OLSEN, J., RICHARDS, M., HEINEMEIER, J., SVEINBJÖRNSDÓTTIR, Á. E., & BENNIKE, P. 2007. Coast-inland mobility and diet in the Danish Mesolithic and Neolithic: evidence from stable isotope values of humans and dogs. *Journal of Archaeological Science*, **34**, 2125–2150.
- FOGEL, M.L., TUROSS, N., JOHNSON, B.J., & MILLER, G.H. 1997. Biogeochemical record of ancient humans. *Organic Geochemistry*, **27**, 275–287.
- FRIEDLI, H., LOSTSCHER, H., OESCHGER, H., SIEGENTHALER, U., & STAUFFER, B. 1986. Ice record of  $^{13}\text{C}/^{12}\text{C}$  ratio of atmospheric  $\text{CO}_2$  in the past two centuries. *Nature*, **324**, 237–238.
- FRIESINGER, H., & FRIESINGER, I. 1975. *5000 Jahre Siedlung im Garser Raum. Die Befestigungsanlagen von Thunau*. Katalogreihe des Krahuletzmuseums, vol. 3. Eggenburg.
- FRIESINGER, H., & FRIESINGER, I. 1991. Ein Vierteljahrhundert Grabungen in Thunau/Gars am Kamp. *Archäologie Österreichs*, **2/1**, 6–22.
- FULLER, B.T., RICHARDS, M.P., & MAYS, S.A. 2003. Stable Carbon and Nitrogen Isotope Variations in Tooth Dentine Serial Sections from Wharram Percy. *Journal of Archaeological Science*, **30**, 1673–1684.
- GANNES, L.Z., MARTINEZ DEL RIO, C., & KOCH, P. 1998. Natural abundance variations in stable isotopes and their potential uses in animal physiological ecology. *Comparative Biochemistry and Physiology*, **119A**, 725–737.
- GOLDYN, B., HROMADA, M., & TRYJANOWSKI, P. 2003. Habitat use and diet of the red fox *Vulpes vulpes* in an agricultural landscape in Poland. *Zeitschrift für Jagdwissenschaften*, **49**, 191–200.
- HANDLEY, L.L., AUSTIN, A.T., STEWART, G.R., ROBINSON, D., SCRIMGEOUR, C.M., RAVEN, J.A., HEATON, T.H.E., & SCHMIDT, S. 1999. The  $^{15}\text{N}$  natural abundance ( $\delta^{15}\text{N}$ ) of ecosystem samples reflects measures of water availability. *Australian Journal of Plant Physiology*, **26**, 185–199.
- HAYES, J.M. 2002. *Practice and principles of isotopic measurements in organic geochemistry*. Woods Hole Oceanographic Institution, Woods Hole, MA 02543, [http://www.gps.caltech.edu/~als/library/other\\_stuff/hayespnp.pdf](http://www.gps.caltech.edu/~als/library/other_stuff/hayespnp.pdf).
- HEDGES, R.E.M. 2002. Bone diagenesis: An overview of processes. *Archaeometry*, **44**, 319–328.
- HEDGES, R.E.M., & REYNARD, L.M. 2007. Nitrogen isotopes and the trophic level of humans in archaeology. *Journal of Archaeological Science*, **34**, 1240–1251.
- HEDGES, R.E.M., CLEMENT, J.G., THOMAS, C.D., & O'CONNEL, T.C. 2007. Collagen turnover in the adult femoral mid-shaft: modelled from anthropogenic radiocarbon tracer measurements. *American Journal of Physical Anthropology*, **133**, 808–816.

- HEINRICH, W., & TESCHLER-NICOLA, M. 1991. Zur Anthropologie des Gräberfeldes F von Gemeinlebarn, Niederösterreich. *Pages 222–262 of: Die Nekropole F von Gemeinlebarn, Niederösterreich* (Habilitation: Neugebauer, J.-W.). Römisch-Germanische Forschungen, vol. 49. Verlag Philipp von Zabern, Mainz am Rhein.
- HEROLD, H. 2008. Der Schanzberg von Gars-Thunau in Niederösterreich. *Archäologisches Korrespondenzblatt*, **38**, 283–299.
- HOEFS, J. 2004. *Stable isotope geochemistry*. 5<sup>th</sup> edn. Springer-Verlag, Berlin.
- HÄRDLE, W., & SIMAR, L. 2007. *Applied Multivariate Statistical Analysis*. 2 edn. Springer-Verlag, Berlin, Heidelberg.
- HUT, G. 1987. *Consultants' group meeting on stable isotope reference samples for geochemical and hydrological investigations (16-18 September 1985, Vienna, Austria) Report to Director General*. Tech. rept. International Atomic Energy Agency.
- IAEA. 2010. *Reference Materials Catalogue - Stable Isotopes*. <http://curem.iaea.org/catalogue/SI>.
- JANSSEN, J., & LAATZ, W. 2007. *Statistische Datenanalyse mit SPSS für Windows*. 6 edn. Springer-Verlag, Berlin.
- JIM, S., JONES, V., AMBROSE, S.H., & EVERSHERD, R.P. 2006. Quantifying dietary macronutrient sources of carbon for bone collagen biosynthesis using natural abundance stable carbon isotope analysis. *British Journal of Nutrition*, **95**, 1055–1062.
- JØRKOV, M.S., HEINEMEIER, J., & LYNNERUP, N. 2007. Evaluating bone collagen extraction methods for stable isotope analysis in dietary studies. *Journal of Archaeological Science*, **34**, 1824–1829.
- JUNQUEIRA, L.C., & CARNEIRO, J. 1996. *Histologie*. 4 edn. Springer Medizin Verlag, Heidelberg.
- KANELUTTI, E. 1990. *Slawen- und Urnenfelderzeitliche Säugetiere von Thunau bei Gars am Kamp (Niederösterreich)*. Ph.D. thesis, Universität Wien.
- KARAMANOS, R.E., VORONEY, R.P., & RENNIE, D.A. 1981. Variation in natural N-15 abundance of central Saskatchewan soils. *Soil Science Society of America Journal*, **45**, 826–828.
- KEENLEYSIDE, A., SCHWARCZ, H., STIRLING, L., & BEN LAZREG, N. 2009. Stable isotopic evidence for diet in a Roman and Late roman population from Leptiminus, Tunisia. *Journal of Archaeological Science*, **36**, 51–63.
- KENDALL, C., & CALDWELL, E.A. 1998. Fundamentals of isotope geochemistry. *In: KENDALL, C., & McDONNELL, J.J. (eds), Isotope Tracers in Catchment Hydrology*, 1 edn. Elsevier, Amsterdam.



- KJELLSTRÖM, A., STORÅ, J., POSSNERT, G., & LINDERHOLM, A. 2009. Dietary patterns and social structures in medieval Sigtuna, Sweden, as reflected in stable isotope values in human skeletal remains. *Journal of Archaeological Science*, **36**, 2689–2699.
- KRUEGER, H.W., & SULLIVAN, C.H. 1984. Models for carbon isotope fractionation between diet and bone. *Pages 205–220 of: TURNLAND, J.F., & JOHNSON, P.E. (eds), Stable isotopes in nutrition.* ACS Symposium Series, vol. 258. American Chemical Society.
- KRYSTEK, M., & ANTON, M. 2007. A weighted total least-squares algorithm for fitting a straight line. *Measurement Science and Technology*, **18**, 3438–3442.
- LAW, I.A., & HEDGES, R.E.M. 1989. A semi-automated bone pretreatment system and the pretreatment of older and contaminated samples. *Radiocarbon*, **31**, 247–253.
- LE HURAY, J.D., & SCHUTKOWSKI, H. 2005. Diet and social status during the La Tène period in Bohemia: Carbon and nitrogen stable isotope analysis of bone collagen from Kutná Hora-Karlov and Radovesice. *Journal of Anthropological Archaeology*, **24**, 135–147.
- LEE-THORP, J.A. 2008. On isotopes and old bones. *Archaeometry*, **6**, 925–950.
- LIBBY, W.F., BERGER, R., MEAD, J.F., ALEXANDER, G.V., & ROSS, J.F. 1964. Replacement rates for human tissue from atmospheric radiocarbon. *Science*, **146**, 1170–1172.
- LIDEN, K., TAKAHASHI, C., & NELSON, D.E. 1995. The effects of lipids in stable carbon isotope analysis and the effects of NaOH treatment on the composition of extracted bone collagen. *Journal of Archaeological Science*, **22**, 321–326.
- LILLIE, M., & JACOBS, K. 2006. Stable isotope analysis of 14 individuals from the Mesolithic cemetery of Vasilyevka II, Dnieper Rapids region, Ukraine. *Journal of Archaeological Science*, **33**, 880–886.
- LONGIN, R. 1971. New method of collagen extraction for radiocarbon dating. *Nature*, **230**, 241–242.
- MANOLAGAS, S.C. 2000. Birth and death of bone cells: Basic regulatory mechanisms and implications for the pathogenesis and treatment of osteoporosis. *Endocrine Reviews*, **21**, 115–137.
- MARIOTTI, A. 1983. Atmospheric nitrogen is a reliable standard for natural  $^{15}\text{N}$  abundance measurements. *Nature*, **303**, 685–687.
- MARIOTTI, A., GERMON, J.C., HUBERT, P., KAISER, P., LETOLLE, R., TARDIEUX, A., & TARDIEUX, P. 1981. Experimental determination of nitrogen kinetic isotope fractionation: some principles; illustration for the denitrification and nitrification processes. *Plant and Soil*, **62**, 413–430.

- MATTEY, D.P. 1997. Gas source mass spectrometry: isotopic composition of lighter elements. *Pages 154–170 of: GILL, R. (ed), Modern analytical geochemistry.* Addison Wesley Longman, Harlow.
- MERCK. 1963. *Reagenzien Merck: Komplexometrische Bestimmungsmethoden mit Titriplex.* Frankfurter Straße 250, 6100 Darmstadt.
- MINAGAWA, M. 1992. Reconstruction of human diet from  $\delta^{13}\text{C}$  and  $\delta^{15}\text{N}$  in contemporary Japanese hair: a stochastic method for estimating multi-source contribution by double isotopic tracers. *Applied Geochemistry*, **7**, 145–158.
- MINAGAWA, M., & WADA, E. 1984. Stepwise enrichment of  $^{15}\text{N}$  along food chains: Further evidence and the relation between  $\delta^{15}\text{N}$  and animal age. *Geochimica et Cosmochimica Acta*, **48**, 1135–1140.
- MÜLDNER, G., & RICHARDS, M.P. 2005. Fast or Feast: Reconstructing Diet in Later Medieval England by Stable Isotope Analysis. *Journal of Archaeological Science*, **32**, 39–48.
- MÜLDNER, G., & RICHARDS, M.P. 2007a. Diet and Diversity at later Medieval Fishergate: The Isotopic Evidence. *American Journal of Physical Anthropology*, **134**, 162–174.
- MÜLDNER, G., & RICHARDS, M.P. 2007b. Stable Isotope Evidence for 1500 Years of Human Diet at the City of York, UK. *American Journal of Physical Anthropology*, **133**, 682–697.
- MOOK, W.G., & KOOPMANS, M. 1983. Seasonal, latitudinal, and secular variations in the abundance and isotopic ratios of atmospheric carbon dioxide, 1. results from land stations. *Journal of Geophysical Research*, **88**, 10915–10933.
- MOOK, W.G., BOMMERSON, J.C., & STAVERMAN, W.H. 1974. Carbon isotope fractionation between dissolved bicarbonate and gaseous carbon dioxide. *Earth and Planetary Science Letters*, **22**, 169–176.
- MURRAY, M., & SCHOENINGER, M.J. 1988. Diet, status and complex social structure in Iron Age Central Europe: some contributions of bone chemistry. *Pages 157–178 of: GIBSON, B., & GESELOWITZ, M. (eds), Tribe and Polity in Late Prehistoric Europe.* Plenum, New York.
- NEUGEBAUER, J.-W. 1991. *Die Nekropole F von Gemeinlebarn, Niederösterreich* (Habilitation, University of Vienna). With contributions by Stadler, P., Heinrich, W., and Teschler-Nicola, M. *Römisch-Germanische Forschungen*, vol. 49. Verlag Philipp von Zabern, Mainz am Rhein.
- NEUGEBAUER, J.-W., NEUGEBAUER-MARESCH, C., TESCHLER-NICOLA, M., & STADLER, P. 1987. *Die Bronzezeit im Osten Österreichs.* Verlag Niederösterreichisches Pressehaus, St. Pölten, Wien.

- NEUGEBAUER, J.-W., LOCHNER, M., NEUGEBAUER-MARESCH, C., & TESCHLER-NICOLA, M. 1994. *Bronzezeit in Ostösterreich*. Verlag Niederösterreichisches Pressehaus, St. Pölten, Wien.
- NICOLAS-SIMONNOT, M.-O., TRÉGUER, V., LECLERC, J.-P., SARDIN, M., BRAJOUX, J.-P., MOY, J., & TAKERKART, G. 1997. Experimental study and modelling of gelatin production from bone powder: elaboration of an overall kinetic scheme for the acid process. *Chemical Engineering Journal*, **67**, 55–64.
- NITSCH, E.K., HUMPHREY, L.T., & HEDGES, R.E.M. 2010. The effect of parity status on  $\delta^{15}\text{N}$ : looking for the "pregnancy effect" in 18th and 19th century London. *Journal of Archaeological Science*, **37**, 3191–3199.
- NOWOTNY, E. 2011. Mehrfachgräber im Gräberfeld von Thunau, Obere Holzwiese. Methodik, Ausprägungen, Deutungsmöglichkeiten. *Archeologické rozhledy*, **63**, 443–465.
- OBENAU, M., & EICHERT, S. 2009. Die Talsiedlung von Thunau am Kamp, NÖ. – Eine Zwischenbilanz (oral presentation by Eichert, S. & abstract). *Internationales ÖGUF-Symposium, Mauterndorf*.
- OBENAU, M., BREIBERT, W., & SZAMEIT, E. 2005. Frühmittelalterliche Bestattungen und Siedlungsbefunde aus Thunau am Kamp, Niederösterreich – ein Vorbericht. *Fundberichte aus Österreich*, **44**, 347–368.
- O'LEARY, M.H. 1980. Determination of heavy-atom isotope effects on enzyme-catalyzed reactions. *Methods in Enzymology*, **64**, 83–104.
- O'LEARY, M.H. 1981. Carbon isotope fractionation in plants. *Phytochemistry*, **20**, 553–567.
- O'LEARY, M.H., MADHAVAN, S., & PANETH, P. 1992. Physical and chemical basis of carbon isotope fractionation in plants. *Plant, Cell and Environment*, **15**, 1099–1104.
- ORTNER, D.J. 2003. *Identification of pathological conditions in human skeletal remains*. 2 edn. Academic Press, Amsterdam.
- PARFITT, A.M. 1994. Osteonal and hemi-osteonal remodeling: The spatial and temporal framework for signal traffic in adult human bone. *Journal of Cellular Biochemistry*, **55**, 273–286.
- PAUL, D., SKRZYPEK, G., & FÓRIZS, I. 2007. Normalization of measured stable isotopic compositions to isotope reference scales - a review. *Rapid Communications in Mass Spectrometry*, **21**, 3006–3014.
- PELLA, E., & COLOMBO, B. 1973. Study of carbon, hydrogen and nitrogen determination by combustion-gas chromatography. *Mikrochimica Acta*, 697–719.

- PETERSON, B.J., & FRY, B. 1987. Stable isotopes in ecosystem studies. *Annual Review of Ecology and Systematics*, **18**, 293–320.
- PLATZNER, I.T. 1997. *Modern isotope ratio mass spectrometry*. John Wiley & Sons, Chichester.
- POPOVTSCHAK, M., ZWIAUER, K., & KOHLER-SCHNEIDER, M. 2003. *Thunau am Kamp – Eine besfestigte Höhensiedlung: Archäobotanik 1965-1995*. Mitteilungen der Prähistorischen Kommission der Österreichischen Akademie der Wissenschaften, vol. 52. Verlag der Österreichischen Akademie der Wissenschaften, Wien.
- PRICE, T.D., SCHOENINGER, M.J., & ARMELAGOS, G.C. 1985. Bone chemistry and past behaviour: an overview. *Journal of Human Evolution*, **14**, 419–447.
- PROWSE, T.L., SCHWARCZ, H.P., SAUNDERS, S.R., MACCHIARELLI, R., & BONDOLI, L. 2005. Isotopic evidence for age-related variation in diet from Isola Sacra, Italy. *American Journal of Physical Anthropology*, **128**, 2–13.
- RAVEN, J.A., COCKEL, C.S., & DE LA ROCHA, C.L. 2008. The evolution of inorganic carbon concentrating mechanisms in photosynthesis. *Philosophical Transactions of the Royal Society B*, **363**, 2641–2650.
- RENNIE, D.A., PAUL, E.A., & JOHNS, L.E. 1976. Natural nitrogen-15 abundance of soil and plant samples. *Canadian Journal of Soil Science*, **56**, 43–50.
- RICHARDS, M.P., & HEDGES, R.E.M. 1999. Stable isotope evidence for similarities in the types of marine foods used by late Mesolithic humans at sites along the Atlantic coast of Europe. *Journal of Archaeological Science*, **26**, 717–722.
- RICHARDS, M.P., HEDGES, R.E.M., MOLLESON, T.I., & VOGEL, J.C. 1998. Stable isotope analysis reveals variations in human diet at the Poundbury Camp cemetery site. *Journal of Archaeological Science*, **25**, 1247–1252.
- RICHARDS, M.P., MAYS, S., & FULLER, B.T. 2002. Stable Carbon and Nitrogen Isotope Values of Bone and Teeth Reflect Weaning Age at the Medieval Wharram Percy Site, Yorkshire, UK. *American Journal of Physical Anthropology*, **119**, 205–210.
- RICHARDS, M.P., JACOBI, R., COOK, J., PETTITT, P.B., & STRINGER, C.B. 2005. Isotopic evidence for the intensive use of marine foods by Late Upper Palaeolithic humans. *Journal of Human Evolution*, **49**, 390–394.
- RICHARDS, M.P., FULLER, B.T., & MOLLESON, T.I. 2006. Stable Isotope Paleodietary Study of Humans and Fauna from the Multi-period (Iron Age, Viking and Late Medieval) site of Newark Bay, Orkney. *Journal of Archaeological Science*, **33**, 122–131.

- RIEDEL, A., & PUCHER, E. 2008. Mittelalterliche Tierknochenfunde aus der Burg Raabs an der Thaya (Niederösterreich). *Beiträge zur Mittelalterarchäologie in Österreich*, **24**, 159–194.
- ROESKE, C.A., & O'LEARY, M.H. 1984. Carbon isotope effects on the enzyme-catalyzed carboxylation of ribulose biphosphate. *Biochemistry*, **23**, 6275–6284.
- RUMPELMAYR, K., PAVLIK, A., WILD, E., & TESCHLER-NICOLA, M. 2011. Assessing the uncertainties of  $\delta^{13}\text{C}$ - and  $\delta^{15}\text{N}$ -values determined by EA-IRMS for palaeodietary studies. *Quaternary International*, **245**, 307–314.
- SCHOENINGER, M.J., & DENIRO, M.J. 1984. Nitrogen and carbon isotopic composition of bone collagen from marine and terrestrial animals. *Geochimica et Cosmochimica Acta*, **48**, 625–639.
- SCHOENINGER, M.J., & MOORE, K. 1992. Bone stable isotope studies in archaeology. *Journal of World Prehistory*, **6**, 247–296.
- SCHOENINGER, M.J., MOORE, K.M., MURRAY, M.L., & KINGSTON, J.D. 1989. Detection of bone preservation in archaeological and fossil samples. *Applied Geochemistry*, **4**, 281–292.
- SCHURR, M.R., & POWELL, M.L. 2005. The role of changing childhood diets in the prehistoric evolution of food production: an isotopic assessment. *American Journal of Physical Anthropology*, **126**, 278–294.
- SCHUTKOWSKI, H. 2006. *Human Ecology*. Springer-Verlag, Berlin, Heidelberg.
- SEALY, J.C., & VAN DER MERWE, N.J. 1988. Social, spatial and chronological patterning in marine food use as determined by  $^{13}\text{C}$  measurements of Holocene human skeletons from the southwestern Cape, South Africa. *World Archaeology*, **20**, 87–102.
- SEMAL, P., & ORBAN, R. 1995. Collagen extraction from recent and fossil bones: quantitative and qualitative aspects. *Journal of Archaeological Science*, **22**, 463–467.
- SENBAYRAM, M., DIXON, L., GOULDING, K.W.T., & BOL, R. 2008. Long-term influence of manure and mineral nitrogen applications on plant and soil  $^{15}\text{N}$  and  $^{13}\text{C}$  values from the Broadbalk Wheat Experiment. *Rapid Communications in Mass Spectrometry*, **22**, 1735–1740.
- SKRZYPEK, G., SADLER, R., & PAUL, D. 2010. Error propagation in normalization of stable isotope data: a Monte Carlo analysis. *Rapid Communications in Mass Spectrometry*, **24**, 2697–2705.
- SMITH, B.H. 1991a. Standards of human tooth formation and dental age assessment. *Pages 143–168 of: KELLEY, M.A., & LARSEN, C.S. (eds), Advances in dental anthropology*. Wiley-Liss., New York.

## Bibliography

- SMITH, B.N., & EPSTEIN, S. 1971. Two categories of  $^{13}\text{C}/^{12}\text{C}$  ratios for higher plants. *Plant Physiology*, **47**, 380–384.
- SMITH, D.L. 1991b. *Probability, statistics, and data uncertainties in nuclear science and technology*. American Nuclear Society, LaGrange Park.
- STADLER, P. 1991. Statistische Auswertungen verschiedener Parameter der Frühbronzezeitlichen Nekropole F von Gemeinlebarn. *Pages 197–221 of: Die Nekropole F von Gemeinlebarn, Niederösterreich* (Habilitation: Neugebauer, J.-W.). Römisch-Germanische Forschungen, vol. 49. Verlag Philipp von Zabern, Mainz am Rhein.
- STEELE, K.W., & DANIEL, R.M. 1978. Fractionation of nitrogen isotopes by animals: a further complication to the use of variations in the natural abundance of  $^{15}\text{N}$  for tracer studies. *Journal of Agricultural Science*, **90**, 7–9.
- STENHOUSE, M.J., & BAXTER, M.S. 1979. The uptake of bomb  $^{14}\text{C}$  in humans. *Pages 324–341 of: BERGER, R., & SUESS, H.E. (eds), Radiocarbon dating*. University of California Press, Berkeley.
- SULLIVAN, C.H., & KRUEGER, H.W. 1981. Carbon isotope analysis in separate chemical phases in modern and fossil bone. *Nature*, **292**, 333–335.
- SZAMEIT, E. 1995. Gars-Thunau – frühmittelalterliche fürstliche Residenz und vorstädtisches Handelszentrum. *Pages 274–282 of: BRACHMANN, H. (ed), Burg – Burgstadt – Stadt. Zur Genese mittelalterlicher nichtagrarischer Zentren in Ostmitteleuropa*. Akademie-Verlag, Berlin.
- SZOMBATHY, J. 1929. *Prähistorische Flachgräber bei Gemeinlebarn in Niederösterreich*. Römisch-Germanische Forschungen, vol. 3. Verlag Philipp von Zabern, Mainz am Rhein.
- TABACHNICK, B., & FIDELL, L.S. 2007. *Using multivariate statistics*. 5th edition edn. Pearson, Boston.
- TESCHLER-NICOLA, M. 1989. Soziale und biologische Differenzierung in der frühen Bronzezeit am Beispiel des Gräberfeldes F von Gemeinlebarn, Niederösterreich. *Annalen des Naturhistorischen Museums in Wien A*, **90**, 135–145.
- TIESZEN, L.L., & FAGRE, T. 1993. Effect of diet quality and composition on the isotopic composition of respiratory  $\text{CO}_2$ , bone collagen, bioapatite, and soft tissues. *Pages 121–155 of: LAMBERT, J.B., & GRUPE, G. (eds), Prehistoric human bone - archaeology at the molecular level*. Springer, Berlin.
- TING, I.P. 1985. Crassulacean acid metabolism. *Annual Reviews of Plant Physiology*, **36**, 595–622.

- TROUGHTON, J.H., CARD, K.A., & HENDY, C.H. 1974. Photosynthetic pathways and carbon isotope discrimination by plants. *Carnegie Institute Washington Yearbook*, **73**, 768–780.
- UREY, H.C., LOWENSTAM, H.A., EPSTEIN, S., & MCKINNEY, C.R. 1951. Measurement of palaeotemperatures and temperatures of the upper Cretaceous of England, Denmark, and the Southeastern United States. *Bulletin of the Geological Society of America*, **62**, 399–416.
- VAN DER MERWE, N.J. 1982. Carbon isotopes, Photosynthesis, and Archaeology. *American Scientist*, **70**, 596–606.
- VAN DER MERWE, N.J. 1989. Natural variation in  $^{13}\text{C}$  concentration and its effect on environmental reconstruction using  $^{13}\text{C}/^{12}\text{C}$  ratios in animal bones. *Pages 105–125 of: PRICE, T.D. (ed), The chemistry of prehistoric human bone*. University Press, Cambridge.
- VAN DER MERWE, N.J., & VOGEL, J.C. 1978.  $^{13}\text{C}$  content of human collagen as a measure of prehistoric diet in Woodland North America. *Nature*, **276**, 815–816.
- VAN KLINKEN, G.J. 1999. Bone collagen quality indicators for palaeodietary and radiocarbon measurements. *Journal of Archaeological Science*, **26**, 687–695.
- VAN KLINKEN, G.J., VAN DER PLICHT, H., & HEDGES, R.E.M. 1994. Bond  $^{13}\text{C}/^{12}\text{C}$  ratios reflect (palaeo-)climatic variations. *Geophysical Research Letters*, **21**, 445–448.
- VOGEL, J.C. 1978. Isotopic assessment of the dietary habits of ungulates. *South African Journal of Science*, **74**, 298–301.
- VOGEL, J.C., & VAN DER MERWE, N.J. 1977. Isotopic evidence for early maize cultivation in New York state. *American Antiquity*, **42**, 238–242.
- VON DER MARK, K. 1999. Structure, biosynthesis and gene regulation of collagens in cartilage and bone. *Pages 18–29 of: SEIBEL, M.J., ROBINS, S.P., & BILEZIKIAN, J.P. (eds), Dynamics of bone and cartilage metabolism*. Academic Press, San Diego London.
- WATZKA, M., BUCHGRABER, K., & WANEK, W. 2006. Natural  $^{15}\text{N}$  abundance of plants and soils under different management practices in a montane grassland. *Soil Biology & Biochemistry*, **38**, 1564–1576.
- WERNER, R.A., & BRAND, W.A. 2001. Referencing strategies and techniques in stable isotope ratio analysis. *Rapid Communications in Mass Spectrometry*, **15**, 501–519.
- WIBERG, K.B. 1955. The deuterium isotope effect. *Chemical Reviews*, **55**, 713–743.

## Bibliography

- WILD, E.M., ARLAMOVSKY, K.A., GOLSER, R., KUTSCHERA, W., PRILLER, A., PUCHEGGER, S., ROM, W., STEIER, P., & VYCUDILIK, W. 2000.  $^{14}\text{C}$  dating with the bomb peak: An application to forensic medicine. *Nuclear Instruments and Methods in Physics Research B*, **172**, 944–950.
- WILD, E.M, GUILLEN, S., KUTSCHERA, W., SEIDLER, H., & STEIER, P. 2007. Radiocarbon dating of the Peruvian Chachapoya/Inka site at the Laguna de los Condores. (Proceedings of the AMS-10 conference). *Nuclear Instruments and Methods in Physics Research B*, **259**, 378–383.
- WILD, E.M, GAUSS, W., FORSTENPOINTNER, G., LINDBLOM, M., SMETANA, R., STEIER, P., THANHEISER, U., & WENINGER, F. 2010.  $^{14}\text{C}$  dating of the Early to late Bronze Age stratigraphic sequence of Aegina Kolonna, Greece. (Proceedings of the AMS-11 conference). *Nuclear Instruments and Methods in Physics Research B*, **268**, 1013–1021.



# List of Abbreviations

AA	amino acid
AD	anno domini
ADP	adenosine diphosphate
AIR	ambient inhalable reservoir
AMS	accelerator mas spectrometry
ANOVA	analysis of variance
ATP	adenosine triphosphate
AV	acceleration voltage
AP	alpha-plates
BC	before christ
BMU	basic multicellular unit
BP	before present
CAM	crassulacean acid metabolism
CE	Common Era
CF	continuous flow
d	day
Da	the unit "Dalton"
EA-IRMS	elemental analyser - isotope ratio mass spectrometry
EI	electron impact
EV	potential difference between filament and ion source block
EX	extraction voltage
f	female
FDI	Fédération Dentaire International
FMA	Frühmittelalter (Early Medieval)
GC	gas chromatography
Gly	glycine
h	hour
HP	half plates
IAEA	International Atomic Energy Agency
id	inner diameter
ID	identity
IR	ion repeller
IRMS	isotope ratio mass spectrometry
m	male
MANOVA	multivariate analysis of variance
MC	current of the solenoid magnet
MS	mass spectrometer

## *Bibliography*

MWCO	molecular weight cut off
n.a.	not applicable
NADP <sup>+</sup>	nicotinamide adenine dinucleotide phosphate
NBS	National Bureau of Standards
n.d.	not determined
OAS	organic analytical standard
od	outer diameter
o.n.	over night
p	poor
P <sub>i</sub>	inorganic phosphate
PEP	phosphoenolpyruvate
PEPc	phosphoenolpyruvate carboxylase
PDB	Pee Dee Belemnite
PL	Phalanx
PTFE	Polytetrafluoroethylene
r	rich
Rubisco	Ribulose-1:5-bisphosphate carboxylase
SD	standard deviation
SILVER	Stable Isotope Laboratory University of Vienna Environmental Research
sol.	solution
SS	source slit
TCD	thermoconductivity detector
TR	trap current
USGS	United States Geological Survey
VERA	Vienna Environmental Research Accelerator
VPDB	Vienna Pee Dee Belemnite
ZP	z-plates

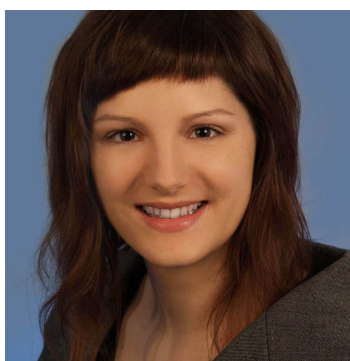
# Acknowledgments

First of all, I want to thank my thesis supervisor Ao. Univ.-Prof. Mag. Dr. Eva Maria Wild for making this work possible and for her commitment during all stages of my thesis work. Many thanks go to Ao. Univ.-Prof. Dr. Maria Teschler-Nicola and co-workers Mag. Friederike Novotny and Ute-Michaela Spannagl-Steiner for providing the access to the sample material and valuable discussions. Mag. Dr. Erich Pucher (1<sup>st</sup> Zoological Department, Natural History Museum of Vienna) is thanked for the identification of the animal samples from the Natural History Museum. Ass. Prof. Dr. Andreas Pavlik deserves my gratitude for his invaluable contributions especially to the uncertainty analysis and statistical part of this work. Ing. Stefan Lehr and Dipl.-Ing.(FH) Johann Lukas are thanked for their technical assistance with the sample preparation and the mass spectrometer respectively. Furthermore, I thank Dr. Hajnalka Herold for her efforts in the selection of the animal samples from Thunau and Mag. Dr. Günther Karl Kunst for the zoological identification of these samples. Special thanks go to my family and friends, but above all to my partner Dipl. Ing. Nicolas Gergaud, who always supported and encouraged me in times of doubt. And of course I would like to thank all the other colleagues at VERA for the wonderful working atmosphere they created, especially Dr. Francesca Quinto, Mag. Leonard Michlmayr, Dr. Jakob Liebl, Mag. Jenny Feige and my "room mates" Dr. Franz Weninger, Daniel Imrich, Mag. Peter Kueß and Dr. Franz Dellinger for all their support and friendship.



## Curriculum Vitae

**Kerstin Rumpelmayr**



E-Mail: k.rumpelmayr@gmail.com

Born: 19<sup>th</sup> December, 1981 (Wels)

## Education

- |                        |   |
|------------------------|---|
| since Sept. 2006       | <b>PhD candidate Chemistry, University of Vienna, Austria</b>   |
| Oct. 2000 – June 2006  | <b>Mag.rer.nat (M.Sc.) Chemistry, University of Vienna, with distinction</b><br><br>Master thesis in Biochemistry:<br>“Stealth-technology: Synthesis and characterization of functional polyethylene glycol derivatives”. |
| Sept. 1996 – June 2000 | Adalbert Stifter secondary school, private school, Linz, Austria:<br>Final exam with distinction  |
| Sept. 1992 – July 1996 | Bundesrealgymnasium Traun (secondary school), Austria   |

## Professional Experience

- |                         |  |
|-------------------------|--|
| since April 2011        | <b>Baxter Biomedical Research Center, Orth/Donau, Austria:</b><br>Validation Specialist, Process Quality Assurance |
| Sept. 2006 – April 2011 | <b>Isotope Research, Faculty of Physics, University of Vienna:</b><br>Scientific employee                          |

Vienna, June 23<sup>rd</sup> 2012



## Publications and Conference Contributions

- RUMPELMAYR, K., PAVLIK, A., WILD, E.M., TESCHLER-NICOLA, M. 2011. Assessing the uncertainties of  $\delta^{13}\text{C}$ - and  $\delta^{15}\text{N}$ -values determined by CF-EA-IRMS for palaeodietary studies. *Quaternary International* **245**, 307-314.
- RUMPELMAYR, K., PAVLIK, A., WILD, E.M., TESCHLER-NICOLA, M. 2010. Assessing the uncertainties of  $\delta^{13}\text{C}$ - and  $\delta^{15}\text{N}$ -values determined by CF-EA-IRMS for palaeodietary studies. (Poster at the *European Geoscience Union General Assembly*, Vienna, May 2-7, 2010). *Geophysical Research Abstracts* **12**, EGU2010-11409.
- RUMPELMAYR, K., WILD, E.M., TESCHLER-NICOLA, M., PAVLIK, A. 2009. Stabil-Isotopenuntersuchungen ( $\delta^{13}\text{C}$  und  $\delta^{15}\text{N}$ ) an den frühmittelalterlichen Skelettresten von Thunau / Gars am Kamp. Talk at the *International ÖGUF-Symposium*, Mauterndorf, Austria, October 21-24, 2009.
- RUMPELMAYR, K., WILD, E.M., TESCHLER-NICOLA, M., PAVLIK, A. in press. Paläodiät-Rekonstruktion mittels Stabil-Isotopenuntersuchungen ( $\delta^{13}\text{C}$  und  $\delta^{15}\text{N}$ ) an den frühmittelalterlichen Skelettresten von Thunau / Gars am Kamp. *Archäologie Österreichs* (Proceedings of the International ÖGUF-Symposium 2009).
- WILD, E.M., RUMPELMAYR, K., STEIER, P., TESCHLER-NICOLA, M., NOVOTNY, F., SPANNAGL-STEINER, M., FRIESINGER, H. 2008. First  $^{14}\text{C}$  and stable isotope results of the Early Medieval site of Gars-Thunau, Lower Austria. Poster at the *Radiocarbon & Archaeology 5th International Symposium*, ETH Zurich, Switzerland, March 25-28, 2008.